รายงานวิจัยฉบับสมบูรณ์

โครงการ อากาศยานไร้คนขับเอนกประสงค์เพื่อสนับสนุนการเกษตรโดยใช้เทคโนโลยีเก็บเกี่ยวพลังงานจากธรรมชาติ

โดย ผศ.ดร.พฤศยน นินทนาวงศา

30 ธันวาคม 2562

สัญญาเลขที่ TRG5880176

รายงานวิจัยฉบับสมบูรณ์

โครงการ อากาศยานไร้คนขับเอนกประสงค์เพื่อสนับสนุนการเกษตรโดยใช้เทคโนโลยีเก็บเกี่ยวพลังงานจากธรรมชาติ

ผศ.ดร.พฤศยน นินทนาวงศา
ภาควิชาวิศวกรรมคอมพิวเตอร์
มหาวิทยาลัยเทคโนโลยีราชมงคลธัญบุรี

สนับสนุนโดยสำนักงานกองทุนสนับสนุนการวิจัยและต้นสังกัด

Abstract

Project Code : TRG5880176

Project Title : Multi-objective Unmanned Aerial Vehicle for Agricultural support powered by ambient energy harvesting

Investigator : Assistant Professor Prusayon Nintanavongsa, Ph.D.
Department of Computer Engineering
Rajamangala University of Technology Thanyaburi

E-mail Address : pn@en.rmutt.ac.th

Project Period : 24 months

This project proposes a new architecture comprised of sensor hardware, protocol, analytical models, and optimized implementation geared towards new self-sustaining system of Unmanned Aerial Vehicle (UAV) and agricultural monitoring stations. The UAV operates by harvesting energy from the environment, together with wireless energy replenishment through ambient energy harvesting monitoring stations, and optimize energy usage under various objective functions, potentially leading to perennial multi-objective agricultural monitoring system. The project is envisaged to play a key role in achieving an optimal efficiency of multi-objective UAVs by (i) designing two routing approaches, called Location-agnostic (LA) and Location-specific (LS) protocols, to facilitate the self-sustaining agricultural monitoring platform, (ii) investigating the impact of sensor mobility on network communications in a smart farm platform, comprising of sensor-equipped UAVs, (iii) offering the performance analysis of perimeter surveillance system comprising of multiple UAVs, and (iv) proposing a system to detect and locate an unauthorized UAV operator using UAV. Through a combination of simulation and experimentation studies, we demonstrate (i) significant energy efficiency and coverage area improvement over the classical routing protocol (ii) how sensor mobility impacts network throughput and delay as well as determine the optimal UAV mobility profile (iii) how numbers of UAVs and their mobility profile have an effect on key network metrics as well as determine the condition of optimality, and (iv) how UAV service ceiling, UAV speed, and antenna directivity have an effect on the key performance metrics of the system, together with, the optimal operating condition.

Keywords : Energy harvesting, Unmanned Aerial Vehicle, agricultural support, perimeter surveillance, unauthorized operator.

บทคัดย่อ

รหัสโครงการ: TRG5880176

ชื่อโครงการ : อากาศยานไร้คนขับเอนกประสงค์เพื่อสนับสนุนการเกษตรโดยใช้เทคโนโลยีเก็บเกี่ยวพลังงานจากธรรมชาติ

ชื่อนักวิจัย : ผศ.ดร.พฤศยน นินทนาวงศา
ภาควิชาวิศวกรรมคอมพิวเตอร์
มหาวิทยาลัยเทคโนโลยีราชมงคลธัญบุรี
อีเมล์ : pn@en.rmutt.ac.th

ระยะเวลาโครงการ : 24 เดือน

โครงการนี้เสนอสถาปัตยกรรมใหม่ซึ่งประกอบไปด้วยเซ็นเซอร์ โปรโตคอล แบบจำลอง และการออกแบบสถานีตรวจสอบสภาพการเพาะปลูกและอากาศยานไร้คนขับที่สามารถทำงานได้ด้วยตนเอง อากาศยานไร้คนขับสามารถทำงานด้วยการรับพลังงานที่ถูกเก็บเกี่ยวจากธรรมชาติโดยสถานีตรวจสอบสภาพการเพาะปลูกและปรับเปลี่ยนการทำงานตามภารกิจและวัตถุประสงค์ต่าง ๆ โครงการนี้มีแนวคิดเพื่อให้อากาศยานไร้คนขับสามารถทำงานด้วยประสิทธิภาพสูงสุดโดย (i) การออกแบบวิธีการหาเส้นทาง 2 วิธี ได้แก่ Location-agnostic (LA) และ Location-specific (LS) protocols เพื่อช่วยการทำงานของสถานีตรวจสอบสภาพการเพาะปลูก (ii) ศึกษาผลการทบของการเคลื่อนที่ของอากาศยานไร้คนขับต่อประสิทธิภาพการสื่อสารในสภาพแวดล้อมการเพาะปลูกแบบอัจฉริยะ (iii) วิเคราะห์ประสิทธิภาพของระบบรักษาความปลอดภัยที่ประกอบไปด้วยกลุ่มของอากาศยานไร้คนขับ (iv) เสนอระบบตรวจจับและระบุตำแหน่งแหล่งสัญญาณที่ไม่ได้รับอนุญาตด้วยอากาศยานไร้คนขับ ด้วยการบูรณาการโดยการจำลองการทำงานบนคอมพิวเตอร์และการทดสอบระบบต้นแบบ ผลการศึกษาแสดงให้เห็น (i) วิธีการหาเส้นทาง 2 วิธีนั้นสามารถเพิ่มประสิทธิภาพในการใช้พลังงานและเพิ่มพื้นที่คลอบคลุมการทำงานของอากาศยานไร้คนขับ (ii) ผลการทบของการเคลื่อนที่ของอากาศยานไร้คนขับต่อ network throughput และ delay พร้อมทั้งเสนอการที่เคลื่อนที่ของอากาศยานไร้คนขับที่ให้ประสิทธิภาพสูงสุด (iii) ผลการทบของกลุ่มของอากาศยานไร้คนขับต่อประสิทธิภาพของระบบรักษาความปลอดภัย (iv) ผลการทบของลักษณะการการเคลื่อนที่ของอากาศยานไร้คนขับ รวมถึงระบบเสาอากาศต่อประสิทธิภาพการตรวจจับและระบุตำแหน่งแหล่งสัญญาณที่ไม่ได้รับอนุญาต

คำสำคัญ : เก็บเกี่ยวพลังงาน, อากาศยานไร้คนขับ, การสนับสนุนการเพาะปลูก, ระบบรักษาความปลอดภัย, ผู้บังคับอากาศยานไร้คนขับที่ไม่ได้รับอนุญาต

Output จากโครงการวิจัยที่ได้รับทุนจาก สกว.

1. ผลงานตีพิมพ์ในวารสารวิชาการนานาชาติ (ระบุชื่อผู้แต่ง ชื่อเรื่อง ชื่อวารสาร ปี เล่มที่ เลขที่ และหน้า) หรือผลงานตามที่คาดไว้ในสัญญาโครงการ
   - P. Nintanavongsa and I. Pitimon, “Detection and Localization of Unauthorized Unmanned Aerial Vehicle Operator using Unmanned Aerial Vehicle,” Information Technology Journal, vol. 15, no. 2, pp. 35-44, December 2019.

2. การนำผลงานวิจัยไปใช้ประโยชน์
   - เชิงวิชาการ (มีการพัฒนาการเรียนการสอน/สร้างนักวิจัยใหม่)
     นำองค์ความรู้ที่ได้จากงานวิจัยไปใช้ในการเรียนการสอนวิชา computer networks และ research methodology ในระดับบัณฑิตศึกษา รวมถึงใช้เป็นองค์ความรู้อ้างอิงสำหรับการทำวิจัยในระดับบัณฑิตศึกษาของมหาวิทยาลัยเทคโนโลยีราชมงคลธัญบุรี

3. อื่นๆ (เช่น ผลงานตีพิมพ์ในวารสารวิชาการในประเทศ การเสนอผลงานในที่ประชุมวิชาการ หนังสือ การจดสิทธิบัตร)
   - P. Nintanavongsa, W. Yaemvachi, and I. Pitimon, “Performance Analysis of Perimeter Surveillance Unmanned Aerial Vehicles,” International Electrical Engineering Congress (IEECON), pp. 1-4, March 2019.
   - P. Nintanavongsa and I. Pitimon, “Impact of Sensor Mobility on UAV-based Smart Farm Communications,” International Electrical Engineering Congress (IEECON), vol. 2, pp. 835-838, March 2017.
   - P. Nintanavongsa, W. Yaemvachi, and I. Pitimon, “A Self-sustaining Unmanned Aerial Vehicle Routing Protocol for Smart Farming,” International Symposium on Intelligent Signal Processing and Communication Systems (ISPACS), pp.459-463, October 2016.

Chapter 1. A Self-sustaining Unmanned Aerial Vehicle Routing Protocol for Smart Farming

Increasing agricultural productivity has been a long quest for farmers and only a few can achieve it. One major factor that hinders them to achieve such goal is the lack of proper agricultural monitoring technique. Recent advancement in technology has enabled the integration of sensor networks and traditional farming, resulting in effective monitoring through smart farming. However, there exists a hefty investment in equipment and infrastructure installation throughout the coverage area. In this chapter, we design two routing approaches, called Location-agnostic (LA) and Location-specific (LS) protocols, to facilitate the self-sustaining agricultural monitoring platform, requiring no infrastructure installation, comprises of Unmanned Aerial Vehicle (UAV) with solar energy harvesting and wireless power transfer capability. The LA protocol does not require location information of monitoring stations to be visited prior to the flight, and is useful for dynamic environment. The LS protocol relies on the complete view of the topology prior to the flight and is suitable for static environment. These protocols determine the optimal UAV routing path from a set of monitoring stations under various conditions.

Two major problems that contribute to low agricultural yield are damage caused by birds and lack of proper farm monitoring techniques [1]. While the exact measure of the loss in yield associated with birds is undocumented, generations of farmers have been performing a number of traditional and conventional techniques to prevent birds from damaging the agricultural area. This not only requires massive hours and manpower but also farmers' unaccountable loss of opportunities as they have to be physically present to repel a flock of birds from their agricultural area. Moreover, it is shown that the agricultural yield can be considerably increased by adopting Information technology to the agricultural area. GranMonte vineyard [2] is one of the examples that obtains a higher crop yield after implementing environmental monitoring stations throughout the agricultural area. With an up-to-date environmental data monitoring, it enables farmers a prompt response to mitigate fluctuation of important variables, i.e., humidity, temperature, that affect the crop yield.

Ambient energy harvesting is the process of scavenging energy from sources in the surrounding environment and store it for later use [3]. The energy sources can be solar, wind, and Radio Frequency (RF). It is an attractive method for overcoming the energy limitations of conventional battery powered wireless devices. Solar energy harvesting through photovoltaic conversion provides the highest power density among other types of energy harvesting. With direct access to sunlight, an average yield of 15 mW/cm^2 is to be expected [4]. The benefit of adopting ambient energy harvesting technology is two-fold. First, it is eco-friendly since no battery is required and hence no toxic waste from battery disposal. Second, it is easy to install and maintain as the infrastructure, i.e., electricity, is not required. The latter is even more pronounced in case of large cultivation area is to be monitored.

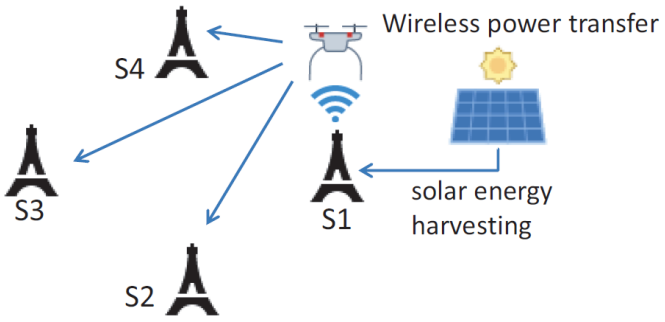

Fig.1. A self-sustaining agricultural monitoring platform

Fig.1 shows a self-sustaining agricultural monitoring platform. It consists of monitoring stations S1, S2, S3 and S4 and the UAV with solar energy harvesting and wireless power transfer capability. The solar energy harvesting enables monitoring stations to be decoupled from infrastructure installation, i.e., electrical cabling, while wireless energy transfer facilitates the UAV energy replenishing without human intervention, i.e., manually mount/dismount battery for recharge. We investigate on how the UAV propagates through a set of monitoring stations, using various routing protocols, and observe its behavior with respect to the following metrics (i) the average flight distance (ii) the average consumed energy, and (iii) the average enclosed area.

The core contributions of our work can be summarized as follows:

- We design a self-sustaining agricultural monitoring plat- form, comprises of Unmanned Aerial Vehicle (UAV) with solar energy harvesting and wireless power transfer capability.
- We propose two routing approaches, called Location-agnostic (LA) and Location-specific (LS) protocols, to facilitate the self-sustaining agricultural monitoring plat- form and demonstrate improvement in crucial metrics over existing routing approach.

RELATED WORK

In recent times, RFID technology is a clear example of wireless power transmission where such a tag operates using the incident RF power emitted by the transmitter [5]. The design of RF energy harvesting circuits has been extensively explored in [3] and the authors show that with a simple yet optimal design and optimization, the prototype can yield almost double the efficiency than that of a major commercially available energy harvesting circuit [6]. Moreover, wireless power transfer via strongly magnetic resonances is investigated by MIT researchers [7]. The authors experimentally demonstrated efficient nonradiative power transfer of 60 watts with 40% efficiency over distances in excess of 2 meters. The concept is later commercialized through the establishment of the WiTricity corporation [8]. This is not only prove that the wireless power transfer is a promising technology but also commercially viable. Recent publication [9] investigates the maximum achievable efficiency in near-field coupled power- transfer systems. The authors also propose a method that effectively decouples the design of the inductive coupling two- port from the problem of loading and power amplifier design. The use of UAV for agricultural purposes is recently pro- posed by Kasetsart

university researchers [10]. The research project is a collaboration between the faculty of engineering, Kasetsart university and the Yamaha motors (Thailand) and aims to effectively plant, deliver fertilizer, and spray pesticide to the cultivation area. The prototype is expected to weight 70 kilograms and able to carry the payload of 29 kilograms. The source of power is fossil fuel with the consumption of 8 liters per 2 hours flight. However, the project has several challenges and issues to be addressed. First, the project relies on a single- objective UAV that is designed to only deliver payload. It does not employ agricultural monitoring or responsive system that reacts to stimuli. Second, the UAV needs to be manually filled once its fuel is exhausted. This incurs not only budget allocation for fuel cost but also time consumed in maintenance of internal combustion engine. Third, environmental impact is a major concern since the UAV employs engine powered by fossil fuel. Not only noise pollution is expected from an internal combustion engine but also the air pollution from its exhaust.

A single Unmanned Aerial Vehicle (UAV) routing problem, where there are multiple depots and the vehicle is allowed to refuel at any depot, is considered in [11] . The objective of the problem is to find a path for the UAV such that each target is visited at least once by the vehicle, the fuel constraint is never violated along the path for the UAV, and the total fuel required by the UAV is a minimum. Computational results show that solutions whose costs are on an average within 1.4% of the optimum can be obtained relatively fast for the problem involving five depots and 25 targets. In [12], a distributed system of autonomous Unmanned Aerial Vehicles (UAVs), able to self-coordinate and cooperate in order to ensure both spatial and temporal coverage of specific time and spatial varying point of interests, is proposed. The authors give a mathematical formulation of the problem as a multi-criteria optimization model are considered simultaneously.

PROTOCOL DESCRIPTION

In this section, we describe the key challenges in protocol design as well as explore our proposed protocols in details.

1) Location-agnostic (LA) protocol: The LA protocol is designed to operate not only under dynamic environment but also requires no information of monitoring stations to be visited. Under this circumstance, monitoring stations are assumed to have Global Positioning System (GPS) equipped and intermittently sending out beacon signal, containing its location. The beacon signal serves two purposes here. First, it provides location information of the sender, enables UAV to calculate its path and navigate properly. Second, it provides a second layer of assurance in case of UAV misses the beacon signal transmitted by the monitoring station. Since neighboring monitoring stations are unlikely to have the same beacon sending interval, they can also provide location information of stations nearby. The concept of using beacon signal to facilitate UAV navigation also makes the LA protocol resilient to dynamic environment, i.e., monitoring stations are mobile. For instance, monitoring stations can be assigned to fine- grained patrol and monitoring while UAV is responsible for coarse-grained patrol and monitoring.

As stated earlier, the LA protocol does not require location information of monitoring station prior to the flight. Once the UAV is fully charged, it takes off and listens to the beacon signal from

monitoring stations in order to determine its first visiting location. Since there may be various monitoring stations in the vicinity, the LA protocol employs the greedy method, i.e., choosing the nearest monitoring station to its current position. In other words, the LA protocol elects the nearest beacon sending monitoring station to be the next visiting location and the process is performed on hop-by-hop basis. Fig. 2(a) shows the topology area of 1000 x 1000 m2 with 5 monitoring stations are deployed. The station number 1 is the only station that has solar energy harvesting and wireless power transfer capability. This implies that the UAV has to originate and terminate its flight at this stations. It also has to perform energy replenishing at this station. The calculated UAV flight path is shown in red and the visiting order is 1, 4, 3, 5, 2, and 1 with the total flight distance of 2,918.55 meters. When the UAV takes off from station 1, it receives beacon signal from both station 3 and station 4. However, upon comparing distance from its current location to location information received from station 3 and station 4, it elects station 4 to be the next visiting point since it is closer to station 4 than station 3. Once it arrives at station 4, it then proceeds to determine the next visiting point. Here, it receives beacon signal from station 2 and station 3 and it chooses to proceed towards station 3 since it is closer to its current position. The process continues in this fashion until it receives no further beacon signal. The UAV then returns to station 1 to disseminate collected information as well as recharging itself. It stays at station 1 until the battery is fully charged and subsequently returns to operation.

2) Location-specific (LS) protocol: Consider the scenario in which location of monitoring stations are predetermined and reconfiguration rarely occurs. In fact, this scenario can be expected in practice since monitoring stations are usually planned, installed, and expected to acquire information at each specific location. We can utilize priori knowledge of monitoring stations' location and perform a more efficient optimization. The LS protocol utilizes the predetermined lo- cation information and performs the flight path calculation. In other words, the LS protocol relies on the complete view of the topology prior to the flight and is suitable for static environment. Unlike the LA protocol where the UAV takes off and determine the next visiting point once it is fully charged, the LS protocol performs the flight path optimization and all visiting points are determined prior to the flight. Fig.2 (b) shows the same topology used in the previous section. Likewise, station 1 is the only station that has solar energy harvesting and wireless power transfer capability and hence the UAV has to originate and terminate its flight at this stations. However, locations of monitoring stations are assumed to be predetermined and they are immobile. This implies that, prior to the flight, the UAV has the complete view of the topology and can determine all points to be visited. The LS protocol heuristically search for the best flight path, that is, the shortest distance that completes the flight. The heuristic search can be performed by going through all possible permutations of monitoring station pairs and choose one that yields the lowest flight distance. One may argue that the flight path computation time can be very large with increasing numbers of monitoring stations. However, it usually takes hours to fully charge the UAV battery and the flight path calculation can be performed simultaneously. Moreover, the flight path calculation is performed by the monitoring station, the station 1 in this case, and poses no burden on energy

consumption to the UAV. Consequently, the computational complexity of the LS protocol deems insignificant in this perspective.

In Fig. 2(b), the calculated UAV flight path using LS protocol is shown in red and the visiting order is 1, 3, 5, 2, 4, and 1 with the total flight distance of 2,801.64 meters. Once the UAV takes off at station 1, it then proceeds to the predetermined visiting points without the need to acquire beacon signal. It is obvious that the LS protocol chooses the longer path, station 1 to station 3, in contrast to that of the LA protocol. Since the environment is static, that is, monitoring stations are immobile, the UAV is bounded to visit all designated monitoring stations and return to station 1. Note that monitoring stations are not required to transmit beacon signal and hence less energy consumption is expected.

The pseudo code of Location-specific (LS) protocol is shown below,

```
Visiting_order = empty stack
while (set of visiting points != Ø)
        randomly pick point k from set of visiting points
        push visiting_order(k)
        set of visiting points = set of visiting points - k
```

3) Random protocol: Fig. 2(c) depicts another way to calculate the UAV flight path via random method. In this case, the assumption is similar to that of the LS protocol, that is, the locations of monitoring stations are assumed to be predetermined and they are immobile. However, there is no flight path calculation prior to the flight and the visiting order of monitoring stations is randomized. Consequently, this method poses negligible time and energy consumption for the flight path calculation. The calculated UAV flight path using random method is shown in red and the visiting order is 1, 4, 5, 2, 3, and 1 with the total flight distance of 3,226 meters. Similar to the LS protocol, once the UAV takes off at station 1, it then proceeds to the predetermined visiting points without the need to acquire beacon signal. Note that each monitoring station will be visited only once in each trip and hence multiple visit is prohibited. This condition is applicable to all three proposed protocols.

The pseudo code of Random protocol is shown below,

```
Min_path = ∞
Find all permutation (set of visiting points)
For each permutation do
        Calculate total path length
        If (total path length < Min_path)
                Min_path = total path length
```

SIMULATION RESULTS

In this section, we thoroughly evaluate our proposed protocols using our custom simulator, developed in MATLAB. We observe the behavior of each protocol with respect to the number of monitoring stations. The simulation parameters are set as follows: The UAV is 3dr iris+ [13] and its specifications and operational characteristics, i.e., current consumption, cruising speed, battery capacity, are from [14]. Additional parameters used in the simulation are present in Table 1. Unless specifically stated, monitoring stations are deployed uniformly at random in 1000 x 1000 m2 grid. While it is possible that the location of the monitoring stations may affect the experiment, i.e., all monitoring stations are deployed in the same location. It is unlikely in practice to implement such deployment. All monitoring stations are assumed to be static and the station 1 is the only station that has solar energy harvesting and wireless power transfer capability and hence the UAV has to originate and terminate its flight at this stations.

We compare the proposed protocols with the random protocol, the order of monitoring station visit is randomly chosen prior to the flight. The random protocol provides the base case and reference protocol for comparison. We perform comparison on three metrics, average flight distance, average consumed energy, and average enclosed area.

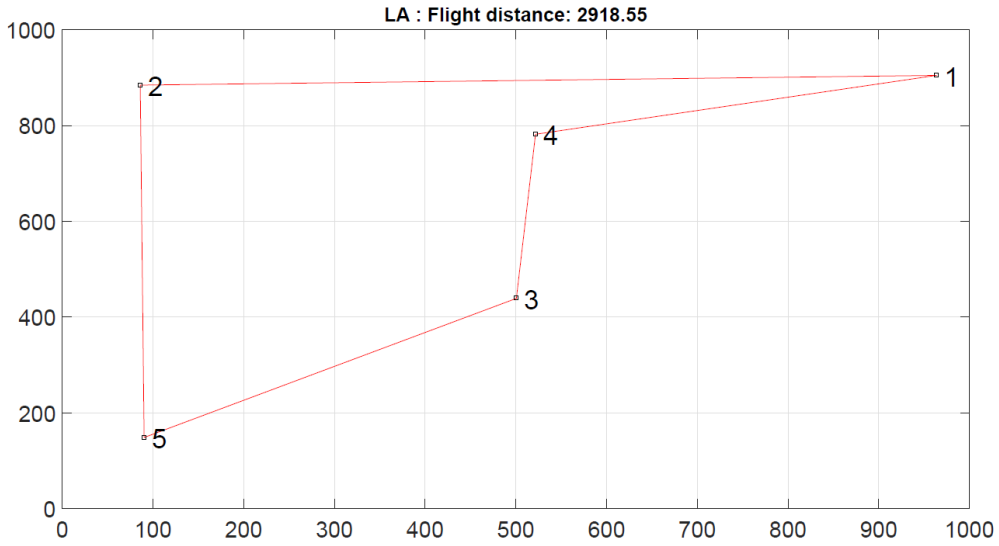

(a)

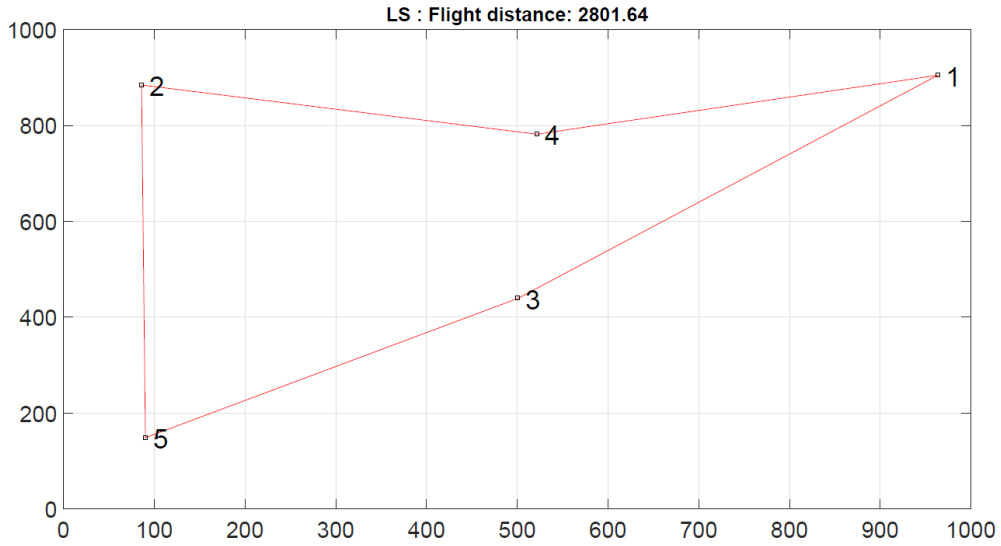

(b)

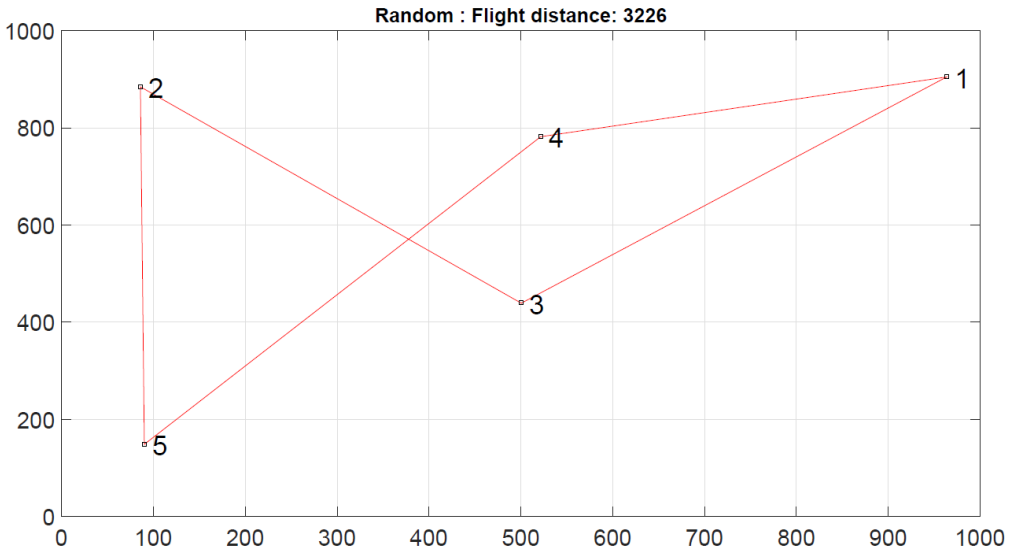

(c)

Fig. 2. Calculated UAV flight path with 5 monitoring stations adopting LA routing protocol (a) LS routing protocol (b) and random protocol (c)

Table 1 Parameter used in simulation

Parameter	**Value**
cruising speed	7.5 m/s
current consumption	21.31 A
cruise ceiling	15.0 m
battery capacity	Lithium-Polymer 5,100 mAh

A. Average flight distance

In this sub-section, we investigate the effect of the number of monitoring stations on the average flight distance for different UAV routing protocols. The average flight distance is defined as the average total distance that the UAV traveled in order to visit all monitoring stations, originating from station 1 and terminating at station 1. Fig. 3 shows the effect of the number of monitoring stations on the average flight distance. The number of monitoring stations, uniformly distributed at random, is varied from 5 to 30. It is clear that the LS protocol delivers the lowest average flight distance among three protocols, approximately 12% lower than the LA protocol. Moreover, the LS protocol delivers monotonically increasing average flight distance with increasing numbers of monitoring stations. The LA protocol yields slightly larger average flight distance than that of the LS protocol and also experiences monotonically increasing average flight distance with increasing numbers of monitoring stations. However, it is expected that the LS protocol offers even lower average flight distance than the LA protocol with increasing numbers of monitoring stations since the difference between these protocols increases with increasing numbers of monitoring stations.

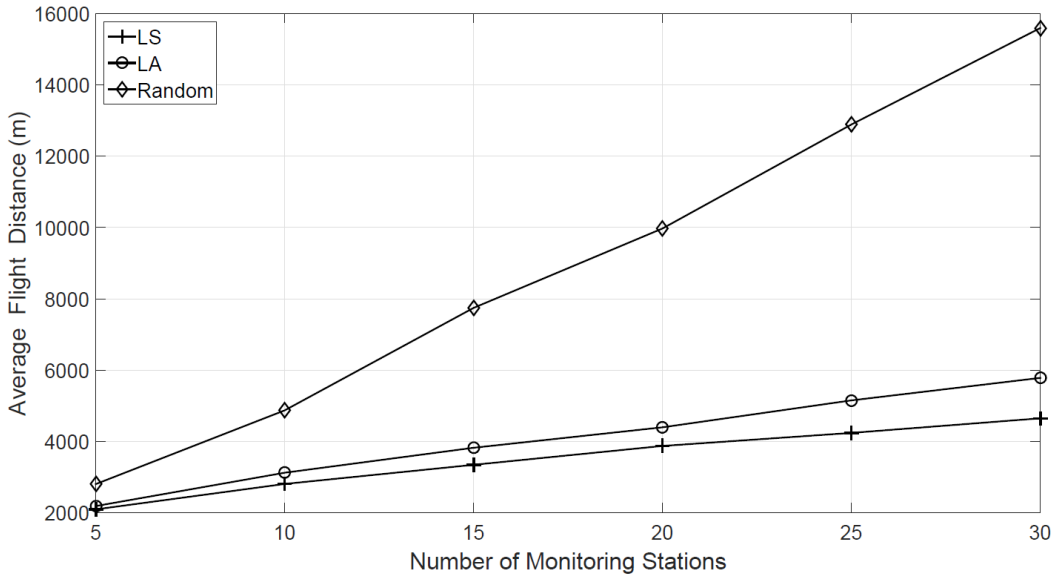

Fig. 3. Effect of the number of monitoring stations on average flight distance

The benefit of pre-flight optimization in the LS proto- col greatly improves the performance as the UAV follows the optimal flight path and ensuring the shortest distance traveled. The per-hop optimization in the LA protocol, although unable to deliver the optimal solution, offers marginally inferior performance compared to the LS protocol. It is also clear that the random protocol performs the worst among three protocols. The average flight distance, even monotonically increases with increasing numbers of monitoring stations, exhibits a higher rate of growth than the LA and LS protocols. The random protocol yields 50% higher average flight distance than the other two protocols even at the lowest number of monitoring stations. Consequently, it may not be a good choice if the average flight distance has to be kept minimum.

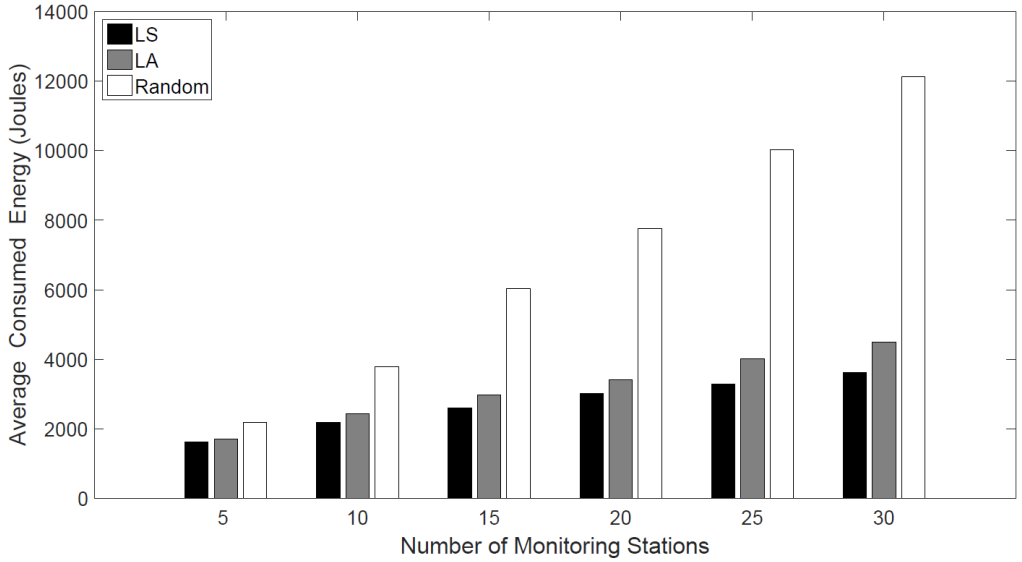

Fig. 4. Effect of the number of monitoring stations on average consumed energy

B. Average consumed energy

Here, we investigate how these three protocols behave when the number of monitoring stations changes. The average consumed energy is a key metric in this section and defined as an average total energy the UAV spent in order to visit all monitoring stations, originating from station 1 and terminating at station 1. The average consumed energy is shown in Fig. 4, wherein the energy consumption of the LA and LS protocols are similar, i.e., monotonically increasing average consumed energy with increasing numbers of monitoring stations. Again, the LS protocol offers the lowest average consumed energy when compared to the LA and random protocols while the random protocol yields the highest energy consumption among three protocols. The average consume energy plot exhibits a similar fashion to the average flight distance shown in the previous section.

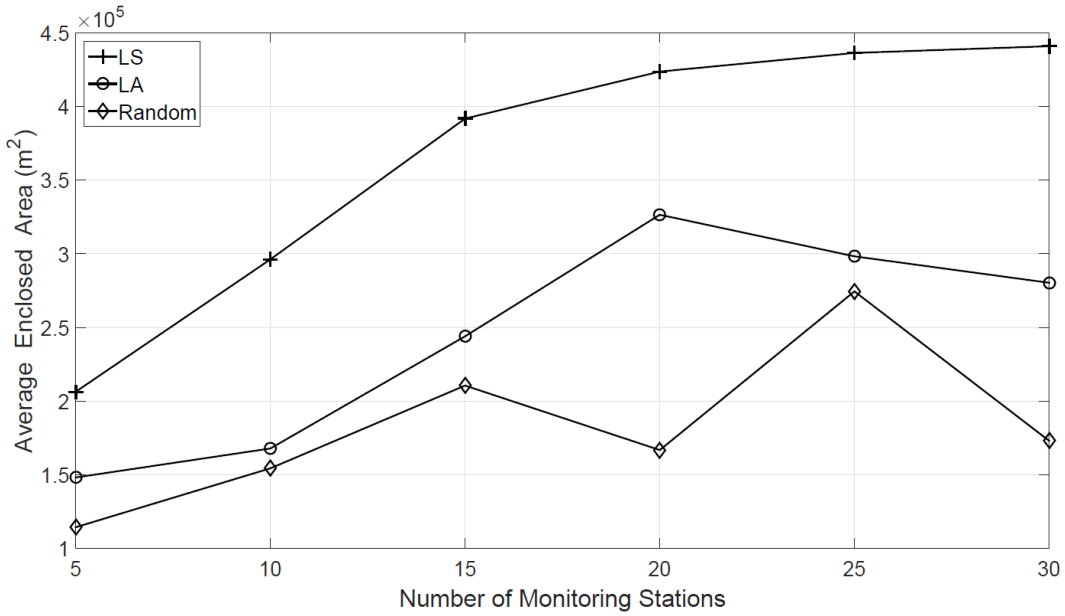

Fig. 5. Effect of the number of monitoring stations on average enclosed area

C. Average enclosed area

The average enclosed area, defined as an average area enclosed by the UAV flight path, is another metric of interest. One of the applications is the surveillance operation and it is crucial to determine the UAV coverage area. Fig. 5 shows the effect of the number of monitoring stations on the average enclosed area for each routing protocol. It is obvious that the LS protocol offers the largest coverage area throughout the range of monitoring stations, approximately 45% and 81% larger than the LA and the random protocols, respectively. However, the average enclosed area curve of the LS protocol exhibits a constant rate of growth until 15 monitoring stations and then gradually decreases towards increasing numbers of monitoring stations. This is not surprising since there is less room for optimization with increasing numbers of monitoring stations placed into the topology. The LA protocol yields the second largest coverage area while the random protocol provides the least amount of coverage area. All three protocols exhibits a similar pattern, that is, the higher the number of monitoring stations, the larger the average enclosed area.

CONCLUSIONS

We design two routing approaches, called Location-agnostic (LA) and Location-specific (LS) protocols, to facilitate the self-sustaining agricultural monitoring platform. The LA protocol optimizes the flight path on-the-fly and is useful for dynamic environment while the LS protocol performs the flight path optimization prior to the flight and is suitable for static environment. Simulation results reveal that the LS and LA protocols largely outperforms the random protocol in average flight distance, average consumed energy, and average enclosed area.

Chapter 2. Impact of Sensor Mobility on UAV-based Smart Farm Communications

Agricultural productivity has long been a key metric for measuring farming efficiency and it has been proven that agricultural productivity can be increased through smart farming. Recently, Unmanned Aerial Vehicle (UAV) has also been incorporated into smart farming in order to provide additional perspectives, i.e., imagery analysis and agricultural surveillance. These UAVs not only perform their specific tasks but also capable of communicating. In this chapter, we investigate the impact of sensor mobility on network communications in a smart farm platform, comprising of sensor-equipped UAVs.

Smart farming, a method of increasing agricultural productivity by incorporating information technology into the traditional farming, is becoming a mainstream method of cultivation adopted by farmers. It is proven in [15] that a higher agricultural productivity can be increased by implementing environmental monitoring stations throughout the agricultural area. With a real-time environmental data monitoring, it enables farmers to respond promptly when fluctuation of critical variables, i.e., water level, temperature, that affect the agricultural productivity occur. Moreover, Food and Agriculture Organization of the United Nations (FAO) announced that food production will have to increase by 70 percent to sustain the global consumption by 2050 [16]. With limited agricultural area and water supply, smart farming is undeniably a promising method to maximize the agricultural productivity.

In addition to environmental monitoring at ground level normally found in smart farming, ones can take advantage from aerial perspective by incorporating UAV into the smart farm platform. At the ground level, useful information, i.e., soil humidity, temperature, and perimeter monitoring, can be collected and exchanged via monitoring stations. On the other hand, UAVs offer additional perspective through aerial monitoring capability. The assigned task can be either active (acting upon the presence of stimuli) or passive (only collecting data). For instance, monitoring stations at the ground level can perform environmental data collection as well as perimeter monitoring. Upon detection of intruders, it sends out the packet, indicating security breach, to the responsible agencies, i.e., central monitoring station and law enforcement unit. Moreover, UAVs not only provide imagery analysis of the agricultural are but also offer in-depth situation awareness by patrolling over the area of breaching upon request. On the contrary, UAVs can also be used to provide important updates and configurations to grounded monitoring stations by traversing towards them.

In order to achieve a seamless operation of the UAV-based smart farming, it is crucial to ensure that the communication efficiency among sensors-equipped devices is at the highest level, that is, operating the network with parameters that yields the highest throughput with respect to an acceptable network delay. We consider a smart farm platform, consisting of sensor- equipped UAVs, and investigate how sensor mobility affects network communications, i.e., network throughput and delay. UAVs with high mobility rate may offer higher level of coverage area since they are travelling at higher speed. However, it is shown in [17] that network communication is very susceptible to high

rate of mobility and the optimal mobility profile should be employed in order to achieve the optimal network throughput.

The core contributions of our work can be summarized as follows:

• We demonstrate how sensor mobility impacts network throughput and delay in a smart farm platform, comprising of sensor-equipped UAVs.

• We determine the optimal UAV mobility profile that yields the optimal network throughput.

RELATED WORK

The concept of smart farming has emerged in the past decade and is gaining more attention recently. It is obvious that even the large presence of land, only a fraction is suitable for agricultural purpose. Moreover, today's agricultural area is decreasing as a result of the economic growth, i.e., rice paddy is converted into habitation through housing development. On the other hand, the world's population is increasing overtime, implying a larger volume of food production needed to keep up with the increasing rate of food consumption. Consequently, there is an urgent need for more efficient agricultural process. In other words, an agricultural productivity has to be increased. This poses even more serious problem if the land available for agricultural propose is diminished. Smart farming is considered to be one of the promising candidates to alleviate aforementioned problem.

Recently, the realization of Internet of Things (IoT) concept is implemented in [18] to provide services for smart city. The authors propose an integrated semantic service platform (ISSP) to support ontological models in various IoT-based service domains of a smart city. The prototype service for a smart office using the ISSP is developed as well as illustration on how the ISSP-based method would help build a smart city. The promise of growing agricultural productivity by adopting IoT-related technologies is discussed in [19] while a connected farm concept, which aims to provide suitable environment for growing crops based on the IoT systems is proposed in [20]. All sensors and actuators for monitoring and growing crops are connected with a gateway installed with a device software platform for IoT systems and the gateway communicates with the IoT service server. Consequently, The IoT service server not only monitors the environmental condition of the connected farm by communicating with the gateway installed into the connected farm, but also talks with expert farming knowledge systems and controls actuators in order to make the farm suitable to grow crops.

The implementation of smart farming with off-the-shelf embedded devices, Raspberry Pi and Arduino Uno, is presented in [21]. The authors investigate an establishment using an Intelligent System which employed an Embedded System and Smart Phone for chicken farming management and problem solving. It is found that the system could monitor weather conditions including humidity, temperature, climate quality, and filter fan in the chicken farm. The system was found to be comfortable for farmers to use as they could effectively control the farm remotely, resulting in cost reduction, asset saving, and productive management in chicken farming.

The use of UAV for agricultural purposes is recently proposed by Kasetsart university researchers [22]. The research project is a collaboration between the faculty of engineering, Kasetsart university and the Yamaha motors (Thailand) and aims to effectively plant, deliver fertilizer,

and spray pesticide to the cultivation area. The prototype is expected to weight 70 kilograms and able to carry the payload of 29 kilograms. The source of power is fossil fuel with the consumption of 8 liters per 2 hours flight. In [23], the authors present a concept of using drones for smart farming and a novel approach to distinguish between different field's plowing techniques by means of an RGB-D sensor is proposed. The proposed technique can be easily integrated in commercially available Unmanned Aerial Vehicles (UAVs). In order to successfully classify the plowing techniques, two different measurement algorithms have been developed. Experimental tests show that the proposed methodology is able to provide a good classification of the field's plowing depths.

The self-sustaining agricultural monitoring platform, comprises of UAV with solar energy harvesting and wireless power transfer capability is proposed in [24]. The authors also propose two routing approaches, called Location-agnostic (LA) and Location-specific (LS) protocols, to facilitate the self-sustaining agricultural monitoring platform and demonstrate improvement in crucial metrics over existing routing approach. The LA protocol does not require location information of monitoring stations to be visited prior to the flight, and is useful for dynamic environment. The LS protocol relies on the complete view of the topology prior to the flight and is suitable for static environment. These protocols determine the optimal UAV routing path from a set of monitoring stations under various conditions. The simulation and experimentation studies demonstrate significant energy efficiency and coverage area improvement over the classical routing protocol.

In [25], the authors consider the case of disjoint farming parcels each including clusters of sensors, organized in a predetermined way according to farming objectives, and propose an UAV Routing Protocol (URP) for crop monitoring where heterogeneous sensor nodes are installed in the large crop field and only selective data from selected sensors is harvested by UAV. The proposed routing protocol takes into account a tradeoff between energy management and data dissemination overhead. The proposed system is validated by simulation and it is found that this system efficiently optimizes the energy utilization for sensor nodes as well as UAV.

SIMULATION PARAMETERS

In this section, we describe the simulation parameters and scenario under consideration. We observe the impact of sensor mobility on network communication using discrete event simulator, ns-2 [26]. The simulation parameters are as follows:

A. UAV mobility profile

The UAV mobility profile consists of both speed and direction of movement. It is crucial to operate UAV at the optimal speed in order to achieve the highest network throughput. Operating UAV at too low speed not only decrease the area of coverage but also unable to utilize the network to its full potential. On the contrary, flying UAV too fast may incur network communication disruption. In this work, the speed of UAV is varied from 5 m/s to 60 m/s with 5 m/s increment.

The direction of UAV movement is another important aspect of UAV mobility profile. We employ the Random WayPoint (RWP) model for UAV movement. The RWP model generate mobility pattern in which each node moves to the random point within the specific area and remains in the

position for certain period, known as pause time, then moves to next point randomly. We employ zero pause time in this work to minimize any possible implication on network throughput measurement.

B. UAV radio profile

It is known that radio module plays a major role in power consumption in battery-operated devices. The radio module equipped in UAV has no exception and it is desirable to use low-power radio module when applicable. The Institute of Electrical and Electronics Engineers (IEEE) 802.15.4 radio standard is employed in this work. In contrast to the IEEE 802.11 radio standard, the IEEE 802.15.4 radio standard is developed for low data rate monitoring and control applications with an emphasis on low-power consumption. We use the carrier sense radius and packet reception radius of 40 m.

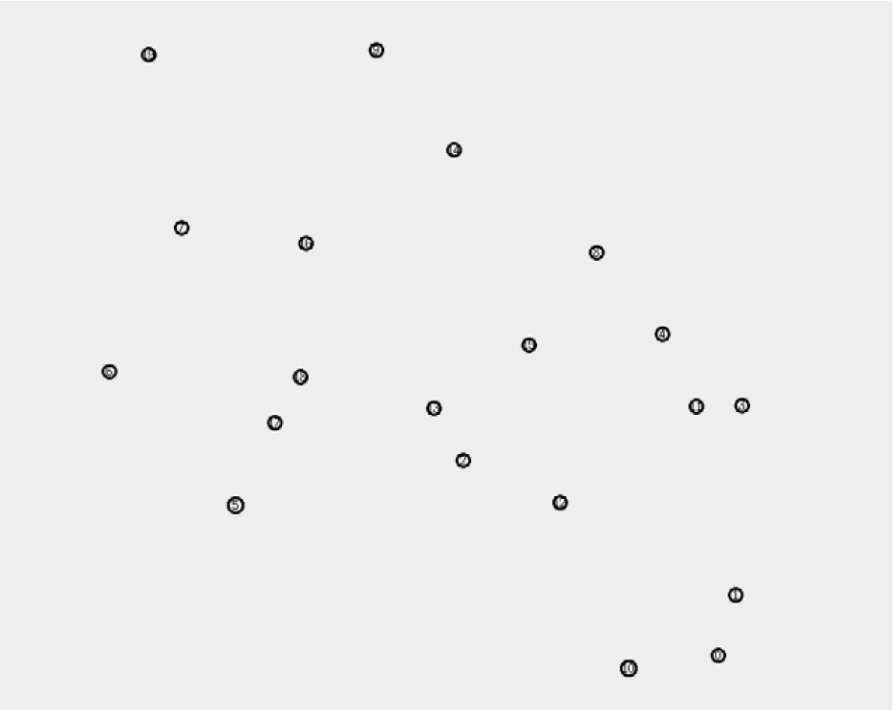

Fig. 6. Placement of UAVs in the deployment area

C. Area of deployment

The area of deployment is 500 x 500 m2 grid and UAVs are deployed uniformly at random. While it is possible that the location of the initial UAV placement may affect the experiment, i.e., UAVs are densely deployed at a particular location. It is unlikely that the initial placement of UAVs incurs any effect on the experiment since UAVs are mobile once the simulation is initiated. Fig. 6 shows the placement of 20 UAVs in the deployment area.

D. Routing protocol and traffic generation

The routing protocol plays a crucial role in packet delivery. In this work, an Ad hoc On-Demand Distance Vector (AODV) [27] is used. AODV is a routing protocol designed for mobile ad hoc networks. It establishes routes to destinations on demand and supports both unicast and multicast routing. We employ the Constant Bit Rate (CBR) traffic for UAV communication. The packet size is set to 512 bytes with the packet generation rate of 2 packets/s. The maximum CBR connection is limited to 20 connections.

SIMULATION RESULTS

In this section, we thoroughly observe the impact of sensor mobility on network communication using ns-2 network simulator. The key metrics under investigation are average network throughput and average network delay. Unless specifically stated, the simulation time is 300 seconds and 20 UAVs are deployed uniformly at random in 500 x 500 m2 grid. The number of iterations for each UAV speed step is set to 10 and the result is obtained through the average value of 10 iterations. This is to prevent outliers from influencing the simulation results.

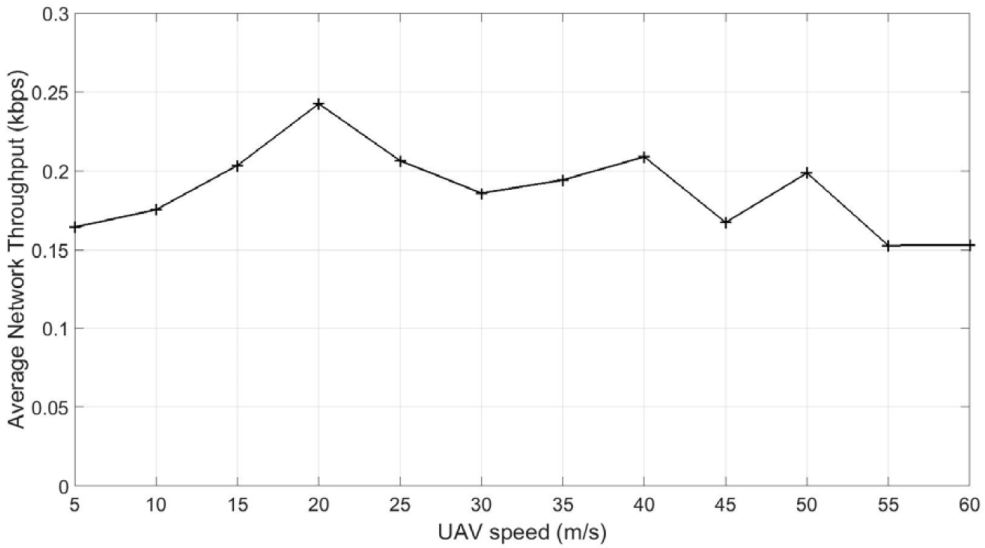

Fig. 7. Effect of the UAV speed on average network throughput

A. Average network throughput

The average network throughput is defined as the average amount of data sent from source and successfully received at the destination over a period of time. It is a key metric for network performance measurement and should be maintained at the highest level possible. We investigate how the UAV speed affects the average network throughput and determine the optimal operational speed of UAVs. Fig. 7 depicts the effect of the UAV speed on average network throughput. The UAV speed is varied from 5 m/s to 60 m/s. It is clear that the UAV speed has an effect on average network throughput, that is, the average network throughput is not constant throughout. In fact, the average network throughput exhibits a constant rate of growth from UAV speed of 5 m/s to 20 m/s

then gradually decreases towards increasing value of UAV speed. At UAV speed of 5 m/s, the network is rather static and routing protocol plays an insignificant role in packet delivery. As the UAV speed increases, the network becomes more dynamic and UAVs are getting more connected.

Consequently, the packet delivery increases thanks to the routing protocol. However, once the network becomes too dynamic due to increasing UAV speed, the higher number of network disruption from disconnected routes. It is obvious that the optimal UAV operational speed is 20 m/s since it yields the highest average network throughput and the network communication is utilized to its full potential at this point.

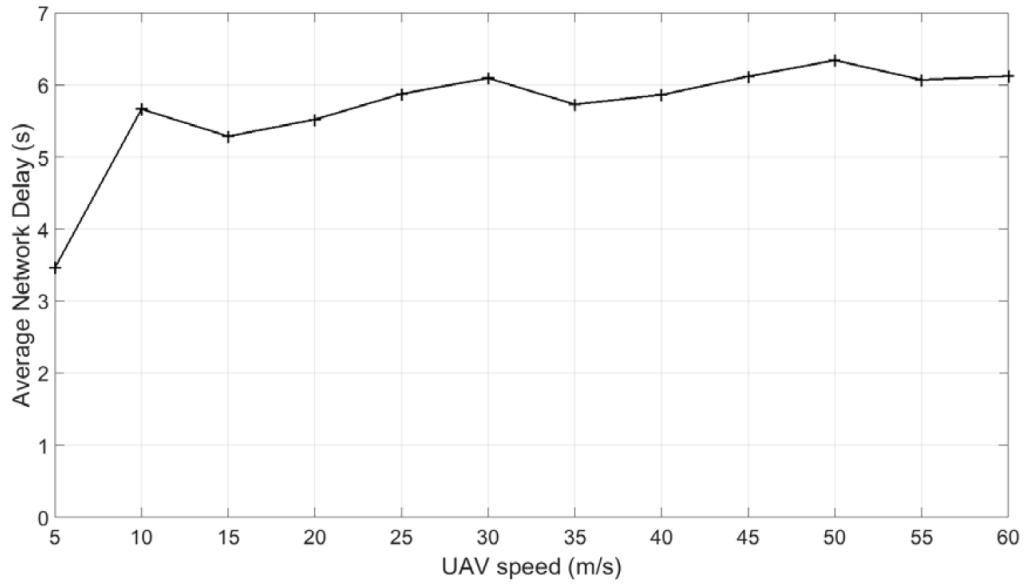

Fig. 8. Effect of the UAV speed on average network delay

B. Average network delay

Another important metric for network performance evaluation is the average network delay. It becomes a critical metric of measurement for time-sensitive communication. In certain types of applications, any increase in network delay may render the application useless. Fig. 8 shows the effect of the UAV speed on average network delay. Again, the UAV speed has an effect on average network delay, that is, the average network delay is not constant throughout. It is obvious that the average network delay monotonically increases with increasing UAV speed. In contrast to the above section, the average network delay grows linearly with increasing UAV speed.

CONCLUSIONS

Smart farming is a promising solution to increase agricultural productivity by incorporating information to the classical farming. It can also be supplemented by introducing UAV for additional perspective. We consider a smart farm platform, consisting of sensor-equipped UAVs, and investigate how sensor mobility affects network communications. We demonstrate how sensor

mobility impacts network throughput and delay in a smart farm as well as determine the optimal UAV mobility profile that yields the optimal network throughput.

Chapter 3. Performance Analysis of Perimeter Surveillance Unmanned Aerial Vehicles

Unmanned Aerial Vehicle (UAV) has seen exceptional growth over the past decade and become easily accessible to everyone. One of the key features that makes UAV attractive is the ability to provide the aerial perspective. This is particular the case for security and military purposes, i.e., security patrol and aerial surveillance. In this chapter, we offer the performance analysis of perimeter surveillance system comprising of multiple UAVs. These UAVs perform a surveillance task along the predefined perimeter and are capable of communicating among them.

Perimeter surveillance plays a major role in any security measures employed throughout the world. This is true in both physical and logical security measures. In physical security measure, the system is designed to detect and deny unauthorized access to facilities and protect them from damage or harm [28]. It involves the use of multiple independent systems, i.e., closed-circuit television camera (CCTV) surveillance, security guards, and protective barriers. In logical security measure, a software suite is usually implemented to ensure that only authorized users can gain an access and perform actions as intended while unauthorized access is detected, denied, and recorded. This is usually accomplished through the use of firewalls, username and password authentication. The aforementioned security measures share the same principle, that is, in order to detect potential attacks, one has to monitor the point of ingress. For example, in case of physical security measure, CCTV surveillance and security guards are used for anomaly detection along the perimeter under monitor. Likewise, firewalls and Intrusion Detection System (IDS) are employed in logical security measure for this regard. To this point, it is undeniable that perimeter surveillance is crucial and plays a vital role in maintaining system integrity.

It is not until recently that UAV has spread its wings into several applications, ranging from recreational purposes to military use. For example, UAV can be used for monitoring forest fire, aerial photography, and border patrol. UAV is gaining its popularity owing to its ability to deliver the aerial perspective. In the old day, perimeter surveillance is an arduous task since one has to allocate time and resource, i.e., managing patrolmen and patrol cycle. Moreover, this method suffers the lack of immediate response since the surveillance is conducted on ground. Any breach can occur between patrol cycle and response can be slow as the backup has to route along perimeter. CCTV surveillance can alleviate the previously stated issue. However, it incurs a heavy investment in equipment installation and is not practical in large area deployment.

UAV is expected to become the mainstream in aerial surveillance since not only its operational cost is much lower than the human-operated aircraft but also eliminates the human risk involved in operating the actual aircraft. In addition to its ability to provide aerial perspective, it does not require infrastructure, i.e., roads and electrical facility, in order to operate. Consequently, UAV is a potential candidate for this purpose. It is globally estimated the market worth of $4.1 billion in commercial UAVs in 2017 and it is expected over 7 million UAVs registration in the United States by 2020 [29].

With the UAV price drastically lowered, UAV begins dominating the perimeter surveillance task. Traditionally, a single large UAV is employed for perimeter surveillance and it only communicates with the base station. Hence, the data communication is simple and network characteristic can easily be determined. Recently, as the lower cost of UAV together with smaller UAV footprint, most civil and public applications can be achieved more efficiently with multi-UAV systems [30]. This system utilizes multiple UAVs, working in a coordinated manner, to provide much higher degree of coverage and scalability. It implies a more complex communication network, that is, communication among UAVs themselves and communication between UAVs and base stations. Consequently, the network characteristic can no longer be easily determined and it is crucial to investigate such scenarios prior to actual deployment.

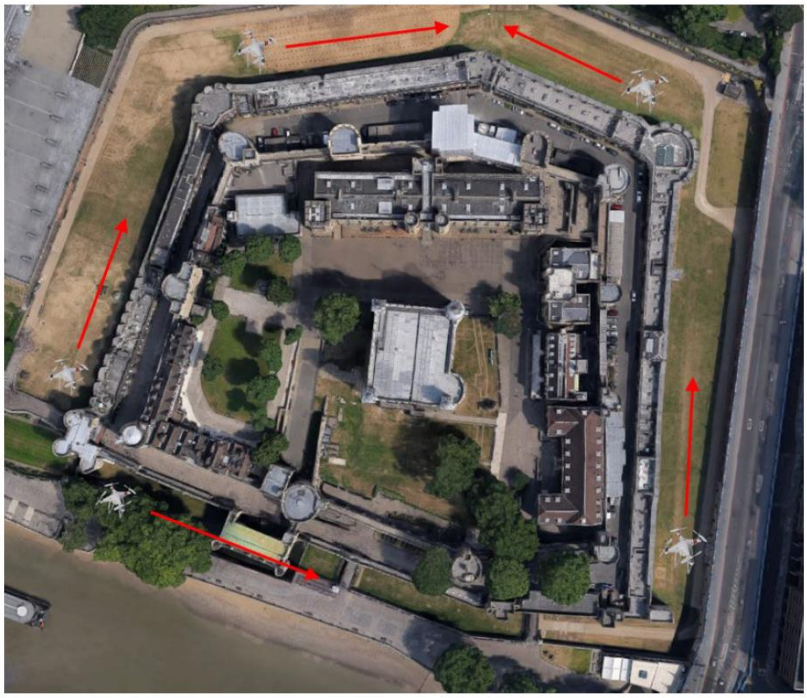

Fig. 9. A perimeter surveillance system using multiple UAVs

Fig. 9 shows a perimeter surveillance system using multiple UAVs. It comprises of UAVs patrolling along the predefined perimeter and are capable of communicating among them, i.e., coordinating flying pattern and signifying alerts. The system can be self-sustaining through energy harvesting technology [31], [32] where UAV battery can be replenished without human intervention. We investigate the impact on packet delivery rate, average packet delay, average system throughput, and average hop count when such system exhibits changes in configurations.

The major contributions of our work can be recapitulated as follows:

• We present a perimeter surveillance system comprising of multiple UAVs. These UAVs perform a surveillance task along the predefined perimeter and are capable of communicating.

• We demonstrate how number of UAVs and their mobility profile have an effect on key network metrics as well as determine the condition of optimality.

RELATED WORK

In [6], a cooperative perimeter surveillance problem is introduced and the authors offer a decentralized solution that accounts for perimeter growth and changing of team members. A precise performance is achieved through small communication range, thanks to a known communication topology and identifying/sharing the critical coordination information. The decentralized approach not only offers scalability but also system robustness. The approach yields finite-time convergence and steady-state optimality.

A surveillance model for multi domain IoT environment, which is supported by reinforced barriers with collision-avoidance using heterogeneous smart UAVs is proposed in [34]. The authors define a problem whose goal is minimizing the maximum movement of UAVs on condition that collision-avoidance among UAVs is guaranteed. The problem is formulated using Integer Linear Programming (ILP) and a novel approach is proposed to solve the problem. Performance analysis of the proposed scheme is evaluated through extensive simulations with various scenarios.

The simulations and implementation of perimeter surveil- lance under communication constraints, performed by teams of UAVs using a Bluetooth communication framework, is presented in [35]. These UAVs perform their task collaboratively and hence efficient communication among them is crucial to ensure proper system operation. Additionally, weight and energy consumption of the payload are maintained at minimum, particularly in micro-UAVs. A coordination variables strategy is implemented to perform the perimeter division.

In [36], the effect of sensor mobility on network communications in a smart farm platform is presented. The platform comprises of sensor-equipped UAVs and are capable of ex- changing data. The experiment is conducted through a custom simulation and the authors demonstrate the influence of sensor mobility on important network metrics. Lastly, the optimal UAV mobility profile is also presented.

SIMULATION PARAMETERS

In this section, the simulation parameters and scenario are discussed in details. We investigate the effect of number of UAVs and their mobility profiles on key network metrics using discrete event simulator, ns-2 [37]. The simulation parameters are as follows:

1) Perimeter surveillance UAV profile: The UAV Perimeter surveillance profile comprises of both direction of UAV movement and UAV speed. For perimeter surveillance, UAVs travel along the boundary of the restricted area. We deploy various numbers of UAVs, ranging from 10 to 90, to observe the network behavior on a different number of UAVs in deployment. Each UAV mobility pattern is generate randomly, that is, each UAV heads toward the random point along the predefined perimeter and remains stationary for certain period, known as pause time, then proceeds to next point randomly. In order to minimize any possible implication on key network metrics measurement, the pause time is set to zero.

In addition, the operational speed of UAV has a critical impact on key network metrics. In sparse UAV deployment, operating UAV at low speed may result in limited connectivity in communication among UAVs and increasing response time due to slower anomaly detection. On the other hand, high UAV mobility rate can cause disruption in network communication under dense UAV deployment. For this purpose, the UAV speed is varied from 0 m/s to 25 m/s with 5 m/s increment.

2) UAV radio profile: For wireless sensors, radio transceiver plays a key role in energy consumption and the radio transceiver installed in the UAV is no exception. It is advisable to employ low-power transceiver when applicable. The IEEE 802.15.4 radio standard is tailored for low data rate communication with an emphasis on low-power consumption. However, the major drawback of IEEE 802.15.4 is the communication range which is quite limited and deemed unsuitable for highly dynamic devices. Moreover, the power consumed by the radio transceiver is negligible when compared to the power consumption of UAV motors. Consequently, we employ the venerable IEEE 802.11 radio standard operating in Ad Hoc mode. Both carrier sense radius and packet reception radius are set to 250 m. We also employ two-ray ground reflection model for the radio propagation model in this work. The two-ray ground reflection model takes into an account both the direct path and a ground reflection path. It is shown that this model yields higher accuracy at a long distance than the free space model [39].

3) Perimeter under surveillance: Without the loss of generality, the restricted area is 1500 x 1500 m^2 grid and UAVs are deployed uniformly at random along the boundary of the restricted area. While it is possible that UAVs are densely populated in particular spots at the beginning of the simulation, it has negligible effect on the simulation validity since UAVs will disperse shortly after the simulation starts.

4) Routing protocol and traffic profile: In multi-hop net- work, the network coverage area is larger than radio range of single a node. As a result, nodes have to act as relays to facilitate packet delivery. Hence, the routing protocol is a critical part in packet delivery. The Ad hoc On-Demand Distance Vector (AODV) [38] is adopted in this work. AODV is a routing protocol specifically tailored for mobile ad hoc networks. The route discovery is performed on demand and can accommodate both unicast and multicast routing. The UAV communication is modeled by Constant Bit Rate (CBR) traffic with the packet generation rate of 10 packets/s. The packet size is 512 bytes and the maximum CBR connection is limited to 30 connections.

SIMULATION RESULTS

We thoroughly investigate the impact of numbers of UAVs and their speed on key network metrics. It is crucial that the network performance is evaluated through multiple network metrics since an individual metric only represents its own perspective. In other words, one has to evaluate as many network metrics at his disposal in order to efficiently capture the network characteristics. In this work, the simulation lasts 250 seconds and each data sample is derived through averaging value of 10 iterations. Consequently, outliers are eliminated and valid simulation results can be obtained.

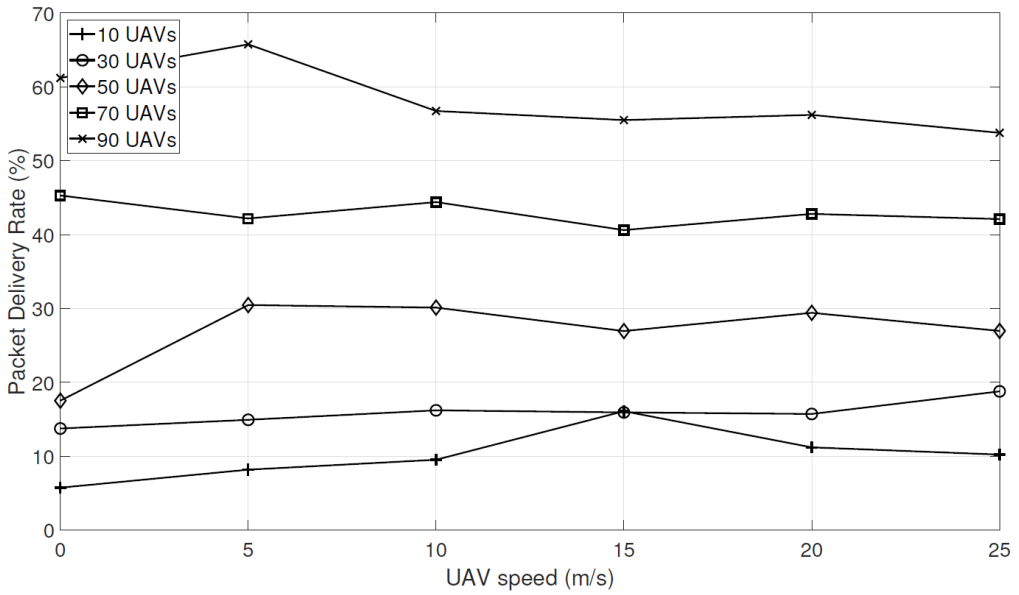

Fig. 10. Effect of UAV speed on packet delivery rate

A. Packet delivery rate

The packet delivery rate defines as the percentage of total packets successfully received to the total packets sent. Fig. 10 shows the effect of UAV speed on packet delivery rate for different numbers of UAVs deployed. It is obvious that, regardless of the number of UAVs deployed, the UAV speed has marginal influence on packet delivery rate as it is mostly constant throughout. However, numbers of UAVs have a direct impact on packet delivery rate, that is, the packet delivery rate increases with the growing numbers of UAVs. It is safe to say that the packet delivery rate is directly proportional to numbers of UAVs deployed. This implies that the UAV speed can be kept at minimum, with negligible effect on packet delivery rate, in order to prolong the UAV flight time.

B. Average packet delay

The average packet delay is a measure of average time required to transmit a packet across a network. It takes both queuing delay and transmission delay into an account. For time-sensitive application, the average packet delay is a crucial metric since certain level of average packet delay can adversely affect some types of applications, i.e., real-time communications. The effect of the UAV speed on average packet delay is shown in Fig. 11. Surprisingly, the average packet delay is marginally susceptible to UAV speed variation. Nevertheless, it is clear that the average packet delay increases as numbers of UAVs increase. In fact, the average packet delay plot exhibits a similar pattern of packet delivery rate plot depicted earlier. It implies that a dense UAV deployment contributes to an increase in average packet delay. That is to say, the larger the number of UAVs deployed, the higher the level of network congestion hence packets end up in a queue, waiting to be transmitted.

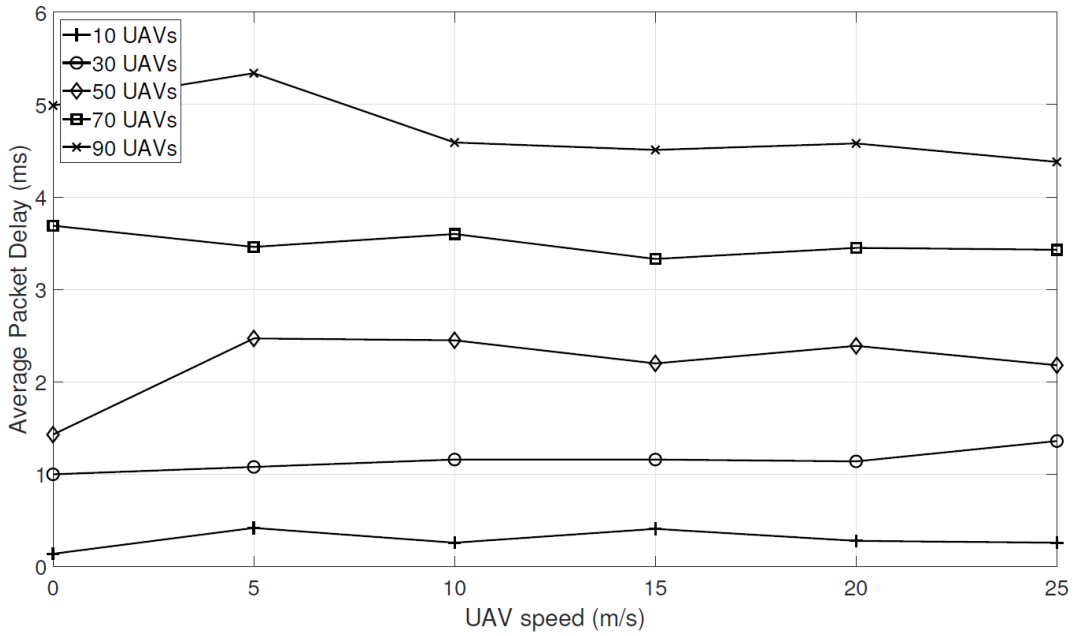

Fig. 11. Effect of UAV speed on average packet delay

C. Average network throughput

The average network throughput defines as the average amount of data successfully received at the destination over a period of time. Note that there is a subtle difference between the packet delivery rate and the average network throughput. For instance, in a congested network, packets may be put in a transmission queue and never be transmitted. These packets will not contribute to the average network throughput because they have never reached the destination. On the contrary, a densely deployed network may benefit from a higher level of connectivity which enables efficient routing. Consequently, packets can be routed to the destination and a higher packet delivery rate is expected. This implies that one can have a system with very high packet delivery rate while its average network throughput hits rock bottom. Fig. 12 shows the effect of UAV speed on average network throughput. It is obvious that the system can benefit from operating UAVs at higher speed. Regardless of the number of UAVs deployed, the average network throughput monotonically increases with increasing UAV speed. However, the system with 10 UAVs deployed offers the highest average network throughput while the least average network throughput occurs in the system with 90UAVs deployed. For the system with 30 UAVs, 50 UAVs, and 70 UAVs, there exists insignificant difference in average network throughput and the different in numbers of UAVs deployed can be considered unimportant. This is in contrast to the packet delivery rate plot shown earlier and it can be presumed that this phenomenon is a result of densely deployed network.

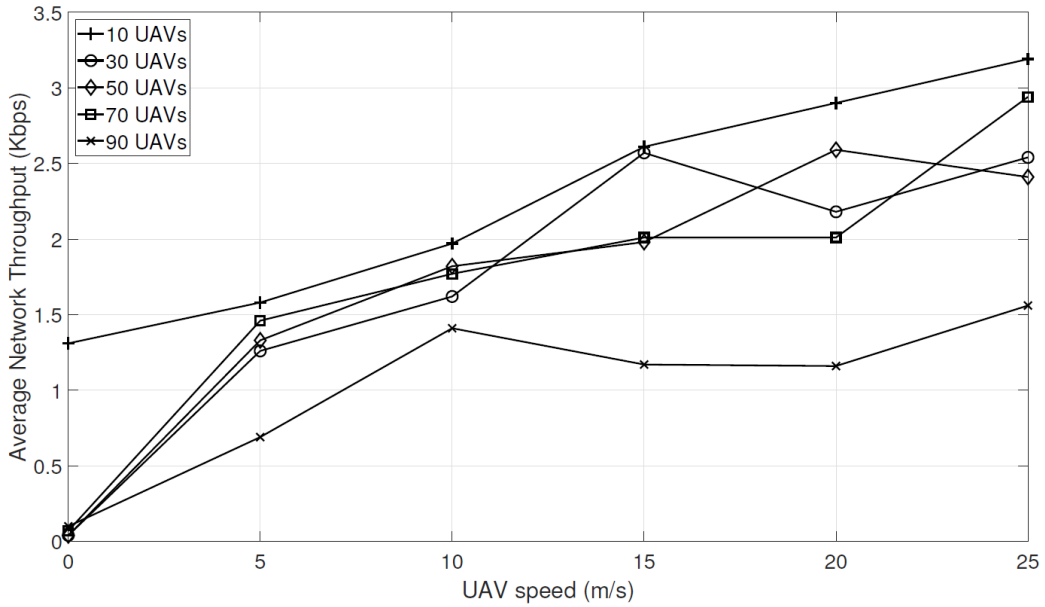

Fig. 12. Effect of UAV speed on average network throughput

D. Average hop count

The average hop count reflects the degree of separation between source and destination. It defines as the number of intermediate network devices through which data must pass between source and destination. Fig. 13 illustrates the effect of UAV speed on average hop count. It is shown that the UAV speed has an influence on the average hop count especially when the number of UAVs is large, i.e., 50 UAVs or more. Furthermore, the average hop count increases with the number of UAVs increases. Note that the larger average hop count implies the more intermediate UAVs required to relay packet to the destined UAV. As a result, the packet accumulates larger queuing and processing delay. This is coincide with earlier findings.

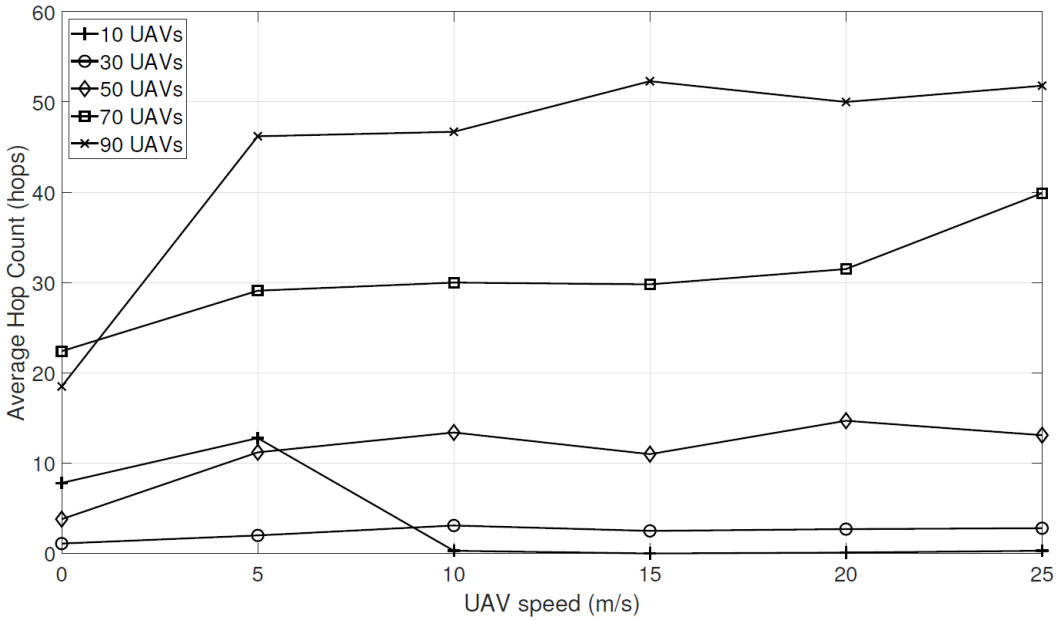

Fig. 13. Effect of UAV speed on average hop count

CONCLUSIONS

We present the performance analysis of perimeter surveil- lance system comprising of multiple UAVs. These UAVs perform a surveillance task along the predefined perimeter and are capable of communicating. We demonstrate how number of UAVs and their mobility profile have an effect on key network metrics as well as determine the condition of optimality. Simulation results reveal that the UAV speed and the number of UAVs deployed have an influence on the average network throughput and the average network hop count. Both the packet delivery rate and the average packet delay are not susceptible to the UAV speed variation. Lastly, both the packet delivery rate and the average packet delay are directly proportional to the number of UAVs deployed.

Chapter 4. Detection and Localization of Unauthorized Unmanned Aerial Vehicle Operator using Unmanned Aerial Vehicle

Unmanned Aerial Vehicle (UAV) has gained popularity recently, in both commercial and leisure purposes. Thanks to the technological advancement and dramatically lower manufacturing cost, UAV becomes very affordable and widely accessible to the public. This poses several critical security issues, ranging from merely loss of privacy to life-threatening incident. Consequently, it is crucial to be able to detect and locate an unauthorized UAV operator in case of critical security breach occurs. In this chapter, we propose a system to detect and locate an unauthorized UAV operator using UAV. This UAV, equipped with a directional antenna, performs unauthorized UAV operator detection and localization tasks by traveling along the predefined path and narrows down the potential area as time passes.

UAV is one of the emerging technologies that has seen a major growth in the recent years. It has secured its places in several applications, ranging from civil to military uses. Civil use of UAV includes aerial photography, filmmaking, and agricultural monitoring while aerial surveillance and reconnaissance are examples of UAV applications for military use. One of the key features that makes UAV attractive is the ability to provide the aerial perspective and its freedom of movement without the need of infrastructure, i.e., roads and electrical facilities. Consequently, it is undeniable that UAV will soon become the workhorse in aerial related applications. In fact, it already replaces human-operated aircraft in aerial photography business since it not only provides a significantly lower in operating cost but also eliminates the human risk involved in operating an actual aircraft. It is globally estimated the market worth of $4.1 billion in commercial UAVs in 2017 and it is expected over 7 million UAVs registration in the United States by 2020 [40].

Since UAV is easily accessible and affordable, several issues involving illegal uses of UAV are increasing rapidly. Breaching of privacy through unauthorized UAV operation is commonly found in most cases. The charge of unauthorized UAV operation spans from misdemeanor to felony offense, depending on the territory the offense occurs [ncsl.org]. However, in an extreme case, i.e., using UAV for malicious purposes, it is not only required that the hostile UAV be rendered harmless but also the need to identify the operator of the hostile UAV. Rendering UAV harmless can be achieved through the use of UAV jammer. UAV jammer interferes the communication between UAV and its operator. As a result, the targeted UAV either drops to the ground or returns to its initial location. Note that the UAV operator is fully aware of the jamming and mostly flees from the scene. Hence, the UAV jammer can prevent malicious UAV from accomplishing its task but cannot locate and apprehend the hostile UAV operator.

Fig. 14. Detection and localization with UAV at high service ceiling.

There exist several methods to detect and locate an unauthorized signal source emitter, i.e., unauthorized UAV operator. Mobile signal tracker and existing communication infrastructures are good examples. However, these facilities are ground-based and have limitations in terms of difficulties in equipment deploying as well as the speed of detection and localization the unauthorized transmitting signal source. In fact, it is almost impossible to employ the existing communication infrastructures for unauthorized UAV detection and localization since they are designed for different purposes from the beginning.

Fig. 14 shows our proposed system for detection and localization of an unauthorized UAV operator using UAV. Initially, the UAV starts of at a higher service ceiling in order to cover a large searching area. However, the location of an unauthorized UAV operator cannot be pinpointed but rather a rough estimate. To narrow down the potential area that an unauthorized UAV operator resides, the UAV identify the potential sector through received signal strength measurement and moves toward the potential sector. The UAV then lower the service ceiling in order to locate an unauthorized UAV operator in fine-grained manner as depicted in Figure 15. Note that the circle signifies the detection range of the UAV.

Fig. 15. Detection and localization with UAV at low service ceiling.

The major contributions of our work can be summarized as follows:

- We propose a system to detect and locate an unauthorized UAV operator using UAV. This UAV, equipped with a directional antenna, performs unauthorized UAV operator detection and localization tasks by traveling along the predefined path and narrows down the potential area as time passes.
- We demonstrate, through simulation studies, how UAV service ceiling, UAV speed, and antenna directivity have an effect on the key performance metrics of the system, together with, the optimal operating condition.

Related Work

Detection and localization of an unauthorized signal source is not new but has been a topic of discussion for a long time. Several techniques have been proposed and received substantial attention from research community. Angle of Arrival (AoA) is a technique that determines the location of signal source by angle estimation between the direction of an incident wave and a certain reference direction [41]-[43]. However, the drawback of AoA is that it is severely affected by non line-of-sight condition. Moreover, the accuracy of AoA is limited by the directivity of the antenna and channel fading, and multipath reflection. The concept of Time of Arrival (TOA) is discussed in [44]-

[46]. In ToA method, the propagation time between the transmitter and the receiver is estimated by calculating the time difference between them, that is, transmitter's time and receiver's time. In [47]-[49], Time Difference of Arrival (TDoA), the localization method based on the measurement of the difference in the arrival times of the signal from the source at multiple nodes, is revisited. The advantage of TDoA is that it is marginally susceptible to multipath reflection and non line-of-sight condition. Lastly, the Received Signal Strength Indication (RSSI) is present in [50]-[54]. In this method, the strength of the received signal at the receiver is translated to the distance between the transmitter and the receiver using Friis transmission equation [55]. However, RSSI is susceptible to multipath reflection and channel fading. A multiplication distance correction factor is introduced in [56] to counteract estimation error and hence drastically improve the accuracy.

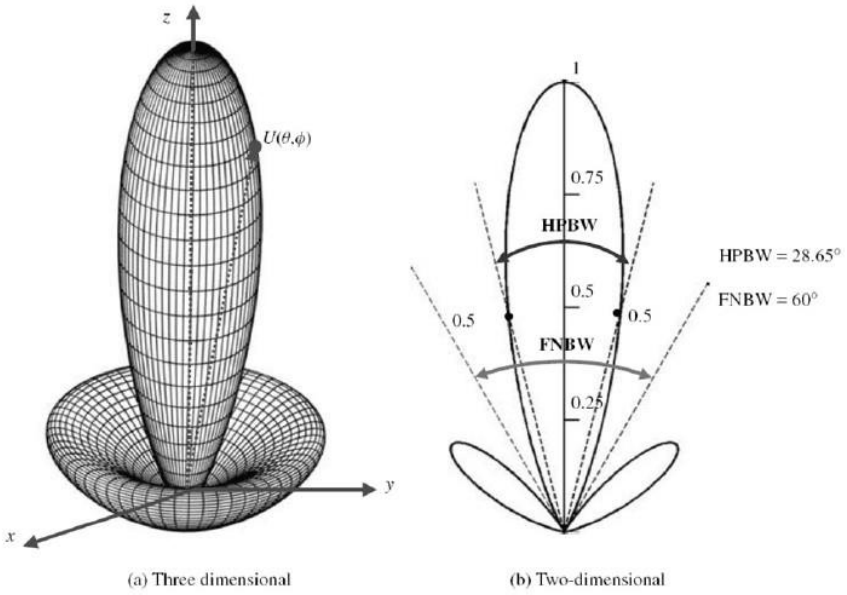

Fig. 16. Radiation pattern of the directional antenna

The Proposed System

One of the key elements of the proposed system that enables an unauthorized UAV operator detection and localization is the directional antenna. The directional antenna is a good candidate for directional finding as it provides a high gain and hence a high sensitivity. However, the sensitivity of the directional antenna can be different according to the design. For example, the directional antenna with narrower beamwidth offers the higher sensitivity compared to the directional antenna with wider beamwidth. On the other hand, the directional antenna with wider beamwidth provides the larger coverage area compared to the directional antenna with narrower beamwidth.

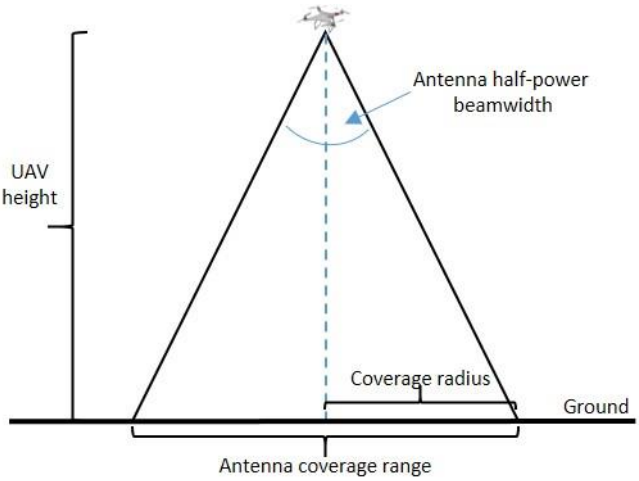

Fig. 17. Coverage area of the UAV equipped with directional antenna

The radiation and reception patterns of the directional antennas are characterized by their beamwidth. The Half Power Beamwidth (HPBW) is the angular separation in which the magnitude of the radiation pattern decreases by 3 dB from the peak of the main beam. Fig. 16 illustrates the radiation pattern of the directional antenna and its HPBW. It is obvious that the larger the HPBW, the larger the coverage area of signal detection. Consequently, if the directional antenna is installed on the UAV in such the way that the directional antenna's main lobe is perpendicular to the ground, that is, the UAV is equipped with the directional antenna underneath and pointing downwards. The coverage area of this directional antenna equipped UAV is shown in Fig. 17. The relationship between UAV service ceiling (UAV height), coverage radius, and HPBW is shown in Equation 1.

$$coverage\ radius\ = \tan\left(\frac{HPBW}{2}\right) \times uav\ height \tag{1}$$

It is shown in Equation 1. that the coverage radius is directly proportion to UAV height and HPBW. In other words, the coverage radius can be increased by increasing UAV height and HPBW. The coverage area, the area that the UAV can detect the presence of an unauthorized UAV operator, can be derived in Equation 2.

$$coverage\ area\ =\ \pi \times coverage\ radius^2 \tag{2}$$

A. Detection of an unauthorized UAV operator

The coverage area shown in Equation 2. is the area that the UAV can detect the presence of an unauthorized UAV operator. In order to provide larger coverage area, the UAV performs the flying pattern as depicted in Fig. 18.

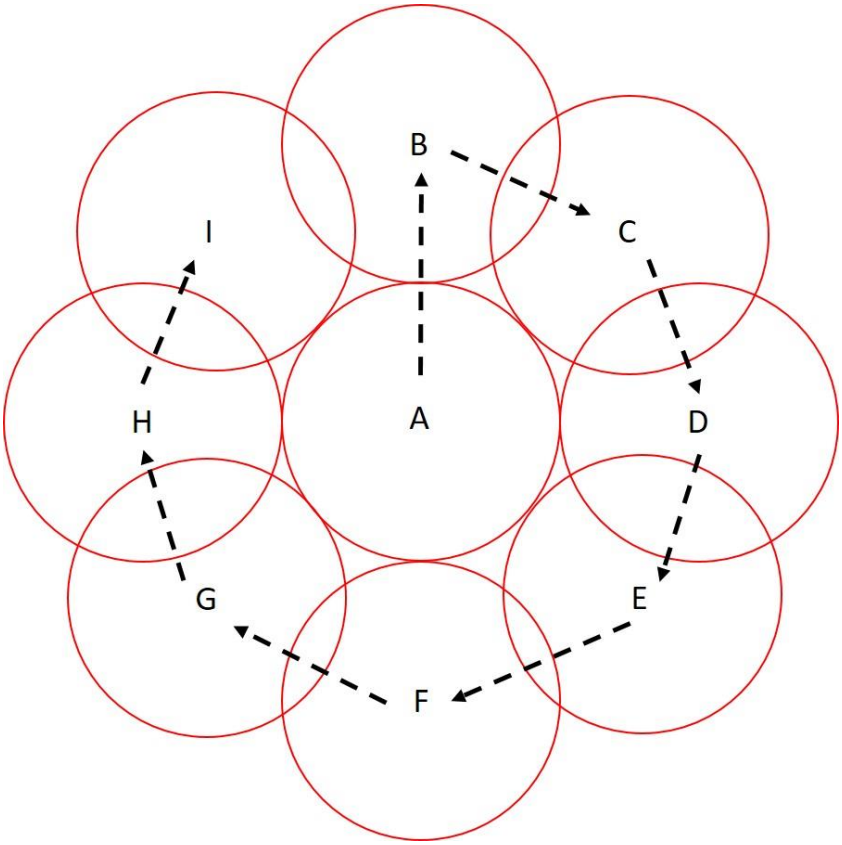

Fig. 18. UAV flying pattern for detection and localization of an unauthorized UAV operator.

The UAV begins detection of an unauthorized UAV operator at the sector A. Again, the circle signifies the detection range of the UAV, that is, the UAV is able to detect the presence of an unauthorized UAV operator if and only if it resides within the circle. Once it accomplishes detection of an unauthorized UAV operator at the sector A, it then proceeds to the sector B and performs detection of an unauthorized UAV operator. Upon completing the detection of an unauthorized UAV operator in sector B, it moves towards the sector C and performs detection of an unauthorized UAV operator. The process carries on in this fashion, a clockwise progression, until it finally reaches the destined sector I. Upon finishing the round of detection, the coverage area of that round can be calculated in Equation 3.

$$coverage\ area_{round} = \pi \times (3 \times coverage\ radius)^2 \tag{3}$$

The signal power perceived by the UAV signifies the distance between the sensing UAV and an unauthorized UAV operator. In other word, the stronger the signal received by the sensing UAV, the closer the UAV to an unauthorized UAV operator. The Friis transmission equation describe the relationship of received power ($P_{receiver}$), transmitted power ($P_{transmitter}$), and distance (d) between transmitter and receiver as shown in Equation 4.

$$P_{receiver} = P_{transmitter} G_t G_r \left(\frac{c}{4\pi f d}\right)^2 \quad (4)$$

where G_t is the antenna gain of transmitter, G_r is the antenna gain of receiver, and are antenna gains, and $\left(\frac{c}{f}\right)$ is the wavelength of the transmitted signal. It is clear that the received signal strength, diminishes with the square of the distance.

As mentioned previously, the circle in Figure 5 signifies the detection range of the UAV. This implies that the maximum degree of separation, that enables the detection of an unauthorized UAV operator, between the sensing UAV and an unauthorized UAV operator lies on the perimeter of the circle. This the maximum degree of separation is simply the hypotenuse in Fig. 4. Consequently, it can be calculated as in Equation 5.

$$distance_{max} = \frac{uav\ height}{\cos(\frac{HPBW}{2})} \quad (5)$$

The lowest level of received signal that the UAV can detect the presence of an unauthorized UAV operator is then derived in Equation 6.

$$P_{receiver\_min} = P_{transmitter} G_t G_r \left(\frac{c}{4\pi f distance_{max}}\right)^2 \quad (6)$$

The signal power received by the UAV in each sector is recorded and will be used in the next section, Localization of an unauthorized UAV operator.

B. Localization of an unauthorized UAV operator

After completion of the detection of an unauthorized UAV operator in each sector, the next phase is to determine the potential sector that an unauthorized UAV operator most likely resides. The signal power received by the UAV in each sector are compared. As mentioned earlier, the stronger the signal received by the sensing UAV, the closer the UAV to an unauthorized UAV operator. Hence, the potential sector that an unauthorized UAV operator most likely resides is the sector that has the highest level of received signal.

Given that the coverage radius of the UAV is *r*, and the centroid of sector A is located at coordinate(X_A, Y_A, Z_A), the centroid of each sector depicted in Fig. 18. can be found as follows:

$$Centroid\ A: (X_A, Y_A, Z_A) \quad (7)$$

$$Centroid\ B: (X_B, Y_B, Z_B) = (X_A, Y_A + 2r, Z_A) \quad (8)$$

$$Centroid\ C: (X_C, Y_C, Z_C) = \left(X_A + \sqrt{2}r, Y_A + \sqrt{2}r, Z_A\right) \quad (9)$$

$$Centroid\ D: (X_D, Y_D, Z_D) = (X_A + 2r, Y_A, Z_A) \quad (10)$$

$$Centroid\ E: (X_E, Y_E, Z_E) = \left(X_A + \sqrt{2}r, Y_A - \sqrt{2}r, Z_A\right) \quad (11)$$

$$Centroid\ F: (X_F, Y_F, Z_F) = (X_A, Y_A + 2r, Z_A) \quad (12)$$

$$Centroid\ G: (X_G, Y_G, Z_G) = \left(X_A - \sqrt{2}r, Y_A - \sqrt{2}r, Z_A\right) \quad (13)$$

$$Centroid\ H: (X_H, Y_H, Z_H) = (X_A - 2r, Y_A, Z_A) \quad (14)$$

$$Centroid\ I: (X_I, Y_I, Z_I) = \left(X_A - \sqrt{2}r, Y_A + \sqrt{2}r, Z_A\right) \quad (15)$$

Once the sector with the highest level of received signal is determined, it is the most likely that an unauthorized UAV operator lies within the sector. The centroid of that corresponding sector is used as the initial sector for the detection of an unauthorized UAV operator in the next round. In other words, the centroid of that corresponding sector becomes the centroid of sector A in the next round of detection of an unauthorized UAV operator.

C. UAV repositioning

Once the potential sector is determined in the previous section, the UAV needs to proceed to the new coordinate and perform the next round of detection of an unauthorized UAV operator. However, only relocating the centroid in X and Y axis will not contribute to the better resolution in detection and localization of an unauthorized UAV operator. It is imperative that the service ceiling of the UAV be lowered in order to capture the signal with higher resolution and hence the more precise localization of an unauthorized UAV operator. We introduce the UAV descending scale, defined as the scaling factor that UAV exhibits in lowering its service ceiling. For example, if the service ceiling of the UAV is at 1000 meters in the first detection round, with the UAV descending scale of 2, the next service ceiling of the UAV in the next round will be 500 meters. UAV descending scale has to be chosen carefully, too large UAV descending scale can lower time to identify the location of an unauthorized UAV operator while too small UAV descending scale can significantly increase time to identify the location of an unauthorized UAV operator and render the system unresponsive. Nevertheless, there is a flip side to the coin. , too large UAV descending scale can result in higher error detection rate of an unauthorized UAV operator while small UAV descending scale can drastically improve detection accuracy of the system.

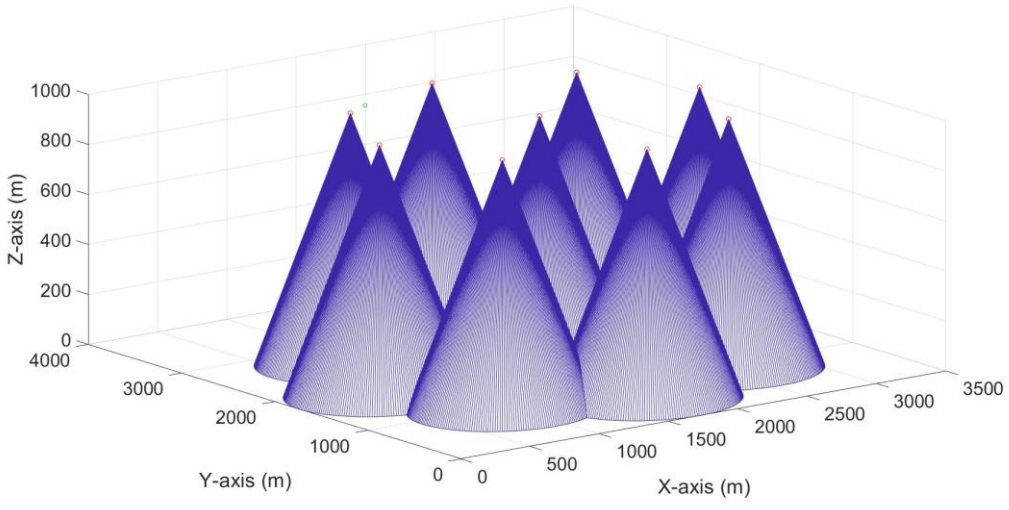

Fig. 19. Coverage area of the proposed system at UAV service ceiling of 1000 meters.

D. System operation example

In order to better understand how the system progresses through different stages of detection and localization of an unauthorized UAV operator. We illustrates the system progression starting at the UAV service ceiling of 1000 meters. Fig. 19 shows the coverage area of the proposed system at UAV service ceiling of 1000 meters. The coverage area of each sector is represented by the cone for each corresponding sector. Consequently, there are 9 cones which correspond to 9 sectors, that is, sector A to sector I. Moreover, the peak of each cone refers to the location that the UAV hovers while performing detection of an unauthorized UAV operator. The UAV starts at sector A then proceeds to sector B, sector C, and so on. Finally, it completes the round of detection of an unauthorized UAV operator at sector I.

Another perspective of the coverage area of the proposed system at UAV service ceiling of 1000 meters can be seen in Fig. 20. Here, the top view of the coverage area of each sector, together with the location of an unauthorized UAV operator in sector I, is presented. It is obvious that each sector has its own coverage and contributes to the larger coverage as a whole.

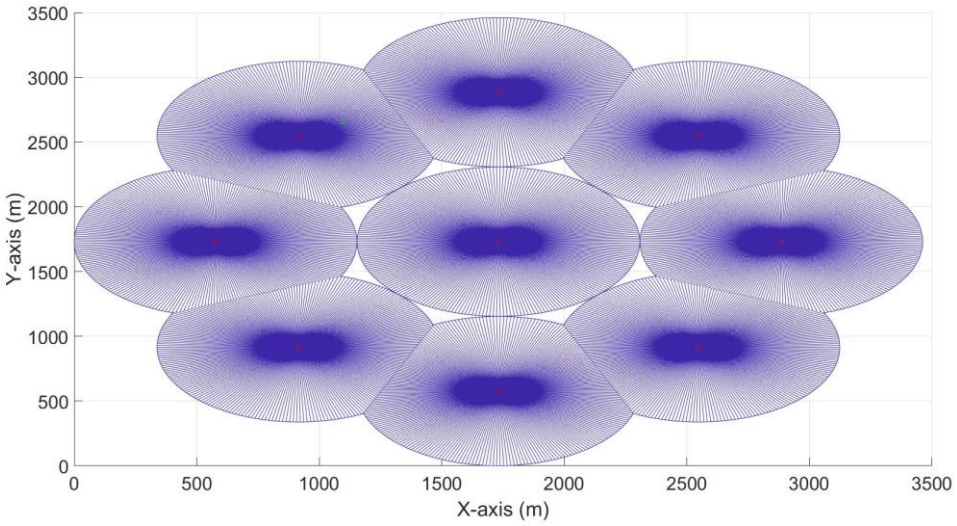

Fig. 20. Coverage area of the proposed system at UAV service ceiling of 1000 meters (top view).

The two dimensional representation of the coverage area of the proposed system can also be depicted in Fig. 21. Here, the side view of the coverage area of the proposed system at UAV service ceiling of 1000 meters is shown and it provides a clear representation of the coverage beam of each sector.

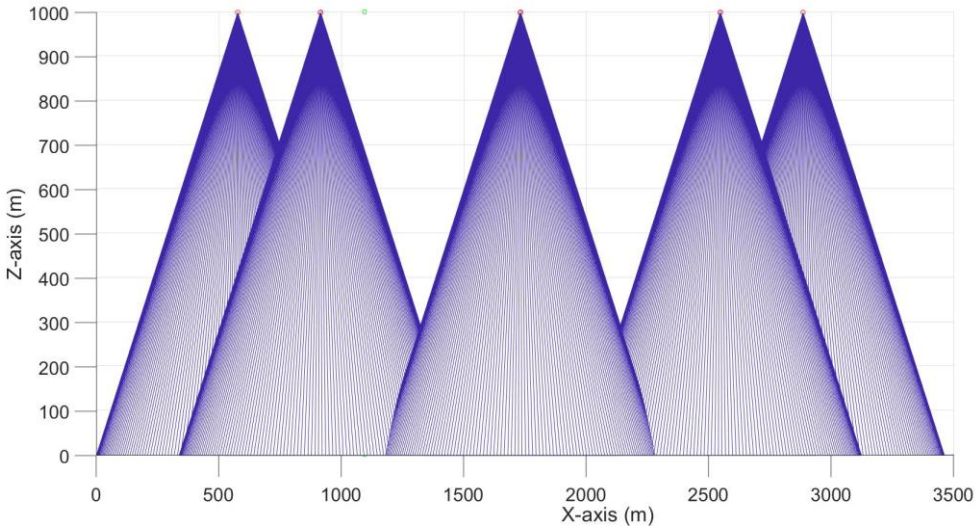

Fig. 21. Coverage area of the proposed system at UAV service ceiling of 1000 meters (side view).

Once the UAV completes the round of detection, the system performs the localization by selecting the potential sector to be the centroid of the next detection round. In this case, since the location of an unauthorized UAV operator is in sector I, the received signal power of sector I is the highest among all sectors. Hence, the centroid of sector I is chosen to be centroid of sector A in the next detection round. The localization process is completed at this point.

The next stage of the system is to reposition the UAV, that is, lowering its service ceiling to better capture the signal resolution. In Fig. 22, the UAV descending scale used is 2.25 and the new UAV service ceiling is 444 meters. The centroid of sector I in the previous detection round becomes the centroid of sector A for the present detection round. The UAV then reiterates through sector A to sector I, like the previous detection round, and records its findings in each sector for localization process.

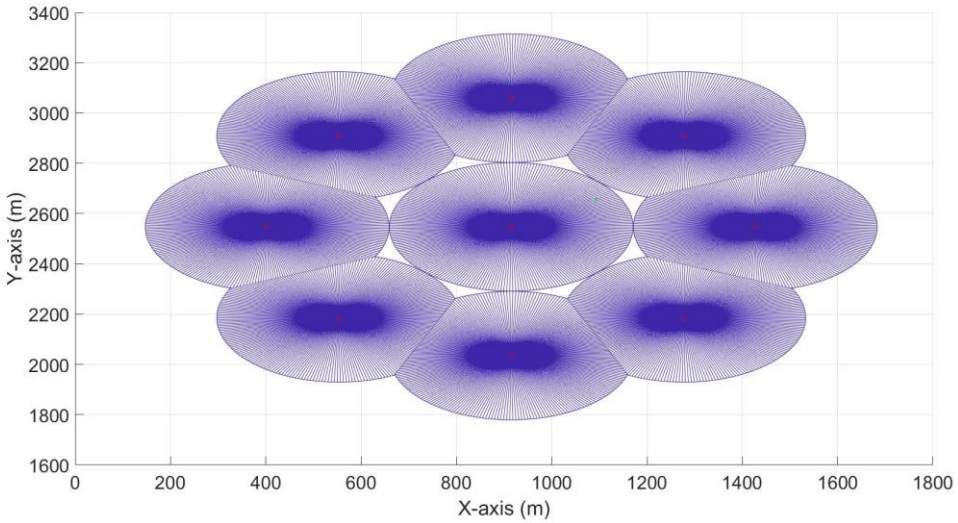

Fig. 22. Coverage area of the proposed system at UAV service ceiling of 444 meters (top view).

The system proceeds through rounds of detection repetitively and finally halts when the predefined UAV service ceiling is achieved, 39 meters in this case. The final round of detection and localization of an unauthorized UAV operator terminates at this point and the corresponding top view of the proposed system can be seen in Fig. 23.

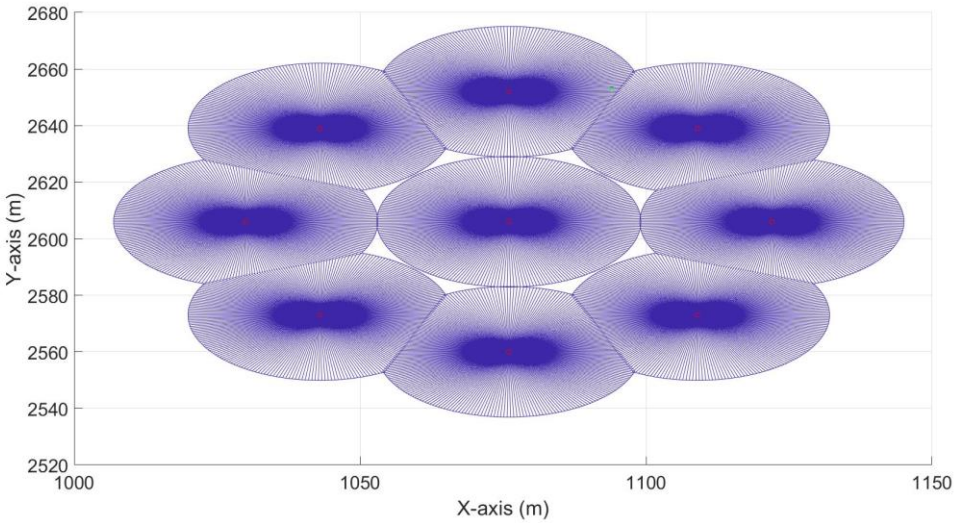

Fig. 23. Coverage area of the proposed system at UAV service ceiling of 39 meters (top view).

Simulation Results

In this section, we thoroughly evaluate our proposed system using our custom simulator, developed in MATLAB. We investigate the effect of UAV service ceiling, UAV speed, and antenna directivity on the key performance metrics of the system. Unless specifically stated, the simulation time is limited to 1,500 seconds and an unauthorized UAV operator is deployed uniformly at random in 2,500 m^2 circular area. The number of iterations for each complete process of detection and localization of an unauthorized UAV operator is set to 50 and the result is obtained through the average value of 50 iterations. This is to prevent outliers from influencing the simulation results.

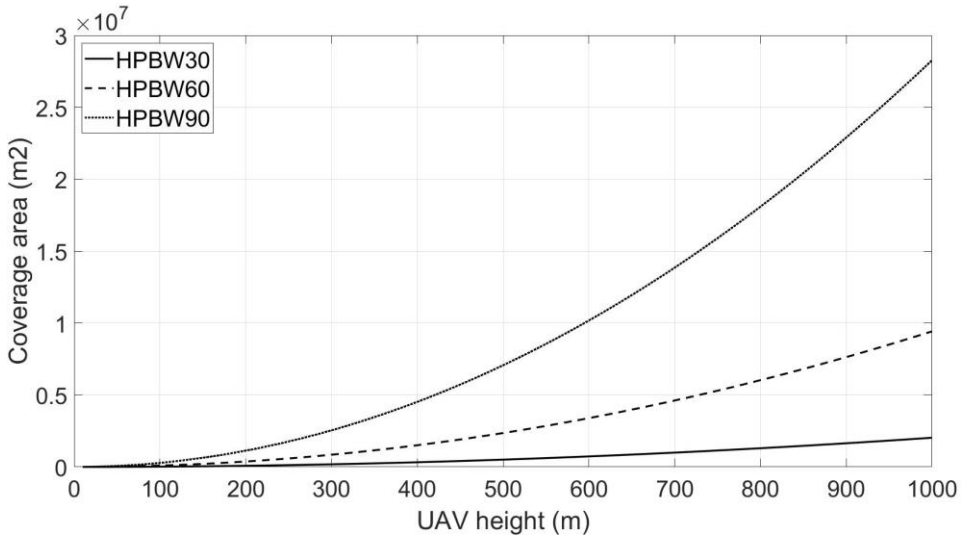

Fig. 24. Effect of UAV height on coverage area of the proposed system for various values of HPBW.

A. Coverage area

The coverage area is one of key performance metrics since it has a major effect on system efficiency, that is, system efficiency is directly proportion to the coverage area. In other words, the larger the coverage area, the faster the detection and localization of an unauthorized UAV operator and hence the higher the system efficiency. Fig. 24 depicts the effect of UAV height on coverage area of the proposed system for various values of HPBW. It is clear that, for the HPBW value of 60 and 90 degrees, the coverage area exhibits a nonlinear increase with increasing UAV height. Consequently, it is preferable to initiate the UAV service ceiling at higher altitude in order to cover a larger area. On the other hand, the UAV equipped with antenna with HPBW of 60 degrees sees negligible benefit on this matter.

The benefit of the proposed system is clearly seen in Fig. 24. For example, if we initiate the UAV service ceiling at 1,000 meters with HPBW of 60 degrees, the coverage area of the system can be as large as 9 km^2. In addition to large coverage area provided by the proposed system, it also offers a fine-grained localization of an unauthorized UAV operator. Fig. 25 illustrates the fine-grained localization of an unauthorized UAV operator offered by the proposed system. It is obvious that the proposed system provides an almost pinpoint location of an unauthorized UAV operator. For instance, if the UAV service ceiling is lowered to 60 meters with HPBW of 60 degrees, the identifiable area of an unauthorized UAV operator can be as small as 400 m^2.

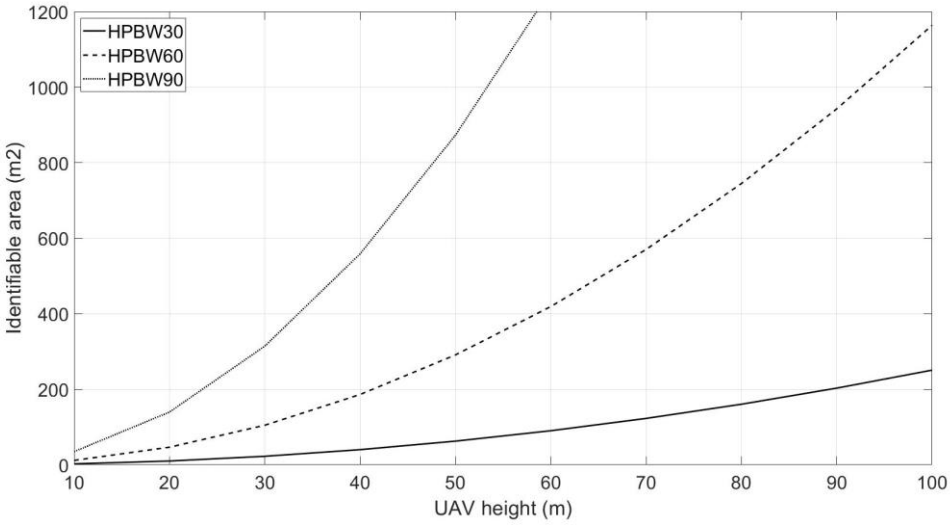

Fig. 25. Fine-grained localization of an unauthorized UAV operator

B. Time to identify an unauthorized UAV operator

Time to identify an unauthorized UAV operator is defined as the time the system takes, from deploying the UAV until the location of an unauthorized UAV operator is determined. It is undeniable that this is the most important key performance metric of the system and it is also preferable to have the lowest value possible. The system that offers low time to identify signal source implies that the location of an unauthorized UAV can be determined promptly and further security measures can be carried out in timely manner. Moreover, since the UAV spends less time in the air, the energy consumption per detection and localization cycle is lower. As a result, the duty cycle of the system is higher and hence improving the system availability. Fig. 26 depicts an effect of UAV descending scale on time to identify an unauthorized UAV operator and its corresponding percentage of identification error. As mentioned previously, UAV descending scale has to be carefully chosen as it can drastically affect the system performance. It is obvious that choosing an arbitrary value of UAV descending scale is not a good idea. In this case, the UAV with HPBW of 60 degrees begins the detection of an unauthorized UAV operator at service ceiling of 1,000 meters. The UAV descending scale is varied from 1.25 to 3.00 with 0.25 step size. It is clear the time to identify an unauthorized UAV operator is not linearly dependent with the UAV descending scale, that is, the time to identify an unauthorized UAV operator exponentially increases once the UAV descending scale is less than 2.0 while it exhibits linear increase with decreasing value of UAV descending scale elsewhere.

It is straight forward to choose the largest value of UAV descending scale if the identification error is omitted. However, it is crucial to investigate as many aspects of the system. Here, the percentage of identification error, defined as the percentage that the system fails to determine the location of an unauthorized UAV operator, is examined for different values of UAV descending scale. It is interesting that it does not exhibits either linear or exponential behavior with UAV descending scale. On the contrary, the percentage of identification error decreases with decreasing value of UAV descending scale, remains constant shortly, and then increases with decreasing value of UAV descending scale. In other words, the percentage of identification error

yields a local minima. Fig. 26 provides an invaluable information about the optimal choice of UAV descending scale, that is, the value of UAV descending scale in which the system yields the optimal performance. It is obvious that the UAV descending scale of 2.35 is the optimal choice since it is where the time to identify signal source and percentage of identification error cross.

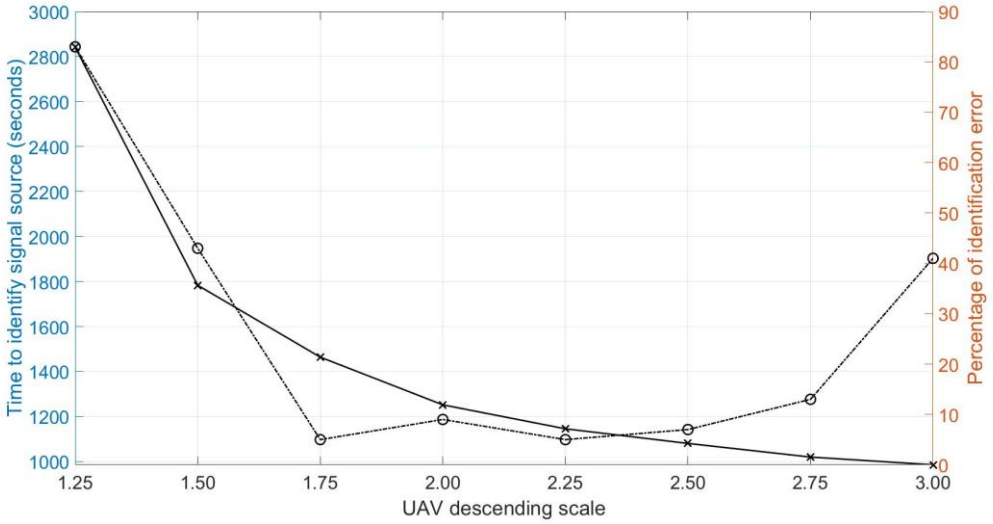

Fig. 26. Effect of UAV descending scale on time to identify an unauthorized UAV operator and its corresponding percentage of identification error.

The effect of UAV speed on time to identify an unauthorized UAV operator is shown in Fig. 27. The UAV speed is varied from 1.25 to 3.00 with 0.25 step size and shown on X-axis while Y-axis shows the time to identify an unauthorized UAV operator. The system is set to terminate detection and localization when UAV service ceiling reaches 40 meters which corresponds to 200 m^2 of an identifiable area for UAV equipped with HPBE of 60 degrees. It is obvious that by increasing the UAV speed, the time to identify an unauthorized UAV operator decreases. Otherwise speaking, the time to identify an unauthorized UAV operator is inversely proportion to the UAV speed. However, the relationship among the two are not linear. The rate of reduction of the time to identify an unauthorized UAV operator is higher during UAV speed of 5 to 15 m/s while it tapers off towards higher UAV speed.

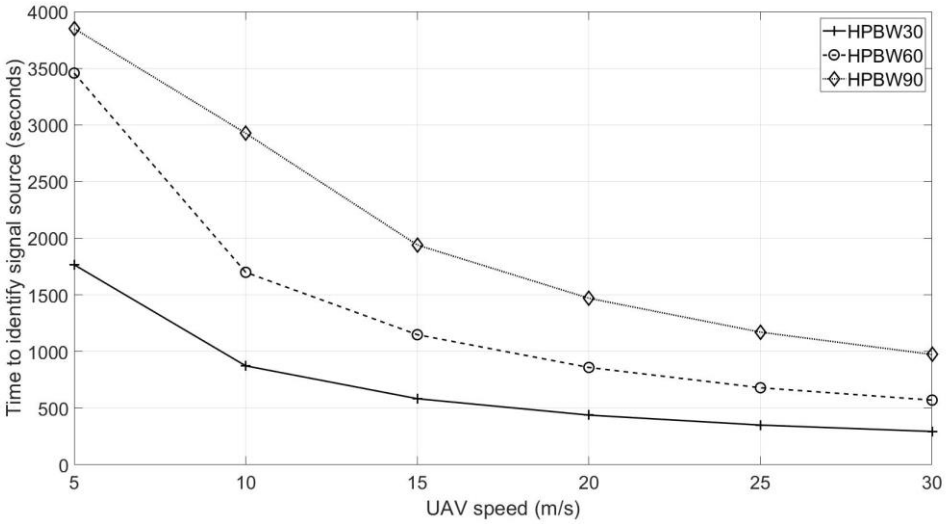

Fig. 27. Effect of UAV speed on time to identify an unauthorized UAV operator.

The HPBW of the antenna also has an effect on the time to identify an unauthorized UAV operator. Three values of HPBW, 30, 60, and 90 degrees, are investigated in Fig. 27. It is clear that all value of HPBW exhibits a similar pattern and the antenna with smaller value of HPBW yields lower value of time to identify an unauthorized UAV operator. However, it should not be concluded that the antenna with a small value of HPBW is preferable since it also offers less coverage area compared to ones with a higher value of HPBW, and vice versa.

Conclusions

UAV has seen an exceptional growth in the recent past and it is highly affordable and accessible than ever before. This poses several critical security issues, ranging from merely loss of privacy to life-threatening incident. It is crucial for the system to not only intercept an unauthorized UAV but also able to locate an unauthorized UAV operator. We propose a system to detect and locate an unauthorized UAV operator by equipping the UAV with a directional antenna. This UAV performs an unauthorized UAV operator detection and localization tasks by traveling along the predefined path and narrows down the potential area as time passes. We demonstrate, through simulation studies, how UAV service ceiling, UAV speed, and antenna directivity have an effect on the key performance metrics of the system, together with, the optimal operating condition.

Chapter 5. Design and Implementation of Agricultural Monitoring Station and Unmanned Aerial Vehicle

The primary purpose of agricultural monitoring station is to sense and report important variables that contribute to agricultural output. Moreover, it also serves secondary purpose, ambient energy harvesting and wireless energy transfer. The monitoring station will be equipped with ambient energy harvester which scavenge ambient energy, i.e. solar, wind, convert it into electrical energy and store it for later use. The agricultural monitoring station comprises of various functional modules. The system diagram of the agricultural monitoring station is shown in Fig 28.

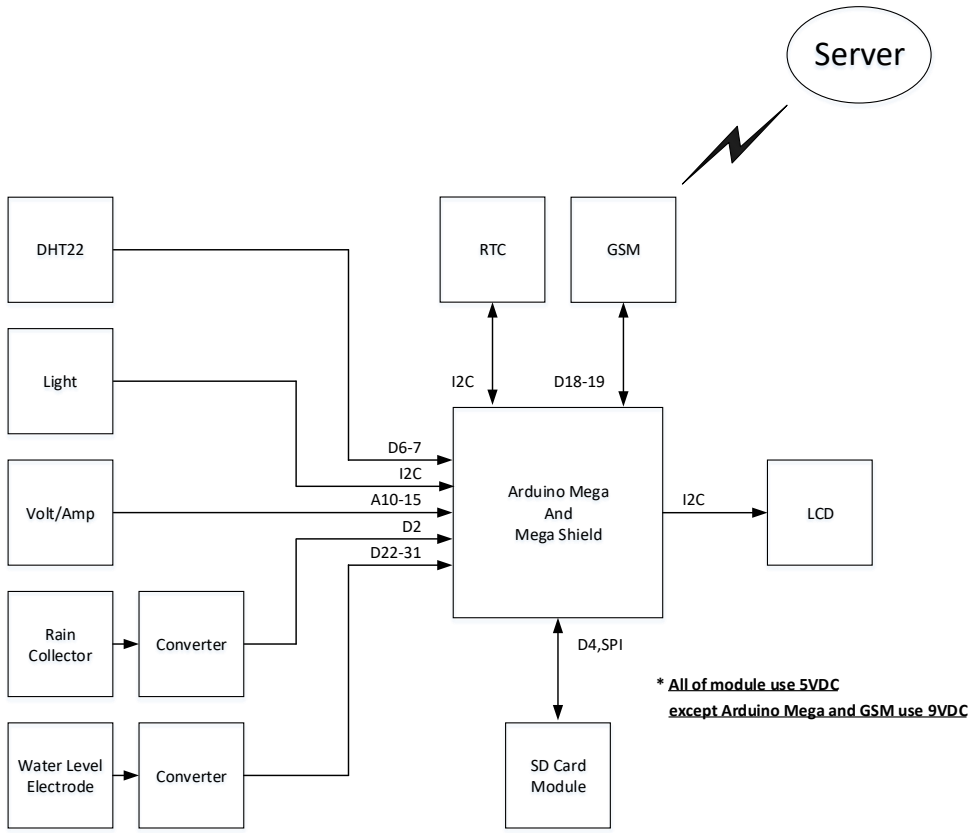

Fig. 28. The system diagram of the agricultural monitoring station

A. Energy harvesting module

Its purpose is to scavenge ambient energy, i.e. solar, wind, convert it into electrical energy and store it for later use. We target to design and develop the energy harvesting module that can scavenge solar energy.

B. Energy transfer module

This module enables energy replenishment to the desirous multi-objective UAV. With wireless energy transfer concept, The UAV does not have to be equipped with any charging connector which implies that no human intervention required.

C. Communication module

The monitoring station will be equipped with a software-defined communication module to realize the newly designed network protocol stated earlier. It is target to be low-power and in compliance with the regulatory domain. We employ 3G GSM Module in this work.

D. Central Processing module

The central processing module is responsible for managing the interoperability of different modules in the agricultural monitoring unit. We target to develop a low-power microcontroller-based platform in this work, that is, an Arduino Mega 2560.

E. Environmental monitoring module

This module is responsible for sensing important environmental variables that contribute to the agricultural output. We target to develop a module that can sense precipitation level, ambient temperature and humidity, water level, solar strength.

F. Energy storage module

The harvested energy will be stored in energy storage module hence it has to pose the following requirements: low discharge rate, high energy density, and environmental friendly. We use the most suitable off-the-shelf energy storage in this work.

G. Localization module

This module is responsible for precise positioning of agricultural monitoring station. It plays a vital role in guiding the multi-objective UAV for energy replenishment as the precise location of the charging station has to be determined. An off-the-shelf Global Positioning System (GPS) module that complies with our acceptable tolerance (2.5 meter radius) is employed in this work.

In this phase, the energy harvesting and charging profile and model are derived and will be further utilized in the network protocol design phase. The component list of the agricultural monitoring station is shown in Table 2.

Table 2. Component list of the agricultural monitoring station

Component	Model
Microcontroller	Arduino MEGA 2560 R3 + Mega Shield
Temperature and humidity sensor	Grove Temperature and Humidity Sensor Pro DHT22
Water level sensor	Omron electrode PS-5S
Precipitation sensor	Davis Instruments Rain Collector 7852
Real Time Clock	Tiny RTC I2C 24C32 DS1307
Solar sensor	Silicon Labs Si1145
Display module	Serial I2C 1602 16×2 Character LCD
Voltage and current sensor	Maxim MAX471/472
Communication module	Quectel 3G Shield (UC20-G)
Localization module	Quectel 3G Shield (UC20-G)
Data storage	SD Card Shield V4.0 and Micro SD Card 32GB

We then describe in details the functionality of each module as follows:

A. Water level sensing

The water level can be measured thanks to the 5-prong Omron electrode PS-5S.The water level detection can be configured to 9 levels, 15 centimeters above or below the ground level, with 2.5 centimeters increment. The circuit diagram of water level detection is shown in Fig. 29.

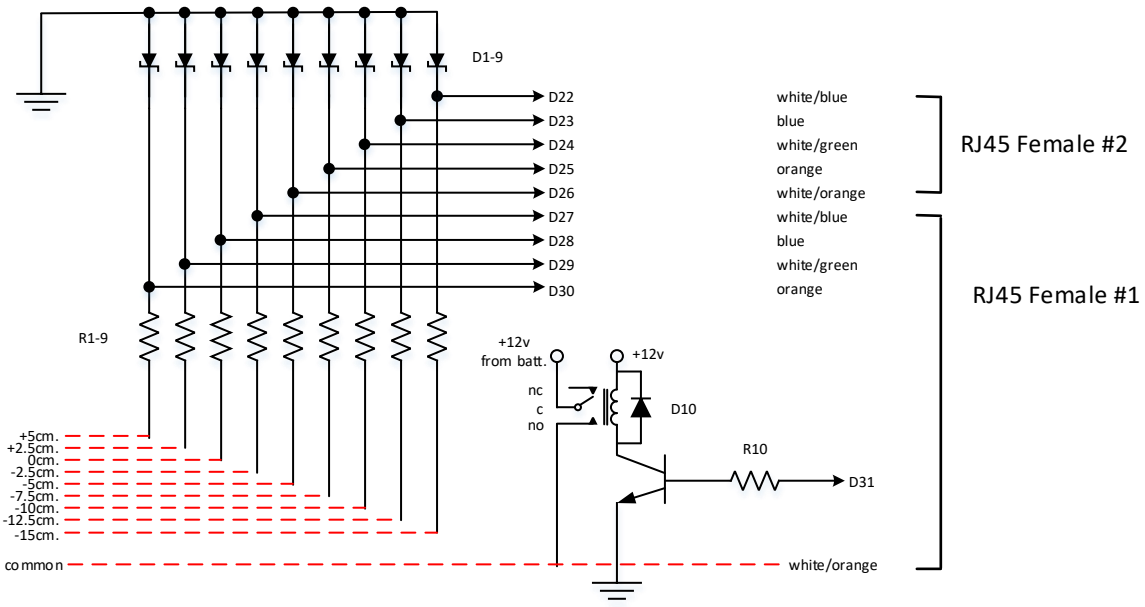

Fig. 29. The circuit diagram of water level detection

The water level detection is carried out when the circuit on each height setting is closed. In other words, the sensing electrode is configured with various heights so that water level can complete the circuit of each water level height settings accordingly. The PIN D31, shown in Fig. 2, can be used to activate the measurement and hence enabling power saving when the measurement is not required. Fig. 30 and Fig. 31 illustrate the electrode connectivity and electrode configuration, respectively.

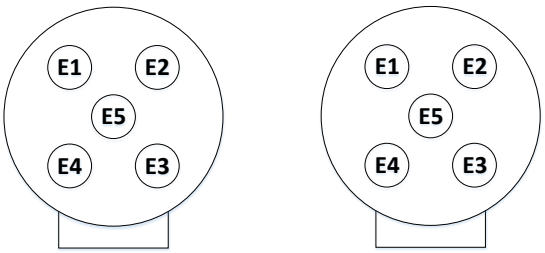

COM	E5 - white/orange	L5: -5	E5 - white/orange
L1: -15	E4 - orange	L5: -2.5	E4 - orange
L2: -12.5	E3 – white/green	L7 : 0	E3 – white/green
L3: -10	E2 - green	L8 : +2.5	E2 - green
L4: -7.5	E1 – white/blue	L9: +5	E1 – white/blue

Fig. 30. The electrode connectivity.

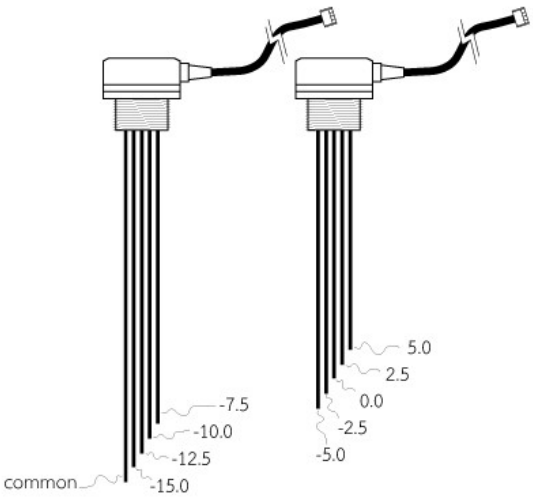

Fig. 31. The electrode configuration.

B. Precipitation level sensing

Precipitation level sensing is made possible through the use of Davis Instruments Rain Collector 7852. Rain enters the collector cone, passes through a debris-filtering screen, and collects in one chamber of the tipping bucket. The bucket tips when it has collected an amount of water equal to the increment in which the collector measures (0.01" or 0.2 mm). As the bucket tips, it causes a switch closure and brings the second tipping bucket chamber into position. The rain water drains out through the screened drains in the base of the collector. Fig. 32 shows the Davis Instruments Rain Collector 7852.

Fig. 32. The Davis Instruments Rain Collector 7852.

Each bucket tip generates a single pulse which then transformed into digital signal. This digital signal is processed by the microcontroller and translated into the precipitation level. In details, the precipitation level per unit time can be calculated by multiplying the number of bucket tips and it's the bucket volume, in this case 0.2 millimeter. The precipitation level measurement circuit is depicted in Fig. 33.

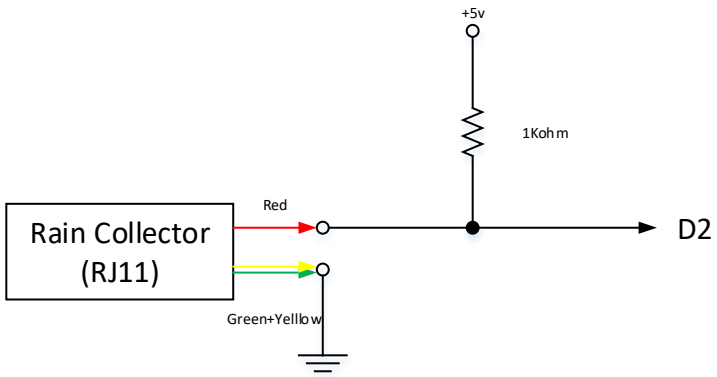

Fig. 33. The precipitation level measurement circuit.

C. Energy harvesting module

The agricultural monitoring station is designed to be self-sustainable with the use of solar energy harvesting. The solar energy is collected through the 50 Watt solar panel and transformed into electrical energy. However, the amount of collected electrical energy is directly proportioned to the solar intensity and can be dangerously harmful to sensitive components in case of an extreme solar intensity occurs. Consequently, it is imperative that the electrical energy directly harvested from the solar panel be regulated

by the solar charge controller. This solar charge controller is responsible for regulating the amount of voltage supplied to the battery during the charging phase, and to the load during the operational phase. The energy harvesting module diagram is shown in Fig. 34.

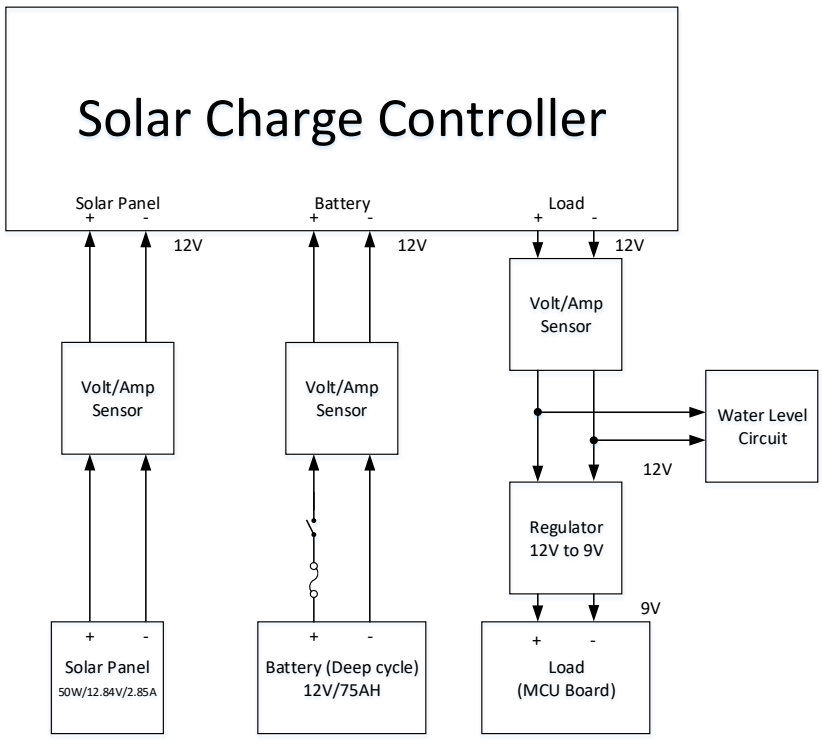

Fig. 34. The energy harvesting module diagram.

In Fig. 34, the energy is stored for later use in the 12-Volt battery and can supply the load of any voltage requirement by the use of voltage regulator. For example, the water level sensing circuit can operate at 12 Volts and hence a directly supply of energy from the battery is plausible. On the other hand, the central processing module needs 9 volts to operate and hence 12-volt to 9-volt voltage regulator is necessary to supply the correct amount of voltage to the load.

The internal of the agricultural monitoring station prototype is illustrated in Fig. 35, consisting of energy storage (12-volt battery), solar charge controller, Communication module, voltage regulators, and central processing module. Fig. 36 shows the agricultural monitoring station prototype in operation.

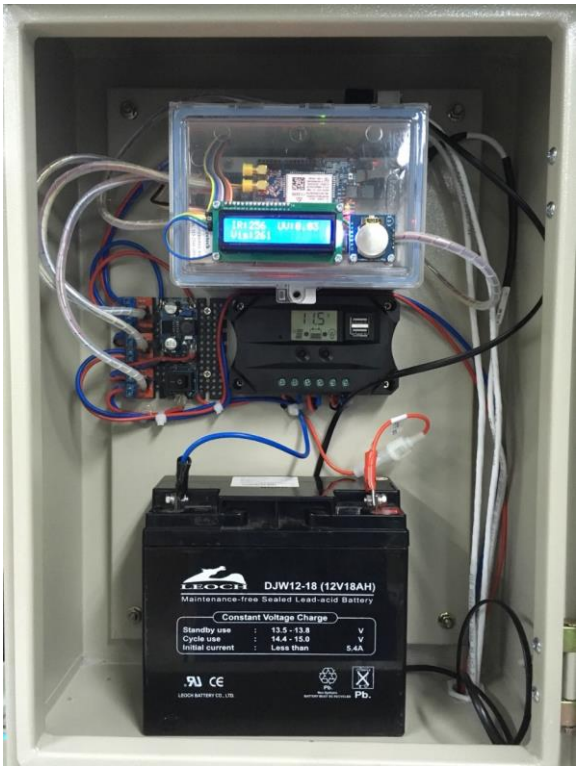

Fig. 35. The internal of the agricultural monitoring station prototype.

Fig. 36. The agricultural monitoring station prototype in operation.

The multi-objective UAV serves various purposes according to user-defined objective functions, i.e., data mule operation, agricultural surveillance, imagery analysis for yield assessment, etc. The multi-objective UAV comprises of the following modules. The system diagram of the multi-objective UAV is shown in Fig. 37.

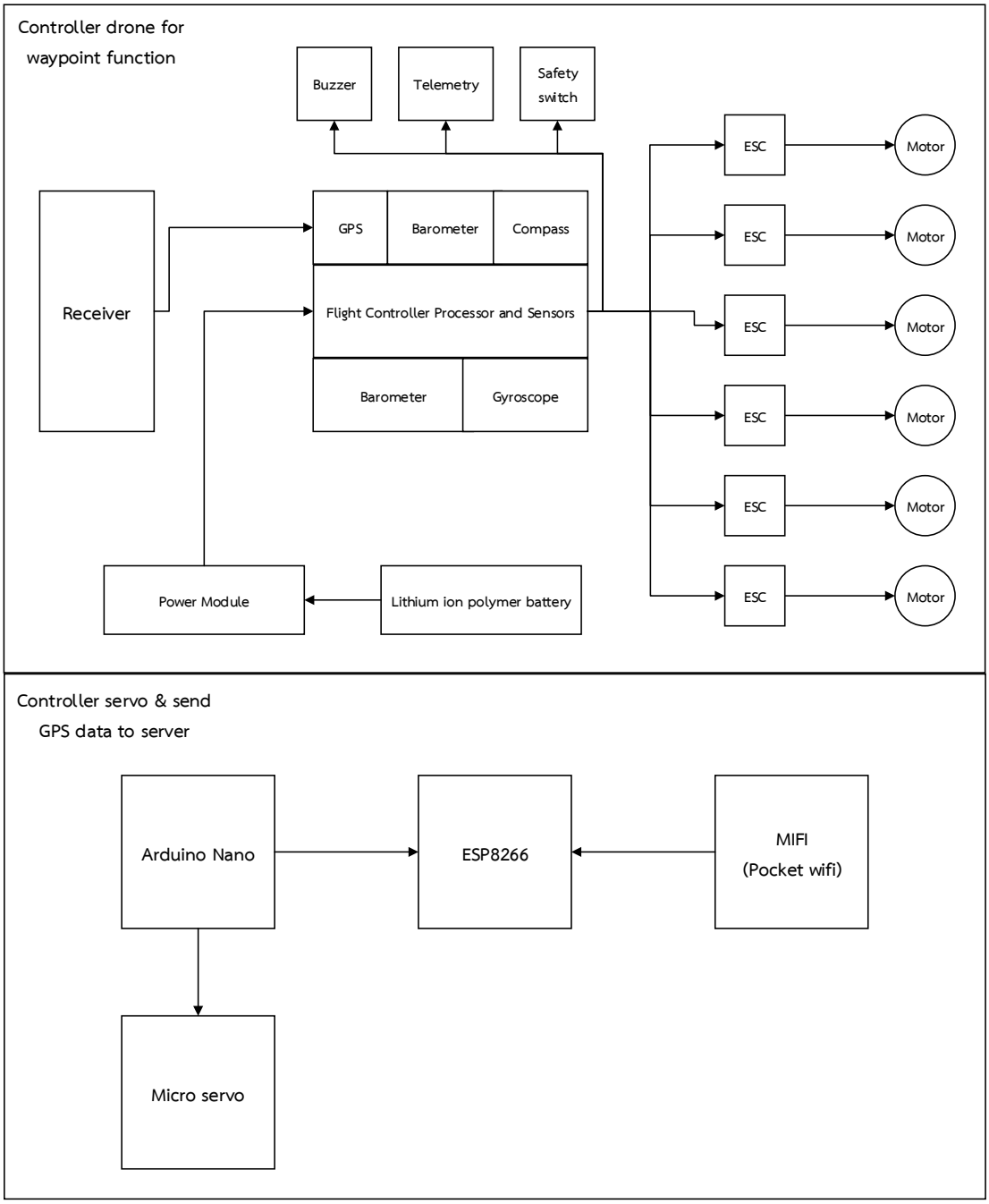

Fig. 37. The system diagram of the multi-objective UAV.

A. Chassis and motors

This is the framework for the multi-objective UAV. We design and fabricate the framework according to our requirements, i.e., ultra lightweight, maneuverability, and payload. We employ the HMF S550 Hexarotor X Copter airframe configuration in this work. The HMF S550 Hexarotor X Copter airframe configuration comprises of 6 motors and their propellers' rotation is shown in Fig. 38. The UAV powertrain is 6 EMAX MT-2216 KV810 brushless motor equipped with Tarot 1055 10-inch carbon fiber propellers. The speed of the motor is governed by HobbyWing XRotor 40A Electronic Speed Controller (ESC).

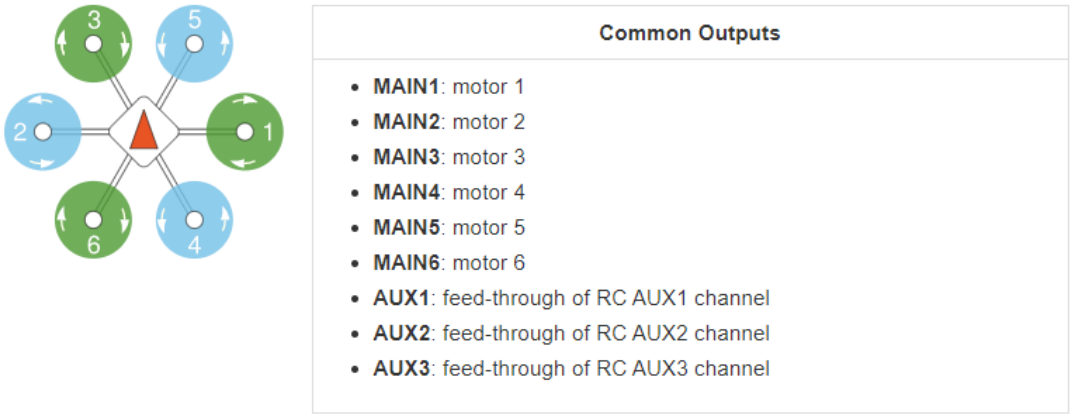

Fig. 38. The Hexarotor X Copter airframe configuration.

B. Programmable flight control module

The multi-objective UAV is equipped with a software-defined flight control module to realize the newly designed protocol stated earlier. It is target to be low-power and deliver a good level of stability as well as ultra-lightweight. A PX4 open-hardware project Pixhawk, an off-the-shelf Programmable flight control module, is chosen in this work. Fig. 39 depicts the PX4 Pixhawk flight control module installed on S550 Hexarotor X Copter airframe. The multi-objective UAV prototype is shown in Fig. 40.

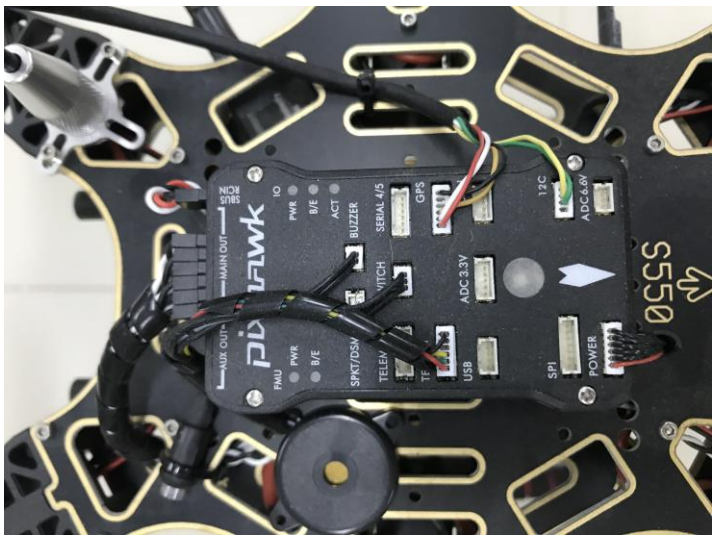

Fig. 39 The PX4 Pixhawk flight control module.

C. Communication module

A software-defined communication module will be equipped in order to realize the newly designed network protocol stated earlier. It is target to be low-power and in compliance with the regulatory domain. We employ both Radio Control (RC) and telemetry Radio. The former is the FrSky telemetry that enables an access to UAV information on a compatible RC transmitter while the latter is Sik Radio compatible telemetry radio. We use the 3DR 915Mhz 500mw Radio Telemetry in this work.

D. Localization module

This module is responsible for precise positioning of the multi-objective UAV. It plays a vital role in guiding the multi-objective UAV for energy replenishment as the precise location of the charging station has to be determined. An off-the-shelf Radio link Ublox M8N Global Positioning System (GPS) module that complies with our acceptable tolerance (2.5 meter radius) is employed in this work.

E. Energy storage module for UAV

The harvested energy will be stored in energy storage module hence it has to pose the following requirements: ultra-lightweight, low discharge rate, high energy density, and environmental friendly. We use 3S 11.1 Volt 3500 mAh 10A Li-Po battery in this work.

Fig. 40 The multi-objective UAV prototype.

References

[1] Managing Bird damage to Fruit and other horticultural crops, Australian government, [Online] http://www.dpi.nsw.gov.au/agriculture/horticulture/pests-diseases- hort/multiple/managing- bird-damage/

[2] GranMonte Smart Vineyard, [Online] http://www.granmonte.com/about- estate.html/

[3] P. Nintanavongsa, U. Muncuk, D. R. Lewis, and K. R. Chowdhury, Design Optimization and Implementation for RF Energy Harvesting Circuits. IEEE Journal on Emerging and Selected Topics in Circuits and Systems, vol. 2, no. 1, pp. 24–33, Mar. 2012.

[4] V. Raghunathan, A. Kansal, J. Hsu, J. Friedman, and M. Srivastava, Design considerations for solar energy harvesting wireless embedded systems. Proc. Of Fourth Intl. Symposium on Information Processing in Sensor Networks (IPSN), pp. 457–462, Apr. 2005.

[5] J. Curty, M. Declercq, C. Dehollain, N. Joehl, Design and Optimization of Passive UHF RFID Systems, Springer, 2007.

[6] Powercast Corporation, Lifetime Power Evaluation and Development Kit. [Online] http://www.powercastco.com/products/development-kits/

[7] A. Kurs, A. Karalis, R. Moffatt, J.D. Joannopoulos, P. Fisher, and M. Soljacic, Wireless Power Transfer via Strongly Coupled Magnetic Resonances. Science Magazine, vol. 317, no. 5834, pp. 83–86, Jul. 2007.

[8] Witricity corporation, [Online] http://witricity.com/

[9] M. Zargham and P. G. Gulak, Maximum Achievable Efficiency in Near-Field Coupled Power-Transfer Systems. IEEE Transactions on Biomedical Circuits and Systems, vol. 6, no. 2, Jun. 2012.

[10] Kasetsart university, [Online] http://www.ku.ac.th/web2012/index.php/

[11] K. Sundar and S. Rathinam, Algorithms for Routing an Unmanned Aerial Vehicle in the Presence of Refueling Depots. IEEE Transactions on Automation Science and Engineering, vol. 11, no. 1, pp. 287–294, Jan. 2014.

[12] F. Guerrieroa, R. Suracea, V. Loscra, and E. Nataliziob, A multi-objective approach for unmanned aerial vehicle routing problem with soft time windows constraints. Applied Mathematical Modelling, vol. 38, no. 3, pp. 839–852, Feb. 2014.

[13] 3D Robotics Incorporation, iris+ drone Kit. [Online] http://www.3dr.com/

[14] Georgia Tech UAV research facility, Electric UAV Flight Time Calculator. [Online] http://www.uavrf.gatech.edu/

[15] GranMonte Smart Vineyard, [Online] http://www.granmonte.com/aboutestate.

[16] 2050: A third more mouths to feed, [Online] http://www.fao.org/news/story/en/item/35571/icode/

[17] A. H. Coarasa, P. Nintanavongsa, S. Sanyal, and K. R. Chowdhury, “Impact of mobile transmitter sources on radio frequency wireless energy harvesting,” Proc. of International Conference on Computing, Networking and Communications (ICNC), pp. 573-577, Jan. 2013.

[18] M. Ryu, J. Kim, and J. Yun, “Integrated semantics service platform for the Internet of Things: a case study of a smart office,” Sensors, vol. 15, no. 1, pp. 2137-2160, Jan. 2015.

[19] A. Savvas, “Farming industry must embrace the Internet of Things to grow enough food,” [Online] http://www.techworld.com/ news/big- data/farming-industry-must-embrace-internet-of-things-3596905/

[20] M. Ryu, J. Yun, T. Miao, I. Ahn, S. Choi, and Jaeho Kim, “Design and implementation of a connected farm for smart farming system,” Proc. of IEEE Sensor, Nov. 2015.

[21] S. Jindarat and P. Wuttidittachotti, “Smart Farm Monitoring Using Raspberry Pi and Arduino,” Proc. of IEEE International Conference on Computer, Communication, and Control Technology (I4CT), Apr. 2015.

[22] Kasetsart university, [Online] http://www.ku.ac.th/web2012/index.php/

[23] P. Tripicchio, M. Satler, G. Dabisias, E. Ruffaldi, and C. A. Avizzano, “Towards Smart Farming and Sustainable Agriculture with Drones,” Proc. of International Conference on Intelligent Environments, Jul. 2015.

[24] P. Nintanavongsa, W. Yaemvachi, and I. Pitimon, “A self-sustaining unmanned aerial vehicle routing protocol for smart farming,” Proc. of International Symposium on Intelligent Signal Processing and Communication Systems (ISPACS), Oct. 2016.

[25] M. Ammad-udin, A, Mansour, D. Le Jeune1, E. H. M. Aggoune, and M. Ayaz, “UAV Routing Protocol for Crop Health Management,” Proc. Of 24th European Signal Processing Conference (EUSIPCO), Sept. 2016.

[26] Ns-2 network simulator, [Online] http://www.isi.edu/nsnam/ns/

[27] Ad hoc On-Demand Distance Vector (AODV) Routing, [Online] https://tools.ietf.org/html/rfc3561

[28] M. L. Garcia, Design and Evaluation of Physical Protection Systems. Butterworth-Heinemann, 2008.

[29] Cooperative Surveillance for UAVs: Enabling safe, secured and efficient UAV operations, [Online] https://www.eurocontrol.int/sites/default/files/events/presentation/session5.5- thales-utm-a-perspective.pdf

[30] L. Gupta, R. Jain and G. Vaszkun, Survey of important issues in UAV communication networks. IEEE Communications Surveys and Tutorials, vol. XX, no. 1, pp. 287–294, November 2015.

[31] P. Nintanavongsa, W. Yaemvachi, and I. Pitimon, A self-sustaining unmanned aerial vehicle routing protocol for smart farming. Proc. of International Symposium on Intelligent Signal Processing and Communication Systems (ISPACS), October 2016.

[32] P. Nintanavongsa, U. Muncuk, D. R. Lewis, and K. R. Chowdhury, Design Optimization and Implementation for RF Energy Harvesting Circuits. IEEE Journal on Emerging and Selected Topics in Circuits and Systems, vol. 2, no. 1, pp. 24–33, March 2012.

[33] D. Kingston, R. W. Beard, and R. S. Holt, Decentralized Perimeter Surveillance Using a Team of UAVs. IEEE TRANSACTIONS ON ROBOTICS, vol. 24, no. 6, pp. 1394–1404, December 2008.

[34] H. Kim and J. Ben-Othman, A Collision-free Surveillance System using Smart UAVs in Multi Domain IoT. IEEE Communications Letters, to appear 2019.

[35] J.M. Aguilar, P.R. Soria, B.C. Arrue, and A. Ollero, Cooperative Perimeter Surveillance Using Bluetooth Framework Under Communication Constraints. Proc. of ROBOT 2017: Third Iberian Robotics Conference, pp. 771–781, December 2017.

[36] P. Nintanavongsa and I. Pitimon, Impact of Sensor Mobility on UAV- based Smart Farm Communications. Proc. of International Electrical Engineering Congress (iEECON), March 2017.

[37] Ns-2 network simulator, [Online] http://www.isi.edu/nsnam/ns/

[38] Ad hoc On-Demand Distance Vector (AODV) Routing, [Online] https://tools.ietf.org/html/rfc3561

[39] T. S. Rappaport, Wireless communications, principles and practice. Prentice Hall, 1996.

[40] Cooperative Surveillance for UAVs: Enabling safe, secured and efficient UAV operations, [Online] https://www.eurocontrol.int/sites/default/files/events/presentation/session5.5-thales-utm-aperspective.pdf

[41] R. Peng and M. L. S ichitiu, “Angle of arrival localization for wireless sensor networks,” in Proceedings of 3rd Annual IEEE Communications Society on Sensor and Adhoc Communications and Networks, January 2006.

[42] S. Tomic, M. Beko, and M. Tuba, “A linear estimator for network localization using integrated RSS and AOA measurements,'” IEEE Signal Processing Letter, vol. 26, no. 3, pp. 405-409, March 2019.

[43] N. Garcia, H. Wymeersch, and D. T. M. Slock, “Optimal precoders for tracking the AoD and AoA of a mmWave path,'” IEEE Transactions on Signal Processing, vol. 66, no. 21, pp. 5718-5729, November 2018.

[44] C.-H. Park and J.-H. Chang, “TOA source localization and DOA estimation algorithms using prior distribution for calibrated source,” Digital Signal Processing, vol. 71, pp. 61-68, December 2017.

[45] M. R. Gholami, S. Gezici, and E. G. Ström, “TW-TOA based positioning in the presence of clock imperfections,” Digital Signal Processing, vol. 59, pp. 19-30, December 2016.

[46] Y. Liu, F. Guo, L. Yang, and W. Jiang, “Source localization using a moving receiver and noisy TOA measurements,” Signal Processing, vol. 119, pp. 185-189, February 2016.

[47] E. Kazikli and S. Gezici, “Hybrid TDOA/RSS based localization for visible light systems,” Digital Signal Processing, vol. 86, pp. 19-28, March 2019.

[48] D. Wang, J. Yin, T. Tang, X. Chen, and Z. Wu, “Quadratic constrained weighted least-squares method for TDOA source localization in the presence of clock synchronization bias: Analysis and solution,” Digital Signal Processing, vol. 82, pp. 237-257, November 2018.

[49] Y. Sun, K. C. Ho, and Q. Wan, “Solution and analysis of TDOA localization of a near or distant source in closed form,” IEEE Transactions on Signal Processing, vol. 67, no. 2, pp. 320-335, January 2019.

[50] P. Abouzar, D. G. Michelson, and M. Hamdi, “RSSI-based distributed self-localization for wireless sensor networks used in precision agriculture,” IEEE Transactions on Wireless Communications, vol. 15, no. 10, pp. 6638-6650, October 2016.

[51] A. E. Lagias, T. D. Lagkas, and J. Zhang, “New RSSI-based tracking for following mobile targets using the law of cosines,” IEEE Wireless Communication Letter, vol. 7, no. 3, pp. 392-395, January 2018.

[52] J. Luomala and I. Hakala, “Analysis and evaluation of adaptive RSSI based ranging in outdoor wireless sensor networks,” Ad Hoc Networks, vol. 87, pp. 100-112, May 2019.

[53] Z. Na, Y. Wang, X. Li, J. Xia, X. Liu, M. Xiong, and W. Lu, “Subcarrier allocation based simultaneous wireless information and power transfer algorithm in 5G cooperative OFDM communication systems,” Physics Communications, vol. 29, pp. 164-170, August 2018.

[54] Z. Na, J. Lv, M. Zhang, B. Peng, M. Xiong, and M. Guan, “GFDM based wireless powered communication for cooperative relay system,” IEEE Access, vol. 7, pp. 50971-50979, April 2019.

[55] T. S. Rappaport, Wireless communications, principles and practice. Prentice Hall, 1996.

[56] L. Gui, M. Yang, P. Fang, and S. Yang, “RSS-based indoor localization using MDCF,” IET Wireless Sensor Systems, vol. 7, no. 4, pp. 98-104, August 2017.

ภาคผนวก

A Self-sustaining Unmanned Aerial Vehicle Routing Protocol for Smart Farming

Prusayon Nintanavongsa, Weerachai Yaemvachi, and Itarun Pitimon
Department of Computer Engineering, Rajamangala University of Technology Thanyaburi, Thailand
Email: {prusayon.n, weerachai.y, itarun.p}@en.rmutt.ac.th

***Abstract*—Increasing agricultural productivity has been a long quest for farmers and only a few can achieve it. One major factor that hinders them to achieve such goal is the lack of proper agricultural monitoring technique. Recent advancement in technology has enabled the integration of sensor networks and traditional farming, resulting in effective monitoring through smart farming. However, there exists a hefty investment in equipment and infrastructure installation throughout the coverage area. We design two routing approaches, called Location-agnostic (LA) and Location-specific (LS) protocols, to facilitate the self-sustaining agricultural monitoring platform, requiring no infrastructure installation, comprises of Unmanned Aerial Vehicle (UAV) with solar energy harvesting and wireless power transfer capability. The LA protocol does not require location information of monitoring stations to be visited prior to the flight, and is useful for dynamic environment. The LS protocol relies on the complete view of the topology prior to the flight and is suitable for static environment. These protocols determine the optimal UAV routing path from a set of monitoring stations under various conditions. Through a combination of simulation and experimentation studies, we demonstrate significant energy efficiency and coverage area improvement over the classical routing protocol.**

***Keywords*—Self sustaining; Routing protocol; Unmanned Aerial Vehicle; Smart farming; Energy harvesting.**

I. Introduction

Two major problems that contribute to low agricultural yield are damage caused by birds and lack of proper farm monitoring techniques [1]. While the exact measure of the loss in yield associated with birds is undocumented, generations of farmers have been performing a number of traditional and conventional techniques to prevent birds from damaging the agricultural area. This not only requires a massive hours and manpower but also farmers' unaccountable loss of opportunities as they have to be physically present to repel a flock of birds from their agricultural area. Moreover, it is shown that the agricultural yield can be considerably increased by adopting Information technology to the agricultural area. GranMonte vineyard [2] is one of the examples that obtains a higher crop yield after implementing environmental monitoring stations throughout the agricultural area. With an up-to-date environmental data monitoring, it enables farmers a prompt response to mitigate fluctuation of important variables, i.e., humidity, temperature, that affect the crop yield.

Ambient energy harvesting is the process of scavenging energy from sources in the surrounding environment and store it for later use [3]. The energy sources can be solar, wind, and Radio Frequency (RF). It is an attractive method for overcoming the energy limitations of conventional battery powered wireless devices. Solar energy harvesting through photovoltaic conversion provides the highest power density among other types of energy harvesting. With direct access to sunlight, an average yield of $15\,\mathrm{mW/cm^2}$ is to be expected [4]. The benefit of adopting ambient energy harvesting technology is two-fold. First, it is eco-friendly since no battery is required and hence no toxic waste from battery disposal. Second, it is easy to install and maintain as the infrastructure, i.e., electricity, is not required. The latter is even more pronounced in case of large cultivation area is to be monitored.

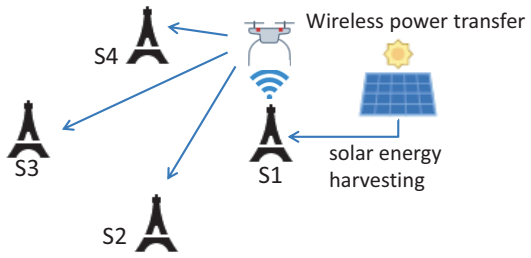

Fig. 1. A self-sustaining agricultural monitoring platform

Fig. 1 shows a self-sustaining agricultural monitoring platform. It consists of monitoring stations $S1$, $S2$, $S3$ and $S4$ and the UAV with solar energy harvesting and wireless power transfer capability. The solar energy harvesting enables monitoring stations to be decoupled from infrastructure installation, i.e., electrical cabling, while wireless energy transfer facilitates the UAV energy replenishing without human intervention, i.e., manually mount/dismount battery for recharge. We investigate on how the UAV propagates through a set of monitoring stations, using various routing protocols, and observe its behavior with respect to the following metrics (i) the average flight distance (ii) the average consumed energy, and (iii) the average enclosed area.

The core contributions of our work can be summarized as follows:

- We design a self-sustaining agricultural monitoring platform, comprises of Unmanned Aerial Vehicle (UAV) with solar energy harvesting and wireless power transfer capability.
- We propose two routing approaches, called Location-

978-1-5090-0629-8/16/$31.00 ©2016 IEEE

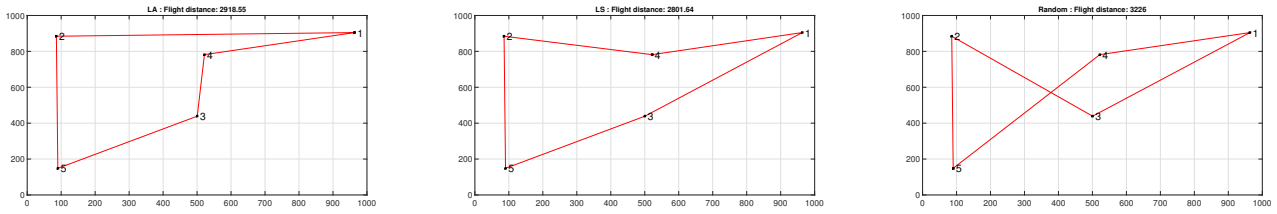

(a) (b) (c)

Fig. 2. Calculated UAV flight path with 5 monitoring stations adopting LA routing protocol (a) LS routing protocol (b) and random protocol (c)

agnostic (LA) and Location-specific (LS) protocols, to facilitate the self-sustaining agricultural monitoring platform and demonstrate improvement in crucial metrics over existing routing approach.

The rest of this paper is organized as follows: In Section II, we give the related work. Our proposed protocols are discussed in detailed in Section III. The simulation results are presented in Section IV. Finally, Section V concludes our work.

II. Related Work

In recent times, RFID technology is a clear example of wireless power transmission where such a tag operates using the incident RF power emitted by the transmitter [5]. The design of RF energy harvesting circuits has been extensively explored in [3] and the authors show that with a simple yet optimal design and optimization, the prototype can yield almost double the efficiency than that of a major commercially available energy harvesting circuit [6]. Moreover, wireless power transfer via strongly magnetic resonances is investigated by MIT researchers [7]. The authors experimentally demonstrated efficient nonradiative power transfer of 60 watts with 40% efficiency over distances in excess of 2 meters. The concept is later commercialized through the establishment of the WiTricity corporation [8]. This is not only prove that the wireless power transfer is a promising technology but also commercially viable. Recent publication [9] investigates the maximum achievable efficiency in near-field coupled power-transfer systems. The authors also propose a method that effectively decouples the design of the inductive coupling two-port from the problem of loading and power amplifier design.

The use of UAV for agricultural purposes is recently proposed by Kasetsart university researchers [10]. The research project is a collaboration between the faculty of engineering, Kasetsart university and the Yamaha motors (Thailand) and aims to effectively plant, deliver fertilizer, and spray pesticide to the cultivation area. The prototype is expected to weight 70 kilograms and able to carry the payload of 29 kilograms. The source of power is fossil fuel with the consumption of 8 liters per 2 hours flight. However, the project has several challenges and issues to be addressed. First, the project relies on a single-objective UAV that is designed to only deliver payload. It does not employ agricultural monitoring or responsive system that reacts to stimuli. Second, the UAV needs to be manually filled once its fuel is exhausted. This incurs not only budget allocation for fuel cost but also time consumed in maintenance of internal combustion engine. Third, environmental impact is a major concern since the UAV employs engine powered by fossil fuel. Not only noise pollution is expected from an internal combustion engine but also the air pollution from its exhaust.

A single Unmanned Aerial Vehicle (UAV) routing problem, where there are multiple depots and the vehicle is allowed to refuel at any depot, is considered in [11] . The objective of the problem is to find a path for the UAV such that each target is visited at least once by the vehicle, the fuel constraint is never violated along the path for the UAV, and the total fuel required by the UAV is a minimum. Computational results show that solutions whose costs are on an average within 1.4% of the optimum can be obtained relatively fast for the problem involving five depots and 25 targets. In [12], a distributed system of autonomous Unmanned Aerial Vehicles (UAVs), able to self-coordinate and cooperate in order to ensure both spatial and temporal coverage of specific time and spatial varying point of interests, is proposed. The authors give a mathematical formulation of the problem as a multi-criteria optimization model are considered simultaneously.

III. Protocol Description

In this section, we describe the key challenges in protocol design as well as explore our proposed protocols in details.

1) Location-agnostic (LA) protocol: The LA protocol is designed to operate not only under dynamic environment but also requires no information of monitoring stations to be visited. Under this circumstance, monitoring stations are assumed to have Global Positioning System (GPS) equipped and intermittently sending out beacon signal, containing its location. The beacon signal serves two purposes here. First, it provides location information of the sender, enables UAV to calculate its path and navigate properly. Second, it provides a second layer of assurance in case of UAV misses the beacon signal transmitted by the monitoring station. Since neighboring monitoring stations are unlikely to have the same beacon sending interval, they can also provide location information of stations nearby. The concept of using beacon signal to facilitate UAV navigation also makes the LA protocol resilient to dynamic environment, i.e., monitoring stations are mobile. For instance, monitoring stations can be assigned to fine-grained patrol and monitoring while UAV is responsible for coarse-grained patrol and monitoring.

As stated earlier, the LA protocol does not require location information of monitoring station prior to the flight. Once the UAV is fully charged, it takes off and listens to the beacon signal from monitoring stations in order to determine its first visiting location. Since there may be various monitoring stations in the vicinity, the LA protocol employs the greedy method, i.e., choosing the nearest monitoring station to its current position. In other words, the LA protocol elects the nearest beacon sending monitoring station to be the next visiting location and the process is performed on hop-by-hop basis. Fig. 2(a) shows the topology area of 1000 x 1000 m^2 with 5 monitoring stations are deployed. The station number 1 is the only station that has solar energy harvesting and wireless power transfer capability. This implies that the UAV has to originate and terminate its flight at this stations. It also has to perform energy replenishing at this station. The calculated UAV flight path is shown in red and the visiting order is 1,4,3,5,2,1 with the total flight distance of 2,918.55 meters. When the UAV takes off from station 1, it receives beacon signal from both station 3 and station 4. However, upon comparing distance from its current location to location information received from station 3 and station 4, it elects station 4 to be the next visiting point since it is closer to station 4 than station 3. Once it arrives at station 4, it then proceeds to determine the next visiting point. Here, it receives beacon signal from station 2 and station 3 and it chooses to proceed towards station 3 since it is closer to its current position. The process continues in this fashion until it receives no further beacon signal. The UAV then returns to station 1 to disseminate collected information as well as recharging itself. It stays at station 1 until the battery is fully charged and subsequently returns to operation.

2) Location-specific (LS) protocol: Consider the scenario in which location of monitoring stations are predetermined and reconfiguration rarely occurs. In fact, this scenario can be expected in practice since monitoring stations are usually planned, installed, and expected to acquire information at each specific location. We can utilize priori knowledge of monitoring stations' location and perform a more efficient optimization. The LS protocol utilizes the predetermined location information and performs the flight path calculation. In other words, the LS protocol relies on the complete view of the topology prior to the flight and is suitable for static environment.

Unlike the LA protocol where the UAV takes off and determine the next visiting point once it is fully charged, the LS protocol performs the flight path optimization and all visiting points are determined prior to the flight. Fig. 2(b) shows the same topology used in the previous section. Likewise, station 1 is the only station that has solar energy harvesting and wireless power transfer capability and hence the UAV has to originate and terminate its flight at this stations. However, locations of monitoring stations are assumed to be predetermined and they are immobile. This implies that, prior to the flight, the UAV has the complete view of the topology and can determine all points to be visited. The LS protocol heuristically search for the best flight path, that is, the shortest distance that completes the flight. The heuristic search can be performed by going through all possible permutations of monitoring station pairs and choose one that yields the lowest flight distance. One may argue that the flight path computation time can be very large with increasing numbers of monitoring stations. However, it usually takes hours to fully charge the UAV battery and the flight path calculation can be performed simultaneously. Moreover, the flight path calculation is performed by the monitoring station, the station 1 in this case, and poses no burden on energy consumption to the UAV. Consequently, the computational complexity of the LS protocol deems insignificant in this perspective.

In Fig. 2(b), the calculated UAV flight path using LS protocol is shown in red and the visiting order is 1, 3, 5, 2, 4, 1 with the total flight distance of 2,801.64 meters. Once the UAV takes off at station 1, it then proceeds to the predetermined visiting points without the need to acquire beacon signal. It is obvious that the LS protocol chooses the longer path, station 1 to station 3, in contrast to that of the LA protocol. Since the environment is static, that is, monitoring stations are immobile, the UAV is bounded to visit all designated monitoring stations and return to station 1. Note that monitoring stations are not required to transmit beacon signal and hence less energy consumption is expected.

TABLE I
PARAMETERS USED IN SIMULATION

Parameter	Value
cruising speed	7.5 $\mathrm{m/s}$
current consumption	21.31 A
cruise ceiling	15.0 m
battery capacity	Lithium-Polymer 5,100 mAh

3) Random protocol: Fig. 2(c) depicts another way to calculate the UAV flight path via random method. In this case, the assumption is similar to that of the LS protocol, that is, the locations of monitoring stations are assumed to be predetermined and they are immobile. However, there is no flight path calculation prior to the flight and the visiting order of monitoring stations is randomized. Consequently, this method poses negligible time and energy consumption for the flight path calculation. The calculated UAV flight path using random method is shown in red and the visiting order is 1, 4, 5, 2, 3, 1 with the total flight distance of 3,226 meters. Similar to the LS protocol, once the UAV takes off at station 1, it then proceeds to the predetermined visiting points without the need to acquire beacon signal.

Note that each monitoring station will be visited only once in each trip and hence multiple visit is prohibited. This condition is applicable to all three proposed protocols.

IV. SIMULATION RESULTS

In this section, we thoroughly evaluate our proposed protocols using our custom simulator, developed in MATLAB. We observe the behavior of each protocol with respect to the number of monitoring stations. The simulation parameters are

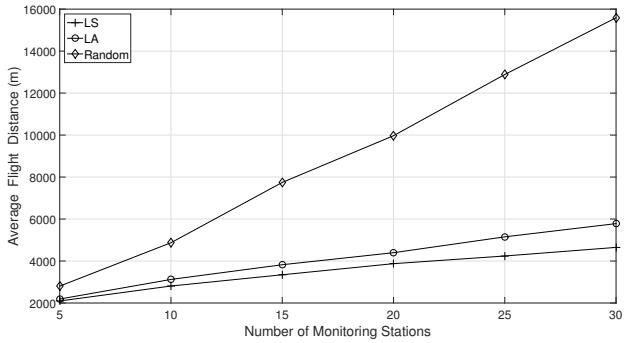

Fig. 3. Effect of the number of monitoring stations on average flight distance

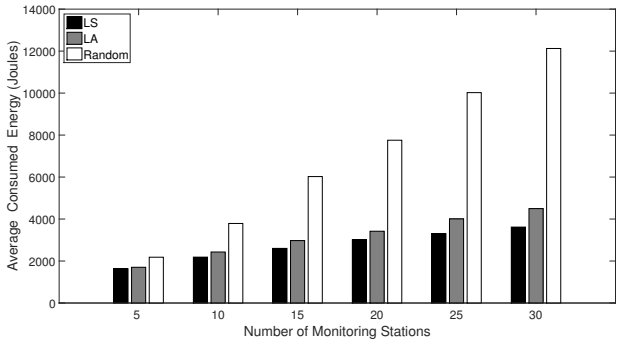

Fig. 4. Effect of the number of monitoring stations on average consumed energy

set as follows: The UAV is 3dr iris+ [13] and its specifications and operational characteristics, i.e., current consumption, cruising speed, battery capacity, are from [14]. Additional parameters used in the simulation are present in Table I. Unless specifically stated, monitoring stations are deployed uniformly at random in 1000 x 1000 m^2 grid. While it is possible that the location of the monitoring stations may affect the experiment, i.e., all monitoring stations are deployed in the same location. It is unlikely in practice to implement such deployment. All monitoring stations are assumed to be static and the station 1 is the only station that has solar energy harvesting and wireless power transfer capability and hence the UAV has to originate and terminate its flight at this stations.

We compare the proposed protocols with the random protocol, the order of monitoring station visit is randomly chosen prior to the flight. The random protocol provides the base case and reference protocol for comparison. We performs comparison on three metrics, average flight distance, average consumed energy, and average enclosed area.

A. Average flight distance

In this sub-section, we investigate the effect of the number of monitoring stations on the average flight distance for different UAV routing protocols. The average flight distance is defined as the average total distance that the UAV traveled in order to visit all monitoring stations, originating from station 1 and terminating at station 1. Fig. 3 shows the effect of the number of monitoring stations on the average flight distance. The number of monitoring stations, uniformly distributed at random, is varied from 5 to 30. It is clear that the LS protocol delivers the lowest average flight distance among three protocols, approximately 12% lower than the LA protocol. Moreover, the LS protocol delivers monotonically increasing average flight distance with increasing numbers of monitoring stations. The LA protocol yields slightly larger average flight distance than that of the LS protocol and also experiences monotonically increasing average flight distance with increasing numbers of monitoring stations. However, it is expected that the LS protocol offers even lower average flight distance than the LA protocol with increasing numbers of monitoring stations since the difference between these protocols increases with increasing numbers of monitoring stations. The benefit of pre-flight optimization in the LS protocol greatly improves the performance as the UAV follows the optimal flight path and ensuring the shortest distance traveled. The per-hop optimization in the LA protocol, although unable to deliver the optimal solution, offers marginally inferior performance compared to the LS protocol. It is also clear that the random protocol performs the worst among three protocols. The average flight distance, even monotonically increases with increasing numbers of monitoring stations, exhibits a higher rate of growth than the LA and LS protocols. The random protocol yields 50% higher average flight distance than the other two protocols even at the lowest number of monitoring stations. Consequently, it may not be a good choice if the average flight distance has to be kept minimum.

B. Average consumed energy

Here, we investigate how these three protocols behave when the number of monitoring stations changes. The average consumed energy is a key metric in this section and defined as an average total energy the UAV spent in order to visit all monitoring stations, originating from station 1 and terminating at station 1. The average consumed energy is shown in Fig. 4, wherein the energy consumption of the LA and LS protocols are similar, i.e., monotonically increasing average consumed energy with increasing numbers of monitoring stations. Again, the LS protocol offers the lowest average consumed energy when compared to the LA and random protocols while the random protocol yields the highest energy consumption among three protocols. The average consume energy plot exhibits a similar fashion to the average flight distance shown in the previous section.

C. Average enclosed area

The average enclosed area, defined as an average area enclosed by the UAV flight path, is another metric of interest. One of the applications is the surveillance operation and it is crucial to determine the UAV coverage area. Fig. 5 shows the effect of the number of monitoring stations on the average enclosed area for each routing protocol. It is obvious that the LS protocol offers the largest coverage area throughout the

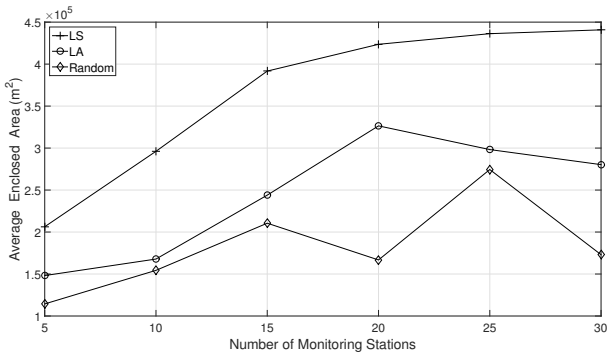

Fig. 5. Effect of the number of monitoring stations on average enclosed area

range of monitoring stations, approximately 45% and 81% larger than the LA and the random protocols, respectively. However, the average enclosed area curve of the LS protocol exhibits a constant rate of growth until 15 monitoring stations and then gradually decreases towards increasing numbers of monitoring stations. This is not surprising since there is less room for optimization with increasing numbers of monitoring stations placed into the topology. The LA protocol yields the second largest coverage area while the random protocol provides the least amount of coverage area. All three protocols exhibits a similar pattern, that is, the higher the number of monitoring stations, the larger the average enclosed area.

V. Conclusions

We design two routing approaches, called Location-agnostic (LA) and Location-specific (LS) protocols, to facilitate the self-sustaining agricultural monitoring platform. The LA protocol optimizes the flight path on-the-fly and is useful for dynamic environment while the LS protocol performs the flight path optimization prior to the flight and is suitable for static environment. Simulation results reveal that the LS and LA protocols largely outperforms the random protocol in average flight distance, average consumed energy, and average enclosed area.

Acknowledgment

This material is based upon work supported by the Rajamangala University of Technology Thanyaburi and Thailand Research Fund under Grant No. TRG5880176.

References

[1] Managing Bird damage to Fruit and other horticultural crops, Australian government, [Online] http://www.dpi.nsw.gov.au/agriculture/horticulture/pests-diseases-hort/multiple/managing- bird-damage/

[2] GranMonte Smart Vineyard, [Online] http://www.granmonte.com/about-estate.html/

[3] P. Nintanavongsa, U. Muncuk, D. R. Lewis, and K. R. Chowdhury, Design Optimization and Implementation for RF Energy Harvesting Circuits. *IEEE Journal on Emerging and Selected Topics in Circuits and Systems*, vol. 2, no. 1, pp. 24–33, Mar. 2012.

[4] V. Raghunathan, A. Kansal, J. Hsu, J. Friedman, and M. Srivastava, Design considerations for solar energy harvesting wireless embedded systems. *Proc. of Fourth Intl. Symposium on Information Processing in Sensor Networks (IPSN)*, pp. 457–462, Apr. 2005.

[5] J. Curty, M. Declercq, C. Dehollain, N. Joehl, Design and Optimization of Passive UHF RFID Systems, Springer, 2007.

[6] Powercast Corporation, Lifetime Power Evaluation and Development Kit. [Online] http://www.powercastco.com/products/development-kits/

[7] A. Kurs, A. Karalis, R. Moffatt, J.D. Joannopoulos, P. Fisher, and M. Soljacic, Wireless Power Transfer via Strongly Coupled Magnetic Resonances. *Science Magazine*, vol. 317, no. 5834, pp. 83–86, Jul. 2007.

[8] Witricity corporation, [Online] http://witricity.com/

[9] M. Zargham and P. G. Gulak, Maximum Achievable Efficiency in Near-Field Coupled Power-Transfer Systems. *IEEE Transactions on Biomedical Circuits and Systems*, vol. 6, no. 2, Jun. 2012.

[10] Kasetsart university, [Online] http://www.ku.ac.th/web2012/index.php/

[11] K. Sundar and S. Rathinam, Algorithms for Routing an Unmanned Aerial Vehicle in the Presence of Refueling Depots. *IEEE Transactions on Automation Science and Engineering*, vol. 11, no. 1, pp. 287–294, Jan. 2014.

[12] F. Guerrieroa, R. Suracea, V. Loscra, and E. Nataliziob, A multi-objective approach for unmanned aerial vehicle routing problem with soft time windows constraints. *Applied Mathematical Modelling*, vol. 38, no. 3, pp. 839–852, Feb. 2014.

[13] 3D Robotics Incorporation, iris+ drone Kit. [Online] http://www.3dr.com/

[14] Georgia Tech UAV research facility, Electric UAV Flight Time Calculator. [Online] http://www.uavrf.gatech.edu/

5th International Electrical Engineering Congress, Pattaya, Thailand, 8-10 March 2017

Impact of Sensor Mobility on UAV-based Smart Farm Communications

Prusayon Nintanavongsa and Itarun Pitimon
Department of Computer Engineering, Rajamangala University of Technology Thanyaburi, Thailand
Email: {prusayon.n, itarun.p}@en.rmutt.ac.th

***Abstract*— Agricultural productivity has long been a key metric for measuring farming efficiency and it has been proven that agricultural productivity can be increased through smart farming. Recently, Unmanned Aerial Vehicle (UAV) has also been incorporated into smart farming in order to provide additional perspectives, i.e., imagery analysis and agricultural surveillance. These UAVs not only perform their specific tasks but also capable of communicating. We investigate the impact of sensor mobility on network communications in a smart farm platform, comprising of sensor-equipped UAVs. Through a simulation study, we demonstrate how sensor mobility impacts network throughput and delay as well as determine the optimal UAV mobility profile.**

Keywords—UAV; sensor; mobility; smart farm; throughput.

I. INTRODUCTION

Smart farming, a method of increasing agricultural productivity by incorporating information technology into the traditional farming, is becoming a mainstream method of cultivation adopted by farmers. It is proven in [1] that a higher agricultural productivity can be increased by implementing environmental monitoring stations throughout the agricultural area. With a real-time environmental data monitoring, it enables farmers to respond promptly when fluctuation of critical variables, i.e., water level, temperature, that affect the agricultural productivity occur. Moreover, Food and Agriculture Organization of the United Nations (FAO) announced that food production will have to increase by 70 percent to sustain the global consumption by 2050 [2]. With limited agricultural area and water supply, smart farming is undeniably a promising method to maximize the agricultural productivity.

In addition to environmental monitoring at ground level normally found in smart farming, ones can take advantage from aerial perspective by incorporating UAV into the smart farm platform. At the ground level, useful information, i.e., soil humidity, temperature, and perimeter monitoring, can be collected and exchanged via monitoring stations. On the other hand, UAVs offer additional perspective through aerial monitoring capability. The assigned task can be either active (acting upon the presence of stimuli) or passive (only collecting data). For instance, monitoring stations at the ground level can perform environmental data collection as well as perimeter monitoring. Upon detection of intruders, it sends out the packet, indicating security breach, to the responsible agencies, i.e., central monitoring station and law enforcement unit. Moreover, UAVs not only provide imagery analysis of the agricultural are but also offer in-depth situation awareness by patrolling over the area of breaching upon request. On the contrary, UAVs can also be used to provide important updates and configurations to grounded monitoring stations by traversing towards them.

In order to achieve a seamless operation of the UAV-based smart farming, it is crucial to ensure that the communication efficiency among sensors-equipped devices is at the highest level, that is, operating the network with parameters that yields the highest throughput with respect to an acceptable network delay. We consider a smart farm platform, consisting of sensor-equipped UAVs, and investigate how sensor mobility affects network communications, i.e., network throughput and delay. UAVs with high mobility rate may offer higher level of coverage area since they are travelling at higher speed. However, it is shown in [3] that network communication is very susceptible to high rate of mobility and the optimal mobility profile should be employed in order to achieve the optimal network throughput.

The core contributions of our work can be summarized as follows:

- We demonstrate how sensor mobility impacts network throughput and delay in a smart farm platform, comprising of sensor-equipped UAVs.
- We determine the optimal UAV mobility profile that yields the optimal network throughput.

The rest of this paper is organized as follows: In Section II, we give the related work. Our simulation parameters are discussed in detailed in Section III. The simulation results are presented in Section IV. Finally, Section V concludes our work.

II. RELATED WORK

The concept of smart farming has emerged in the past decade and is gaining more attention recently. It is obvious that even the large presence of land, only a fraction is suitable for agricultural purpose. Moreover, today's agricultural area is decreasing as a result of the economic growth, i.e., rice paddy is converted into habitation through housing development. On the other hand, the world's population is increasing overtime, implying a larger volume of food production needed to keep up with the increasing rate of food consumption. Consequently, there is an urgent need for more efficient agricultural process. In other words, an agricultural productivity has to be increased. This poses even more serious problem if the land available for

978-1-5090-4666-9/17/$31.00 ©2017 IEEE

agricultural propose is diminished. Smart farming is considered to be one of the promising candidates to alleviate aforementioned problem.

Recently, the realization of Internet of Things (IoT) concept is implemented in [4] to provide services for smart city. The authors propose an integrated semantic service platform (ISSP) to support ontological models in various IoT-based service domains of a smart city. The prototype service for a smart office using the ISSP is developed as well as illustration on how the ISSP-based method would help build a smart city. The promise of growing agricultural productivity by adopting IoT-related technologies is discussed in [5] while a connected farm concept, which aims to provide suitable environment for growing crops based on the IoT systems is proposed in [6]. All sensors and actuators for monitoring and growing crops are connected with a gateway installed with a device software platform for IoT systems and the gateway communicates with the IoT service server. Consequently, The IoT service server not only monitors the environmental condition of the connected farm by communicating with the gateway installed into the connected farm, but also talks with expert farming knowledge systems and controls actuators in order to make the farm suitable to grow crops.

The implementation of smart farming with off-the-shelf embedded devices, Raspberry Pi and Arduino Uno, is presented in [7]. The authors investigate an establishment using an Intelligent System which employed an Embedded System and Smart Phone for chicken farming management and problem solving. It is found that the system could monitor weather conditions including humidity, temperature, climate quality, and filter fan in the chicken farm. The system was found to be comfortable for farmers to use as they could effectively control the farm remotely, resulting in cost reduction, asset saving, and productive management in chicken farming.

The use of UAV for agricultural purposes is recently proposed by Kasetsart university researchers [8]. The research project is a collaboration between the faculty of engineering, Kasetsart university and the Yamaha motors (Thailand) and aims to effectively plant, deliver fertilizer, and spray pesticide to the cultivation area. The prototype is expected to weight 70 kilograms and able to carry the payload of 29 kilograms. The source of power is fossil fuel with the consumption of 8 liters per 2 hours flight. In [9], the authors present a concept of using drones for smart farming and a novel approach to distinguish between different field's plowing techniques by means of an RGB-D sensor is proposed. The proposed technique can be easily integrated in commercially available Unmanned Aerial Vehicles (UAVs). In order to successfully classify the plowing techniques, two different measurement algorithms have been developed. Experimental tests show that the proposed methodology is able to provide a good classification of the field's plowing depths.

The self-sustaining agricultural monitoring platform, comprises of UAV with solar energy harvesting and wireless power transfer capability is proposed in [10] . The authors also propose two routing approaches, called Location-agnostic (LA) and Location-specific (LS) protocols, to facilitate the self-sustaining agricultural monitoring platform and demonstrate improvement in crucial metrics over existing routing approach. The LA protocol does not require location information of monitoring stations to be visited prior to the flight, and is useful for dynamic environment. The LS protocol relies on the complete view of the topology prior to the flight and is suitable for static environment. These protocols determine the optimal UAV routing path from a set of monitoring stations under various conditions. The simulation and experimentation studies demonstrate significant energy efficiency and coverage area improvement over the classical routing protocol.

In [11], the authors consider the case of disjoint farming parcels each including clusters of sensors, organized in a predetermined way according to farming objectives, and propose an UAV Routing Protocol (URP) for crop monitoring where heterogeneous sensor nodes are installed in the large crop field and only selective data from selected sensors is harvested by UAV. The proposed routing protocol takes into account a tradeoff between energy management and data dissemination overhead. The proposed system is validated by simulation and it is found that this system efficiently optimizes the energy utilization for sensor nodes as well as UAV.

III. Simulation Parameters

In this section, we describe the simulation parameters and scenario under consideration. We observe the impact of sensor mobility on network communication using discrete event simulator, ns-2 [12]. The simulation parameters are as follows:

A. UAV mobility profile

The UAV mobility profile consists of both speed and direction of movement. It is crucial to operate UAV at the optimal speed in order to achieve the highest network throughput. Operating UAV at too low speed not only decrease the area of coverage but also unable to utilize the network to its full potential. On the contrary, flying UAV too fast may incur network communication disruption. In this work, the speed of UAV is varied from 5 m/s to 60 m/s with 5 m/s increment.

The direction of UAV movement is another important aspect of UAV mobility profile. We employ the Random WayPoint (RWP) model for UAV movement. The RWP model generate mobility pattern in which each node moves to the random point within the specific area and remains in the position for certain period, known as pause time, then moves to next point randomly. We employ zero pause time in this work to minimize any possible implication on network throughput measurement.

B. UAV radio profile

It is known that radio module plays a major role in power consumption in battery-operated devices. The radio module equipped in UAV has no exception and it is desirable to use low-power radio module when applicable. The Institute of Electrical and Electronics Engineers (IEEE) 802.15.4 radio standard is employed in this work. In contrast to the IEEE 802.11 radio standard, the IEEE 802.15.4 radio standard is developed for low data rate monitoring and control applications with an emphasis on low-power consumption. We use the carrier sense radius and packet reception radius of 40 m.

C. Area of deployment

The area of deployment is 500 x 500 m^2 grid and UAVs are deployed uniformly at random. While it is possible that the location of the initial UAV placement may affect the experiment, i.e., UAVs are densely deployed at a particular location. It is unlikely that the initial placement of UAVs incurs any effect on the experiment since UAVs are mobile once the simulation is initiated. Fig. 1 shows the placement of 20 UAVs in the deployment area.

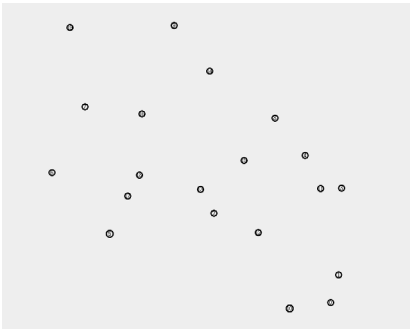

Fig. 1. Placement of UAVs in the deployment area

D. Routing protocol and traffic generation

The routing protocol plays a crucial role in packet delivery. In this work, an Ad hoc On-Demand Distance Vector (AODV) [13] is used. AODV is a routing protocol designed for mobile ad hoc networks. It establishes routes to destinations on demand and supports both unicast and multicast routing. We employ the Constant Bit Rate (CBR) traffic for UAV communication. The packet size is set to 512 bytes with the packet generation rate of 2 packets/s. The maximum CBR connection is limited to 20 connections.

IV. Simulation Results

In this section, we thoroughly observe the impact of sensor mobility on network communication using ns-2 network simulator. The key metrics under investigation are average network throughput and average network delay. Unless specifically stated, the simulation time is 300 seconds and 20 UAVs are deployed uniformly at random in 500 x 500 m^2 grid. The number of iterations for each UAV speed step is set to 10 and the result is obtained through the average value of 10 iterations. This is to prevent outliers from influencing the simulation results.

A. Average network throughput

The average network throughput is defined as the average amount of data sent from source and successfully received at the destination over a period of time. It is a key metric for network performance measurement and should be maintained at the highest level possible. We investigate how the UAV speed affects the average network throughput and determine the optimal operational speed of UAVs. Fig. 2 depicts the effect of the UAV speed on average network throughput. The UAV speed is varied from 5 m/s to 60 m/s. It is clear that the UAV speed has an effect on average network throughput, that is, the average network throughput is not constant throughout. In fact, the average network throughput exhibits a constant rate of growth from UAV speed of 5 m/s to 20 m/s then gradually decreases towards increasing value of UAV speed. At UAV speed of 5 m/s, the network is rather static and routing protocol plays an insignificant role in packet delivery. As the UAV speed increases, the network becomes more dynamic and UAVs are getting more connected. Consequently, the packet delivery increases thanks to the routing protocol. However, once the network becomes too dynamic due to increasing UAV speed, the higher number of network disruption from disconnected routes. It is obvious that the optimal UAV operational speed is 20 m/s since it yields the highest average network throughput and the network communication is utilized to its full potential at this point.

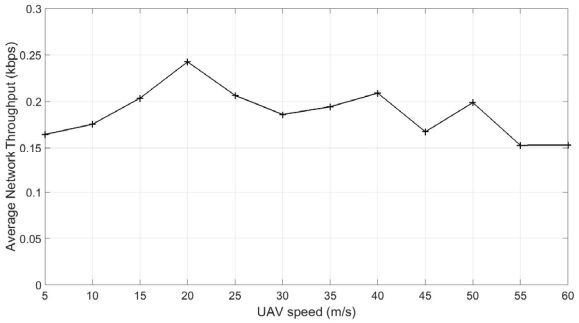

Fig. 2. Effect of the UAV speed on average network throughput

B. Average network delay

Another important metric for network performance evaluation is the average network delay. It becomes a critical metric of measurement for time-sensitive communication. In certain types of applications, any increase in network delay may render the application useless. Fig. 3 shows the effect of the UAV speed on average network delay. Again, the UAV speed has an effect on average network delay, that is, the average network delay is not constant throughout. It is obvious that the average network delay monotonically increases with increasing UAV speed. In contrast to the above section, the average network delay grows linearly with increasing UAV speed.

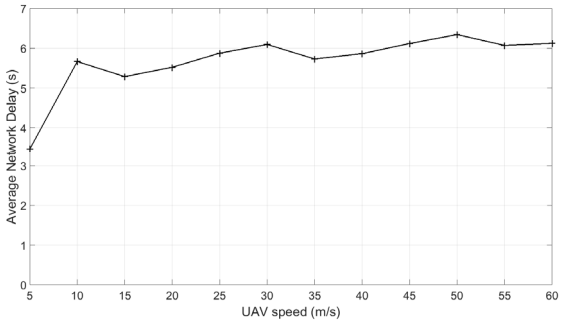

Fig. 3. Effect of the UAV speed on average network delay

V. CONCLUSIONS

Smart farming is a promising solution to increase agricultural productivity by incorporating information to the classical farming. It can also be supplemented by introducing UAV for additional perspective. We consider a smart farm platform, consisting of sensor-equipped UAVs, and investigate how sensor mobility affects network communications. We demonstrate how sensor mobility impacts network throughput and delay in a smart farm as well as determine the optimal UAV mobility profile that yields the optimal network throughput.

ACKNOWLEDGMENT

This material is based upon work supported by the Rajamangala University of Technology Thanyaburi and Thailand Research Fund under Grant No. TRG5880176.

REFERENCES

[1] GranMonte Smart Vineyard, [Online] http://www.granmonte.com/aboutestate.

[2] 2050: A third more mouths to feed, [Online] http://www.fao.org/news/story/en/item/35571/icode/

[3] A. H. Coarasa, P. Nintanavongsa, S. Sanyal, and K. R. Chowdhury, "Impact of mobile transmitter sources on radio frequency wireless energy harvesting," Proc. of International Conference on Computing, Networking and Communications (ICNC), pp. 573-577, Jan. 2013.

[4] M. Ryu, J. Kim, and J. Yun, "Integrated semantics service platform for the Internet of Things: a case study of a smart office," Sensors, vol. 15, no. 1, pp. 2137-2160, Jan. 2015.

[5] A. Savvas, "Farming industry must embrace the Internet of Things to grow enough food," [Online] http://www.techworld.com/ news/big-data/farming-industry-must-embrace-internet-of-things-3596905/

[6] M. Ryu, J. Yun, T. Miao, I. Ahn, S. Choi, and Jaeho Kim, "Design and implementation of a connected farm for smart farming system," Proc. of IEEE Sensor, Nov. 2015.

[7] S. Jindarat and P. Wuttidittachotti, "Smart Farm Monitoring Using Raspberry Pi and Arduino," Proc. of IEEE International Conference on Computer, Communication, and Control Technology (I4CT), Apr. 2015.

[8] Kasetsart university, [Online] http://www.ku.ac.th/web2012/index.php/

[9] P. Tripicchio, M. Satler, G. Dabisias, E. Ruffaldi, and C. A. Avizzano, "Towards Smart Farming and Sustainable Agriculture with Drones," Proc. of International Conference on Intelligent Environments, Jul. 2015.

[10] P. Nintanavongsa, W. Yaemvachi, and I. Pitimon, "A self-sustaining unmanned aerial vehicle routing protocol for smart farming," Proc. of International Symposium on Intelligent Signal Processing and Communication Systems (ISPACS), Oct. 2016.

[11] M. Ammad-udin, A, Mansour, D. Le Jeune1, E. H. M. Aggoune, and M. Ayaz, "UAV Routing Protocol for Crop Health Management," Proc. of 24th European Signal Processing Conference (EUSIPCO), Sept. 2016.

[12] Ns-2 network simulator, [Online] http://www.isi.edu/nsnam/ns/

[13] Ad hoc On-Demand Distance Vector (AODV) Routing, [Online] https://tools.ietf.org/html/rfc3561

Performance Analysis of Perimeter Surveillance Unmanned Aerial Vehicles

Prusayon Nintanavongsa, Weerachai Yaemvachi, and Itarun Pitimon
Department of Computer Engineering, Rajamangala University of Technology Thanyaburi, Thailand
Email: {prusayon.n, weerachai.y, itarun.p}@en.rmutt.ac.th

***Abstract*—Unmanned Aerial Vehicle (UAV) has seen exceptional growth over the past decade and become easily accessible to everyone. One of the key features that makes UAV attractive is the ability to provide the aerial perspective. This is particular the case for security and military purposes, i.e., security patrol and aerial surveillance. This paper offers the performance analysis of perimeter surveillance system comprising of multiple UAVs. These UAVs perform a surveillance task along the predefined perimeter and are capable of communicating. The key metrics under investigations are packet delivery rate, average packet delay, average network throughput, and average hop count. Through a simulation study, we demonstrate how numbers of UAVs and their mobility profile have an effect on key network metrics as well as determine the condition of optimality.**

***Keywords*—Performance analysis; Throughput; Unmanned Aerial Vehicle; Perimeter; Surveillance.**

I. Introduction

Perimeter surveillance plays a major role in any security measures employed throughout the world. This is true in both physical and logical security measures. In physical security measure, the system is designed to detect and deny unauthorized access to facilities and protect them from damage or harm [1]. It involves the use of multiple independent systems, i.e., closed-circuit television camera (CCTV) surveillance, security guards, and protective barriers. In logical security measure, a software suite is usually implemented to ensure that only authorized users can gain an access and perform actions as intended while unauthorized access is detected, denied, and recorded. This is usually accomplished through the use of firewalls, username and password authentication. The aforementioned security measures share the same principle, that is, in order to detect potential attacks, one has to monitor the point of ingress. For example, in case of physical security measure, CCTV surveillance and security guards are used for anomaly detection along the perimeter under monitor. Likewise, firewalls and Intrusion Detection System (IDS) are employed in logical security measure for this regard. To this point, it is undeniable that perimeter surveillance is crucial and plays a vital role in maintaining system integrity.

It is not until recently that UAV has spread its wings into several applications, ranging from recreational purposes to military use. For example, UAV can be used for monitoring forest fire, aerial photography, and boarder patrol. UAV is gaining its popularity owing to its ability to deliver the aerial perspective. In the old day, perimeter surveillance is an arduous task since one has to allocate time and resource, i.e., managing patrolmen and patrol cycle. Moreover, this method suffers the lack of immediate response since the surveillance is conducted on ground. Any breach can occur between patrol cycle and response can be slow as the backup has to route along perimeter. CCTV surveillance can alleviate the previously stated issue. However, it incurs a heavy investment in equipment installation and is not practical in large area deployment.

UAV is expected to become the mainstream in aerial surveillance since not only its operational cost is much lower than the human-operated aircraft but also eliminates the human risk involved in operating the actual aircraft. In addition to its ability to provide aerial perspective, it does not require infrastructure, i.e., roads and electrical facility, in order to operate. Consequently, UAV is a potential candidate for this purpose. It is globally estimated the market worth of $4.1 billion in commercial UAVs in 2017 and it is expected over 7 millions UAVs registration in the United States by 2020 [2].

With the UAV price drastically lowered, UAV begins dominating the perimeter surveillance task. Traditionally, a single large UAV is employed for perimeter surveillance and it only communicates with the base station. Hence, the data communication is simple and network characteristic can easily be determined. Recently, as the lower cost of UAV together with smaller UAV footprint, most civil and public applications can be achieved more efficiently with multi-UAV systems [3]. This system utilizes multiple UAVs, working in a coordinated manner, to provide much higher degree of coverage and scalability. It implies a more complex communication network, that is, communication among UAVs themselves and communication between UAVs and base stations. Consequently, the network characteristic can no longer be easily determined and it is crucial to investigate such scenarios prior to actual deployment.

Fig. 1 shows a perimeter surveillance system using multiple UAVs. It comprises of UAVs patrolling along the predefined perimeter and are capable of communicating among them, i.e., coordinating flying pattern and signifying alerts. The system can be self-sustaining through energy harvesting technology [4], [5] where UAV battery can be replenished without human intervention. We investigate the impact on packet delivery rate, average packet delay, average system throughput, and average hop count when such system exhibits changes in

978-1-7281-0729-5/19/$31.00

configurations.

The major contributions of our work can be recapitulated as follows:

- We present a perimeter surveillance system comprising of multiple UAVs. These UAVs perform a surveillance task along the predefined perimeter and are capable of communicating.
- we demonstrate how number of UAVs and their mobility profile have an effect on key network metrics as well as determine the condition of optimality.

The rest of this paper is sectioned as follows: The related work is given in Section II. The simulation parameters and scenario under investigation are discussed in details in Section III. The simulation results are revealed in Section IV. Finally, Section V concludes our work.

II. Related Work

In [6], a cooperative perimeter surveillance problem is introduced and the authors offer a decentralized solution that accounts for perimeter growth and changing of team members. A precise performance is achieved through small communication range, thanks to a known communication topology and identifying/sharing the critical coordination information. The decentralized approach not only offers scalability but also system robustness. The approach yields finite-time convergence and steady-state optimality.

A surveillance model for multi domain IoT environment, which is supported by reinforced barriers with collision-avoidance using heterogeneous smart UAVs is proposed in [7]. The authors define a problem whose goal is minimizing the maximum movement of UAVs on condition that collision-avoidance among UAVs is guaranteed. The problem is formulated using Integer Linear Programming (ILP) and a novel approach is proposed to solve the problem. Performance analysis of the proposed scheme is evaluated through extensive simulations with various scenarios.

The simulations and implementation of perimeter surveillance under communication constraints, performed by teams of UAVs using a Bluetooth communication framework, is presented in [8]. These UAVs perform their task collaboratively and hence efficient communication among them is crucial to ensure proper system operation. Additionally, weight and energy consumption of the payload are maintained at minimum, particularly in micro-UAVs. A coordination variables strategy is implemented to perform the perimeter division.

In [9], the effect of sensor mobility on network communications in a smart farm platform is presented. The platform comprises of sensor-equipped UAVs and are capable of exchanging data. The experiment is conducted through a custom simulation and the authors demonstrate the influence of sensor mobility on important network metrics. Lastly, the optimal UAV mobility profile is also presented.

III. Simulation Parameters

In this section, the simulation parameters and scenario are discussed in details. We investigate the effect of number of UAVs and their mobility profiles on key network metrics using discrete event simulator, ns-2 [10]. The simulation parameters are as follows:

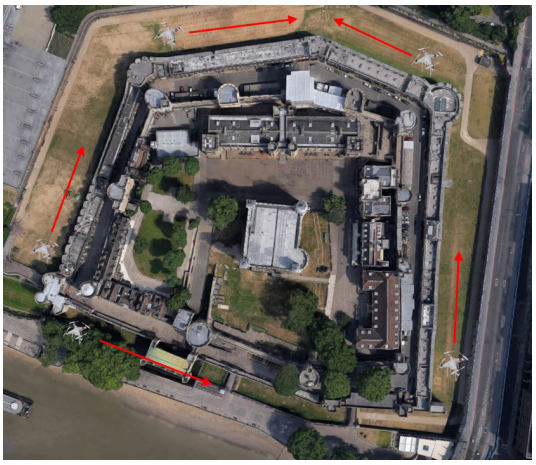

Fig. 1. A perimeter surveillance system using multiple UAVs

1) Perimeter surveillance UAV profile: The UAV Perimeter surveillance profile comprises of both direction of UAV movement and UAV speed. For perimeter surveillance, UAVs travel along the boundary of the restricted area. We deploy various numbers of UAVs, ranging from 10 to 90, to observe the network behavior on a different number of UAVs in deployment. Each UAV mobility pattern is generate randomly, that is, each UAV heads toward the random point along the predefined perimeter and remains stationary for certain period, known as pause time, then proceeds to next point randomly. In order to minimize any possible implication on key network metrics measurement, the pause time is set to zero.

In addition, the operational speed of UAV has a critical impact on key network metrics. In sparse UAV deployment, operating UAV at low speed may result in limited connectivity in communication among UAVs and increasing response time due to slower anomaly detection. On the other hand, high UAV mobility rate can cause disruption in network communication under dense UAV deployment. For this purpose, the UAV speed is varied from 0 $\mathrm{m/s}$ to 25 $\mathrm{m/s}$ with 5 $\mathrm{m/s}$ increment.

2) UAV radio profile: For wireless sensors, radio transceiver plays a key role in energy consumption and the radio transceiver installed in the UAV is no exception. It is advisable to employ low-power transceiver when applicable. The IEEE 802.15.4 radio standard is tailored for low data rate communication with an emphasis on low-power consumption. However, the major drawback of IEEE 802.15.4 is the communication range which is quite limited and deemed unsuitable for highly dynamic devices. Moreover, the power consumed by the radio transceiver is negligible when compared to the power consumption of UAV motors. Consequently, we employ the venerable IEEE 802.11 radio standard operating in Ad Hoc mode. Both carrier sense radius and packet reception radius are set to 250 m. We also employ two-ray ground reflection model for the radio propagation model in this work. The two-

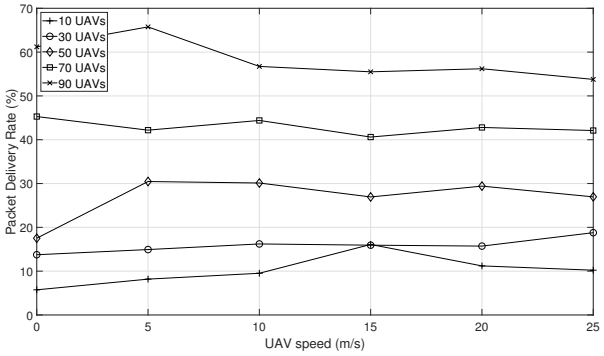

Fig. 2. Effect of UAV speed on packet delivery rate

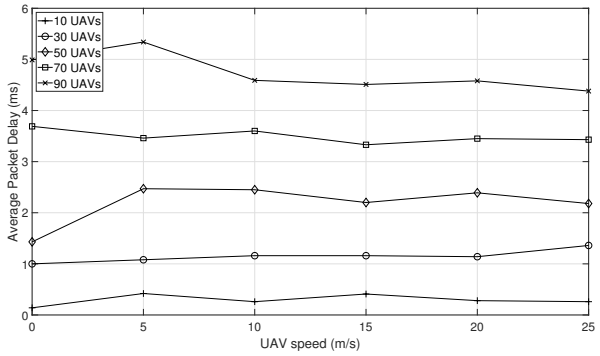

Fig. 3. Effect of UAV speed on average packet delay

ray ground reflection model takes into an account both the direct path and a ground reflection path. It is shown that this model yields higher accuracy at a long distance than the free space model [12].

3) Perimeter under surveillance: Without the loss of generality, the restricted area is 1500 x 1500 m^2 grid and UAVs are deployed uniformly at random along the boundary of the restricted area. While it is possible that UAVs are densely populated in particular spots at the beginning of the simulation, it has negligible effect on the simulation validity since UAVs will disperse shortly after the simulation starts.

4) Routing protocol and traffic profile: In multi-hop network, the network coverage area is larger than radio range of single a node. As a result, nodes have to act as relays to facilitate packet delivery. Hence, the routing protocol is a critical part in packet delivery. The Ad hoc On-Demand Distance Vector (AODV) [11] is adopted in this work. AODV is a routing protocol specifically tailored for mobile ad hoc networks. The route discovery is performed on demand and can accommodate both unicast and multicast routing. The UAV communication is modeled by Constant Bit Rate (CBR) traffic with the packet generation rate of 10 $\mathrm{packets/s}$. The packet size is 512 bytes and the maximum CBR connection is limited to 30 connections.

IV. Simulation Results

We thoroughly investigate the impact of numbers of UAVs and their speed on key network metrics. It is crucial that the network performance is evaluated through multiple network metrics since an individual metric only represents its own perspective. In other words, one has to evaluate as many network metrics at his disposal in order to efficiently capture the network characteristics. In this work, the simulation lasts 250 seconds and each data sample is derived through averaging value of 10 iterations. Consequently, outliers are eliminated and valid simulation results can be obtained.

A. Packet delivery rate

The packet delivery rate defines as the percentage of total packets successfully received to the total packets sent. Fig. 2 shows the effect of UAV speed on packet delivery rate for different numbers of UAVs deployed. It is obvious that, regardless of the number of UAVs deployed, the UAV speed has marginal influence on packet delivery rate as it is mostly constant throughout. However, numbers of UAVs have a direct impact on packet delivery rate, that is, the packet delivery rate increases with the growing numbers of UAVs. It is safe to say that the packet delivery rate is directly proportional to numbers of UAVs deployed. This implies that the UAV speed can be kept at minimum, with negligible effect on packet delivery rate, in order to prolong the UAV flight time.

B. Average packet delay

The average packet delay is a measure of average time required to transmit a packet across a network. It takes both queuing delay and transmission delay into an account. For time-sensitive application, the average packet delay is a crucial metric since certain level of average packet delay can adversely affect some types of applications, i.e., real-time communications. The effect of the UAV speed on average packet delay is shown in Fig. 3. Surprisingly, the average packet delay is marginally susceptible to UAV speed variation. Nevertheless, it is clear that the average packet delay increases as numbers of UAVs increase. In fact, the average packet delay plot exhibits a similar pattern of packet delivery rate plot depicted earlier. It implies that a dense UAV deployment contributes to an increase in average packet delay. That is to say, the larger the number of UAVs deployed, the higher the level of network congestion hence packets end up in a queue, waiting to be transmitted.

C. Average network throughput

The average network throughput defines as the average amount of data successfully received at the destination over a period of time. Note that there is a subtle difference between the packet delivery rate and the average network throughput. For instance, in a congested network, packets may be put in a transmission queue and never be transmitted. These packets will not contribute to the average network throughput because they have never reached the destination. On the contrary, a densely deployed network may benefit from a higher level of connectivity which enables efficient routing. Consequently,

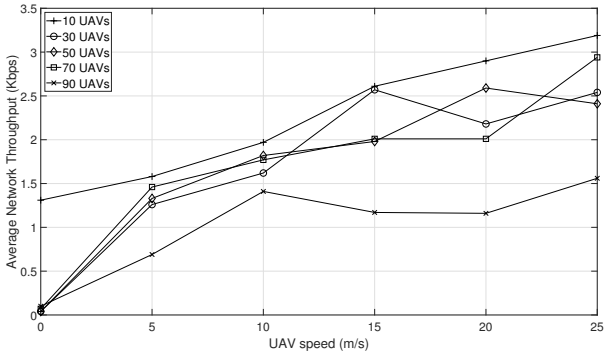

Fig. 4. Effect of UAV speed on average network throughput

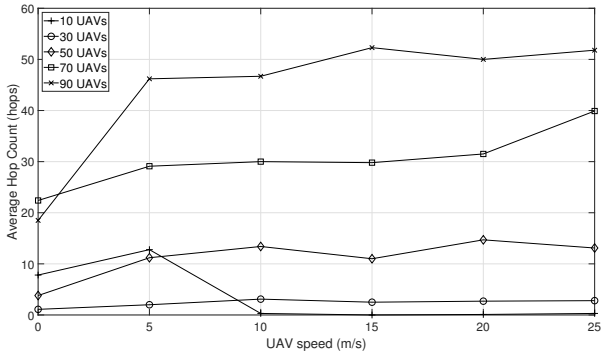

Fig. 5. Effect of UAV speed on average hop count

packets can be routed to the destination and a higher packet delivery rate is expected. This implies that one can have a system with very high packet delivery rate while its average network throughput hits rock bottom. Fig. 4 shows the effect of UAV speed on average network throughput. It is obvious that the system can benefit from operating UAVs at higher speed. Regardless of the number of UAVs deployed, the average network throughput monotonically increases with increasing UAV speed. However, the system with 10 UAVs deployed offers the highest average network throughput while the least average network throughput occurs in the system with 90 UAVs deployed. For the system with 30 UAVs, 50 UAVs, and 70 UAVs, there exists insignificant difference in average network throughput and the different in numbers of UAVs deployed can be considered unimportant. This is in contrast to the packet delivery rate plot shown earlier and it can be presumed that this phenomenon is a result of densely deployed network.

D. Average hop count

The average hop count reflects the degree of separation between source and destination. It defines as the number of intermediate network devices through which data must pass between source and destination. Fig. 5 illustrates the effect of UAV speed on average hop count. It is shown that the UAV speed has an influence on the average hop count especially when the number of UAVs is large, i.e., 50 UAVs or more. Furthermore, the average hop count increases with the number of UAVs increases. Note that the larger average hop count implies the more intermediate UAVs required to relay packet to the destined UAV. As a result, the packet accumulates larger queuing and processing delay. This is coincide with earlier findings.

V. Conclusions

We present the performance analysis of perimeter surveillance system comprising of multiple UAVs. These UAVs perform a surveillance task along the predefined perimeter and are capable of communicating. we demonstrate how number of UAVs and their mobility profile have an effect on key network metrics as well as determine the condition of optimality. Simulation results reveal that the UAV speed and the number of UAVs deployed have an influence on the average network throughput and the average network hop count. Both the packet delivery rate and the average packet delay are not susceptible to the UAV speed variation. Lastly, both the packet delivery rate and the average packet delay are directly proportional to the number of UAVs deployed.

Acknowledgment

This material is based upon work supported by Thailand Research Fund (TRF) under Grant No. TRG5880176.

References

[1] M. L. Garcia, Design and Evaluation of Physical Protection Systems. *Butterworth-Heinemann*, 2008.

[2] Cooperative Surveillance for UAVs: Enabling safe, secured and efficient UAV operations, [Online] https://www.eurocontrol.int/sites/default/files/events/presentation/session5.5-thales-utm-a-perspective.pdf

[3] L. Gupta, R. Jain and G. Vaszkun, Survey of important issues in UAV communication networks. *IEEE Communications Surveys and Tutorials*, vol. XX, no. 1, pp. 287–294, November 2015.

[4] P. Nintanavongsa, W. Yaemvachi, and I. Pitimon, A self-sustaining unmanned aerial vehicle routing protocol for smart farming. *Proc. of International Symposium on Intelligent Signal Processing and Communication Systems (ISPACS)*, October 2016.

[5] P. Nintanavongsa, U. Muncuk, D. R. Lewis, and K. R. Chowdhury, Design Optimization and Implementation for RF Energy Harvesting Circuits. *IEEE Journal on Emerging and Selected Topics in Circuits and Systems*, vol. 2, no. 1, pp. 24–33, Mar. 2012.

[6] D. Kingston, R. W. Beard, and R. S. Holt, Decentralized Perimeter Surveillance Using a Team of UAVs. *IEEE TRANSACTIONS ON ROBOTICS*, vol. 24, no. 6, pp. 1394–1404, Dec. 2008.

[7] H. Kim and J. Ben-Othman, A Collision-free Surveillance System using Smart UAVs in Multi Domain IoT. *IEEE Communications Letters*, to appear 2019.

[8] J.M. Aguilar, P.R. Soria, B.C. Arrue, and A. Ollero, Cooperative Perimeter Surveillance Using Bluetooth Framework Under Communication Constraints. *Proc. of ROBOT 2017: Third Iberian Robotics Conference*, pp. 771–781, December 2017.

[9] P. Nintanavongsa and I. Pitimon, Impact of Sensor Mobility on UAV-based Smart Farm Communications. *Proc. of International Electrical Engineering Congress (iEECON)*, March 2017.

[10] Ns-2 network simulator, [Online] http://www.isi.edu/nsnam/ns/

[11] Ad hoc On-Demand Distance Vector (AODV) Routing, [Online] https://tools.ietf.org/html/rfc3561

[12] T. S. Rappaport, Wireless communications, principles and practice. *Prentice Hall*, 1996.

Detection and Localization of Unauthorized Unmanned Aerial Vehicle Operator using Unmanned Aerial Vehicle

Prusayon Nintanavongsa* and Itarun Pitimon*

Received : November 29, 2019
Revised : December 23, 2019
Accepted : December 25, 2019

Abstract

Unmanned Aerial Vehicle (UAV) has gained popularity recently, in both commercial and leisure purposes. Thanks to the technological advancement and dramatically lower manufacturing cost, UAV becomes very affordable and widely accessible to the public. This poses several critical security issues, ranging from merely loss of privacy to life-threatening incident. Consequently, it is crucial to be able to detect and locate an unauthorized UAV operator in case of critical security breach occurs. We propose a system to detect and locate an unauthorized UAV operator using UAV. This UAV, equipped with a directional antenna, performs unauthorized UAV operator detection and localization tasks by traveling along the predefined path and narrows down the potential area as time passes. The key performance metrics under investigation are coverage area, identifiable area, time to identify an unauthorized UAV operator, and error rate. We demonstrate, through simulation studies, how UAV service ceiling, UAV speed, and antenna directivity have an effect on the key performance metrics of the system, together with, the optimal operating condition.

Keywords: Unmanned Aerial Vehicle, Detection, Localization, Unauthorized Operator.

1. Introduction

UAV is one of the emerging technologies that has seen a major growth in the recent years. It has secured its places in several applications, ranging from civil to military uses. Civil use of UAV includes aerial photography, filmmaking, and agricultural monitoring while aerial surveillance and reconnaissance are examples of UAV applications for military use. One of the key features that makes UAV attractive is the ability to provide the aerial perspective and its freedom of movement without the need of infrastructure, i.e., roads and electrical facilities. Consequently, it is undeniable that UAV will soon become the workhorse in aerial related applications. In fact, it already replaces human-operated aircraft in aerial photography business since it not only provides a significantly lower in operating cost but also eliminates the human risk involved in operating an actual aircraft. It is globally estimated the market worth of $4.1 billion in commercial UAVs in 2017 and it is expected over 7 million UAVs registration in the United States by 2020 [1].

Since UAV is easily accessible and affordable, several issues involving illegal uses of UAV are increasing rapidly. Breaching of privacy through unauthorized UAV operation is commonly found in most cases. The charge of unauthorized UAV operation spans from misdemeanor to felony offense, depending on the territory the offense occurs [ncsl.org]. However, in an extreme case, i.e., using UAV for malicious purposes, it is not only required that the hostile UAV be rendered harmless but also the need to identify the operator of the hostile UAV. Rendering UAV harmless can be achieved through the use of UAV jammer. UAV jammer interferes the communication between UAV and its operator. As a result, the targeted UAV either drops to the ground or returns to its initial location. Note that the UAV operator is fully aware of the jamming and mostly flees from the scene. Hence, the UAV jammer can prevent malicious UAV from accomplishing its

* *Department of computer engineering, Faculty of engineering, Rajamangala University of Technology Thanyaburi.*

task but cannot locate and apprehend the hostile UAV operator.

There exist several methods to detect and locate an unauthorized signal source emitter, i.e., unauthorized UAV operator. Mobile signal tracker and existing communication infrastructures are good examples. However, these facilities are ground-based and have limitations in terms of difficulties in equipment deploying as well as the speed of detection and localization the unauthorized transmitting signal source. In fact, it is almost impossible to employ the existing communication infrastructures for unauthorized UAV detection and localization since they are designed for different purposes from the beginning.

Figure 1. *Detection and locaization with UAV at high service ceiling.*

Figure 1 shows our proposed system for detection and localization of an unauthorized UAV operator using UAV. Initially, the UAV starts of at a higher service ceiling in order to cover a large searching area. However, the location of an unauthorized UAV operator cannot be pinpointed but rather a rough estimate. To narrow down the potential area that an unauthorized UAV operator resides, the UAV identify the potential sector through received signal strength measurement and moves toward the potential sector. The UAV then lower the service ceiling in order to locate an unauthorized UAV operator in fine-grained manner as depicted in Figure 2. Note that the circle signifies the detection range of the UAV.

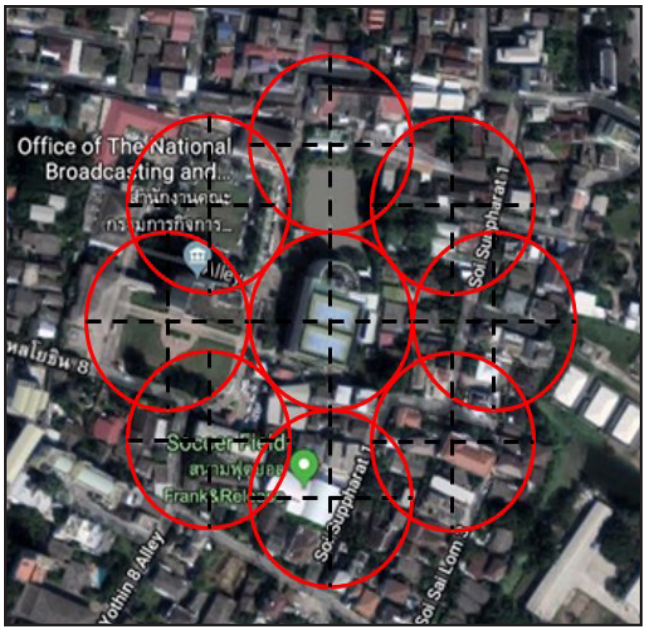

Figure 2. *Detection and locaization with UAV at low service ceiling.*

The major contributions of our work can be summarized as follows:

• We propose a system to detect and locate an unauthorized UAV operator using UAV. This UAV, equipped with a directional antenna, performs unauthorized UAV operator detection and localization tasks by traveling along the predefined path and narrows down the potential area as time passes.

• We demonstrate, through simulation studies, how UAV service ceiling, UAV speed, and antenna directivity have an effect on the key performance metrics of the system, together with, the optimal operating condition.

The rest of this paper is organized as follows: The related work is given in Section 2. The proposed system are discussed in details in Section 3. The simulation results are revealed in Section 4. Finally, Section 5 concludes our work.

2. Related Work

Detection and localization of an unauthorized signal source is not new but has been a topic of discussion for a long time. Several techniques have been proposed and received substantial attention from research community. Angle of Arrival (AoA) is a technique that determines the location of signal source by angle estimation between the direction of an incident wave

and a certain reference direction [2], [3], [4]. However, the drawback of AoA is that it is severely affected by non line-of-sight condition. Moreover, the accuracy of AoA is limited by the directivity of the antenna and channel fading, and multipath reflection. The concept of Time of Arrival (TOA) is discussed in [5], [6], [7]. In ToA method, the propagation time between the transmitter and the receiver is estimated by calculating the time difference between them, that is, transmitter's time and receiver's time. In [8], [9], [10], Time Difference of Arrival (TDoA), the localization method based on the measurement of the difference in the arrival times of the signal from the source at multiple nodes, is revisited. The advantage of TDoA is that it is marginally susceptible to multipath reflection and non line-of-sight condition. Lastly, the Received Signal Strength Indication (RSSI) is present in [11]-[15]. In this method, the strength of the received signal at the receiver is translated to the distance between the transmitter and the receiver using Friis transmission equation [16]. However, RSSI is susceptible to multipath reflection and channel fading. A multiplication distance correction factor is introduced in [17] to counteract estimation error and hence drastically improve the accuracy.

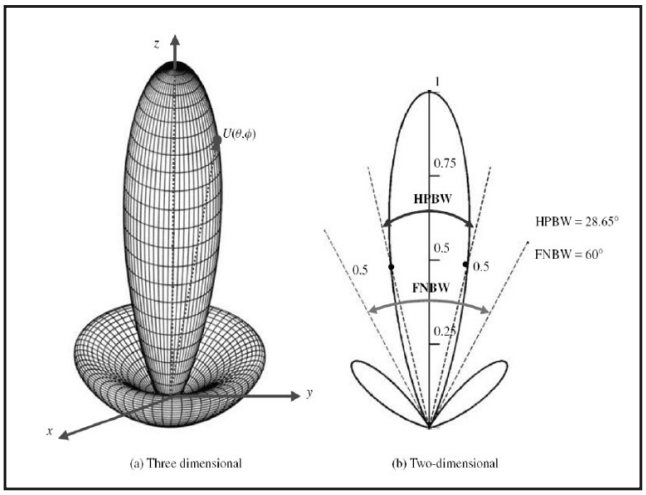

Figure 3. *Radiation pattern of the directional antenna.*

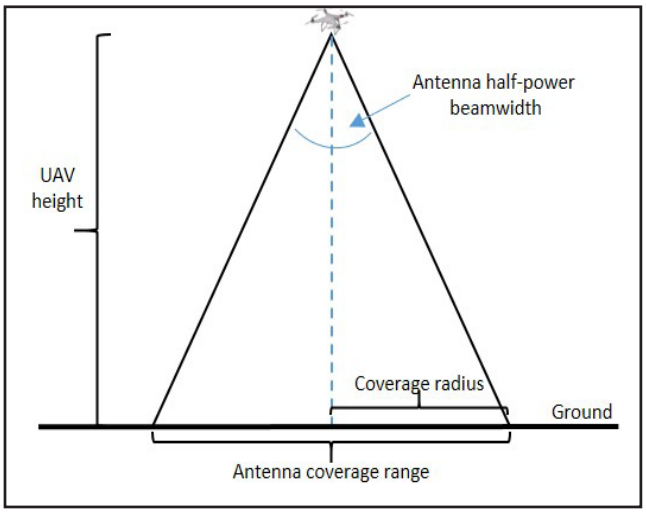

Figure 4. *Coverage area of the UAV equipped with directional antenna.*

3. The Proposed System

One of the key elements of the proposed system that enables an unauthorized UAV operator detection and localization is the directional antenna. The directional antenna is a good candidate for directional finding as it provides a high gain and hence a high sensitivity. However, the sensitivity of the directional antenna can be different according to the design. For example, the directional antenna with narrower beamwidth offers the higher sensitivity compared to the directional antenna with wider beamwidth. On the other hand, the directional antenna with wider beamwidth provides the larger coverage area compared to the directional antenna with narrower beamwidth.

The radiation and reception patterns of the directional antennas are characterized by their beamwidth. The Half Power Beamwidth (HPBW) is the angular separation in which the magnitude of the radiation pattern decreases by 3 dB from the peak of the main beam. Figure 3 illustrates the radiation pattern of the directional antenna and its HPBW. It is obvious that the larger the HPBW, the larger the coverage area of signal detection. Consequently, if the directional antenna is installed on the UAV in such the way that the directional antenna's main lobe is perpendicular to the ground, that is, the UAV is equipped with the directional antenna underneath and pointing downwards. The coverage area of this directional antenna equipped UAV is shown in Figure 4. The relationship between UAV service ceiling (UAV height), coverage radius, and HPBW is shown in Equation 1.

$$coverage\ radius = \tan\frac{HPBW}{2} \times uav\ height \quad (1)$$

It is shown in Equation 1. that the coverage radius is directly proportion to UAV height and HPBW. In other words, the coverage radius can be increased by increasing UAV height and HPBW. The coverage area, the area that the UAV can detect the presence of an unauthorized UAV operator, can be derived in Equation 2.

$$coverage\ area = \pi \times coverage\ radius^2 \quad (2)$$

3.1 Detection of an Unauthorized UAV Operator

The coverage area shown in Equation 2. is the area that the UAV can detect the presence of an unauthorized UAV operator. In order to provide larger coverage area, the UAV performs the flying pattern as depicted in Figure 5. The UAV begins detection of an unauthorized UAV operator at the sector A. Again, the circle signifies the detection range of the UAV, that is, the UAV is able to detect the presence of an unauthorized UAV operator if and only if it resides within the circle. Once it accomplishes detection of an unauthorized UAV operator at the sector A, it then proceeds to the sector B and performs detection of an unauthorized UAV operator. Upon completing the detection of an unauthorized UAV operator in sector B, it moves towards the sector C and performs detection of an unauthorized UAV operator. The process carries on in this fashion, a clockwise progression, until it finally reaches the destined sector I. Upon finishing the round of detection, the coverage area of that round can be calculated in Equation 3.

$$coverage\ area around_{round} = \pi \times (3 \times coverage\ radius)^2 \quad (3)$$

The signal power perceived by the UAV signifies the distance between the sensing UAV and an unauthorized UAV operator. In other word, the stronger the signal received by the sensing UAV, the closer the UAV to an unauthorized UAV operator. The Friis transmission equation describe the relationship of received power ($P_{receiver}$), transmitted power ($P_{transmitter}$), and distance (d) between transmitter and receiver as shown in Equation 4.

$$p_{receiver} = p_{tranmitter} G_t G_r \left(\frac{c}{4\pi fd}\right)^2 \quad (4)$$

where G_t is the antenna gain of transmitter, G_r is the antenna gain of receiver, and are antenna gains, and $\left(\frac{c}{f}\right)$ is the wavelength of the transmitted signal. It is clear that the received signal strength, diminishes with the square of the distance.

As mentioned previously, the circle in Figure 5 signifies the detection range of the UAV. This implies that the maximum degree of separation, that enables the detection of an unauthorized UAV operator, between the sensing UAV and an unauthorized UAV operator lies on the perimeter of the circle. This the maximum degree of separation is simply the hypotenuse in Figure 4. Consequently, it can be calculated as in Equation 5.

$$distance_{max} = \frac{uav\ height}{\cos\left(\frac{HPBW}{2}\right)} \quad (5)$$

The lowest level of received signal that the UAV can detect the presence of an unauthorized UAV operator is then derived in Equation 6

$$p_{receiver\_\min} = p_{tranmitter} G_t G_r \left(\frac{c}{4\pi f\ distance_{\max}}\right)^2 \quad (6)$$

The signal power received by the UAV in each sector is recorded and will be used in the next section, Localization of an unauthorized UAV operator.

3.2 Localization of an Unauthorized UAV Operator

After completion of the detection of an unauthorized UAV operator in each sector, the next phase is to determine the potential sector that an unauthorized UAV operator most likely resides. The signal power received by the UAV in each sector are compared. As mentioned earlier, the stronger the signal received by the sensing UAV, the closer the UAV to an unauthorized UAV operator. Hence, the potential sector that an unauthorized UAV operator most likely resides is the sector that has the highest level of received signal.

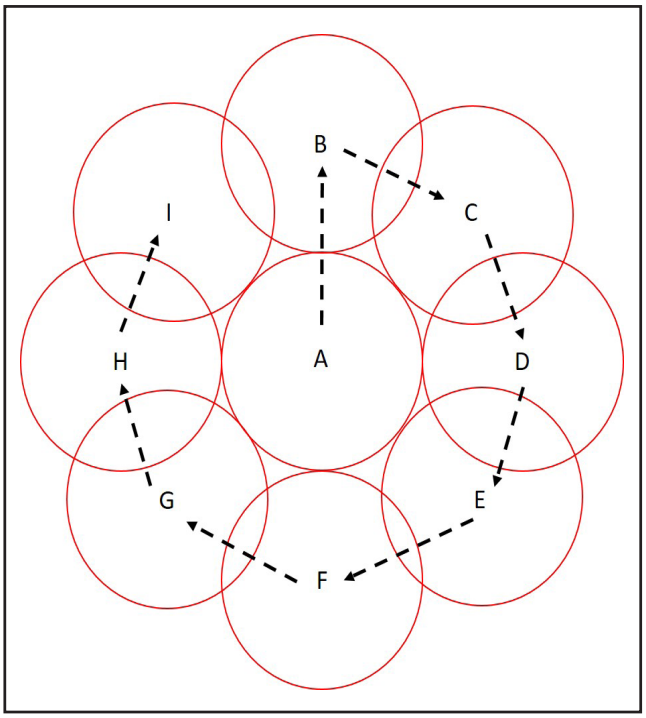

Figure 5. *UAV flying pattern for detection and localization of an unauthorized UAV operator.*

Given that the coverage radius of the UAV is r, and the centroid of sector A is located at coordinate(X_A, Y_A, Z_A), the centroid of each sector depicted in Figure 5. can be found as follows:

$$\textit{Centroid A}: (X_A, Y_A, Z_A) \quad (7)$$

$$\textit{Centroid B}: (X_B, Y_B, Z_B) = (X_A, Y_A+2r, Z_A) \quad (8)$$

$$\textit{Centroid C}: (X_C, Y_C, Z_C) = (X_A+\sqrt{2r}, Y_A+\sqrt{2r}, Z_A) \quad (9)$$

$$\textit{Centroid D}: (X_D, Y_D, Z_D) = (X_A+2r, Y_A, Z_A) \quad (10)$$

$$\textit{Centroid E}: (X_E, Y_E, Z_E) = (X_A+\sqrt{2r}, Y_A-\sqrt{2r}, Z_A) \quad (11)$$

$$\textit{Centroid F}: (X_F, Y_F, Z_F) = (X_A, Y_A+2r, Z_A) \quad (12)$$

$$\textit{Centroid G}: (X_G, Y_G, Z_G) = (X_A-\sqrt{2r}, Y_A-\sqrt{2r}, Z_A) \quad (13)$$

$$\textit{Centroid H}: (X_H, Y_H, Z_H) = (\mathrm{X}_A\text{-}2\mathrm{r}, \mathrm{Y}_A, \mathrm{Z}_A) \quad (14)$$

$$\textit{Centroid I}: (X_I, Y_I, Z_I) = (X_A-\sqrt{2r}, Y_A+\sqrt{2r}, Z_A) \quad (15)$$

Once the sector with the highest level of received signal is determined, it is the most likely that an unauthorized UAV operator lies within the sector. The centroid of that corresponding sector is used as the initial sector for the detection of an unauthorized UAV operator in the next round. In other words, the centroid of that corresponding sector becomes the centroid of sector A in the next round of detection of an unauthorized UAV operator.

3.3 UAV Repositioning

Once the potential sector is determined in the previous section, the UAV needs to proceed to the new coordinate and perform the next round of detection of an unauthorized UAV operator. However, only relocating the centroid in X and Y axis will not contribute to the better resolution in detection and localization of an unauthorized UAV operator. It is imperative that the service ceiling of the UAV be lowered in order to capture the signal with higher resolution and hence the more precise localization of an unauthorized UAV operator. We introduce the UAV descending scale, defined as the scaling factor that UAV exhibits in lowering its service ceiling. For example, if the service ceiling of the UAV is at 1000 meters in the first detection round, with the UAV descending scale of 2, the next service ceiling of the UAV in the next round will be 500 meters. UAV descending scale has to be chosen carefully, too large UAV descending scale can lower time to identify the location of an unauthorized UAV operator while too small UAV descending scale can significantly increase time to identify the location of an unauthorized UAV operator and render the system unresponsive. Nevertheless, there is a flip side to the coin. , too large UAV descending scale can result in higher error detection rate of an unauthorized UAV operator while small UAV descending scale can drastically improve detection accuracy of the system.

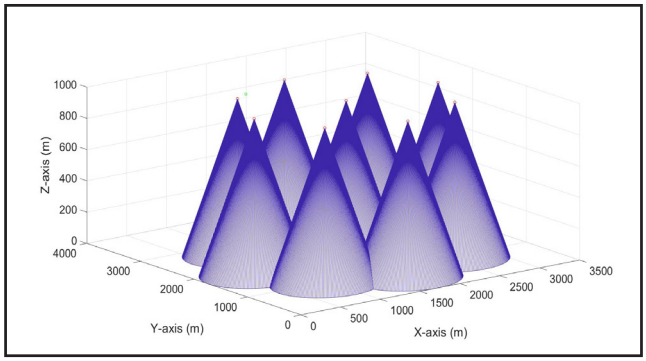

Figure 6. *Coverage area of the proposed system at UAV service ceiling of 1000 meters.*

3.4 System Operation Example

In order to better understand how the system progresses through different stages of detection and localization of an unauthorized UAV operator. We illustrates the system progression starting at the UAV service ceiling of 1000 meters. Figure 6 shows the coverage area of the proposed system at UAV service ceiling of 1000 meters. The coverage area of each sector is represented by the cone for each corresponding sector. Consequently, there are 9 cones which correspond to 9 sectors, that is, sector A to sector I. Moreover, the peak of each cone refers to the location that the UAV hovers while performing detection of an unauthorized UAV operator. The UAV starts at sector A then proceeds to sector B, sector C, and so on. Finally, it completes the round of detection of an unauthorized UAV operator at sector I.

Another perspective of the coverage area of the proposed system at UAV service ceiling of 1000 meters can be seen in Figure 7. Here, the top view of the coverage area of each sector, together with the location of an unauthorized UAV operator in sector I, is presented. It is obvious that each sector has its own coverage and contributes to the larger coverage as a whole.

The two dimensional representation of the coverage area of the proposed system can also be depicted in Figure 8. Here, the side view of the coverage area of the proposed system at UAV service ceiling of 1000 meters is shown and it provides a clear represention of the coverage beam of each sector.

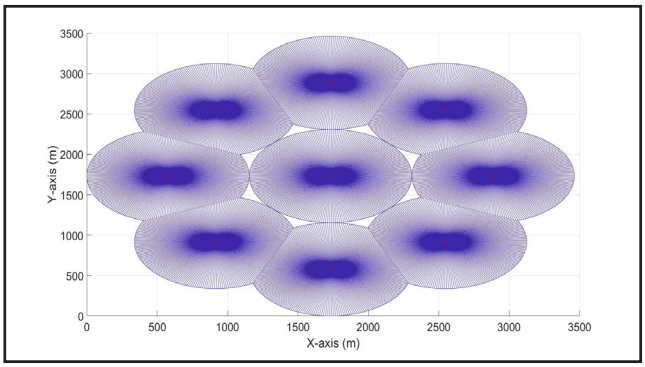

Figure 7. *Coverage area of the proposed system at UAV service ceiling of 1000 meters (top view).*

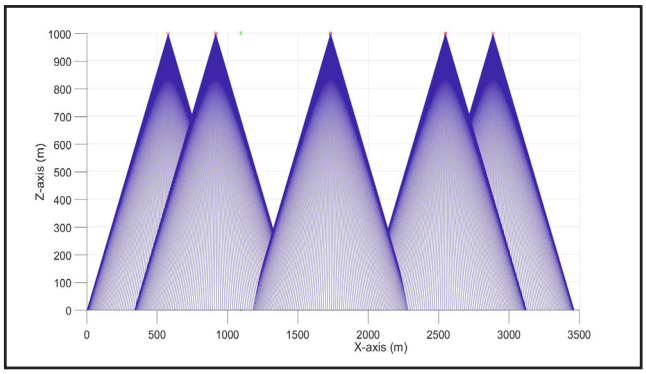

Figure 8. *Coverage area of the proposed system at UAV service ceiling of 1000 meters (side view).*

Once the UAV completes the round of detection, the system performs the localization by selecting the potential sector to be the centroid of the next detection round. In this case, since the location of an unauthorized UAV operator is in sector I, the received signal power of sector I is the highest among all sectors. Hence, the centroid of sector I is chosen to be centroid of sector A in the next detection round. The localization process is completed at this point.

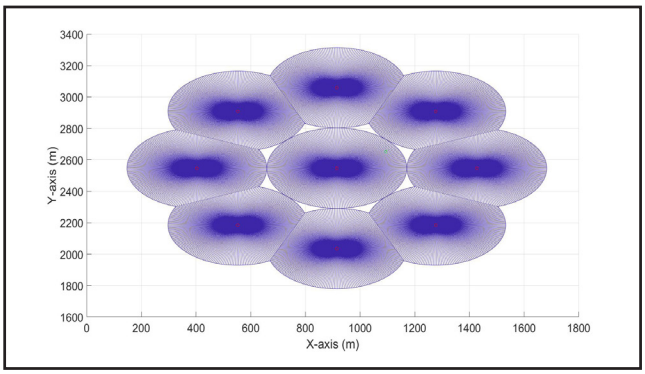

Figure 9. *Coverage area of the proposed system at UAV service ceiling of 444 meters (top view).*

The next stage of the system is to reposition the UAV, that is, lowering its service ceiling to better capture the signal resolution. In Figure 9, the UAV descending scale used is 2.25 and the new UAV service ceiling is 444 meters. The centroid of sector I in the previous detection round becomes the centroid of sector A for the present detection round. The UAV then reiterates through sector A to sector I, like the previous detection round, and records its findings in each sector for localization process.

The system proceeds through rounds of detection repetitively and finally halts when the predefined UAV service ceiling is achieved, 39 meters in this case. The final round of detection and localization of an unauthorized UAV operator terminates at this point and the corresponding top view of the proposed system can be seen in Figure 10.

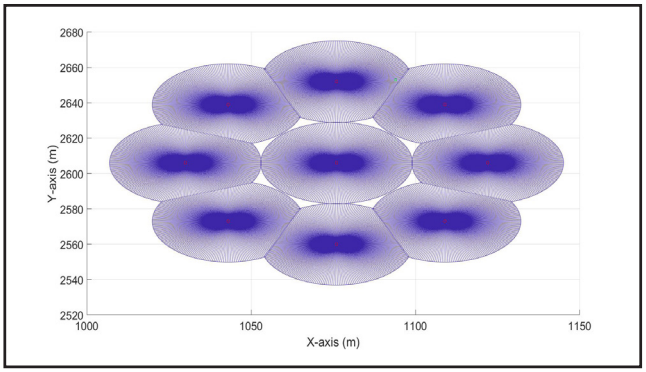

Figure 10. *Coverage area of the proposed system at UAV service ceiling of 39 meters (top view).*

4. Simulation Results

In this section, we thoroughly evaluate our proposed system using our custom simulator, developed in MATLAB. We investigate the effect of UAV service ceiling, UAV speed, and antenna directivity on the key performance metrics of the system. Unless specifically stated, the simulation time is limited to 1,500 seconds and an unauthorized UAV operator is deployed uniformly at random in 2,500 m2 circular area. The number of iterations for each complete process of detection and localization of an unauthorized UAV operator is set to 50 and the result is obtained through the average value of 50 iterations. This is to prevent outliers from influencing the simulation results.

4.1 Coverage Area

The coverage area is one of key performance metrics since it has a major effect on system efficiency, that is, system efficiency is directly proportion to the coverage area. In other words, the larger the coverage area, the faster the detection and localization of an unauthorized UAV operator and hence the higher the system efficiency. Figure 11 depicts the effect of UAV height on coverage area of the proposed system for various values of HPBW. It is clear that, for the HPBW value of 60 and 90 degrees, the coverage area exhibits a nonlinear increase with increasing UAV height. Consequently, it is preferable to initiate the UAV service ceiling at higher altitude in order to cover a larger area. On the other hand, the UAV equipped with antenna with HPBW of 60 degrees sees negligible benefit on this matter.

The benefit of the proposed system is clearly see in Figure 11. For example, if we initiate the UAV service ceiling at 1,000 meters with HPBW of 60 degrees, the coverage area of the system can be as large as 9 km2. In addition to large coverage area provided by the proposed system, it also offers a fine-grained localization of an unauthorized UAV operator. Figure 12 illustrates the fine-grained localization of an unauthorized UAV operator offered by the proposed system. It is obvious that the proposed system provides an almost pinpoint location of an unauthorized UAV operator. For instance, if the UAV service ceiling is lowered to 60 meters with HPBW of 60 degrees, the identifiable area of an unauthorized UAV operator can be as small as 400 m2.

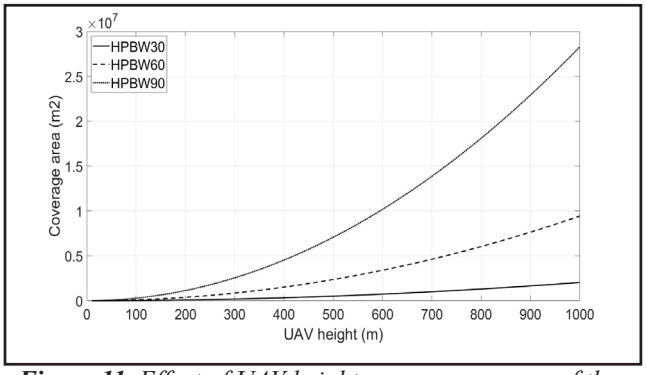

Figure 11. *Effect of UAV height on coverage area of the proposed system for various values of HPBW.*

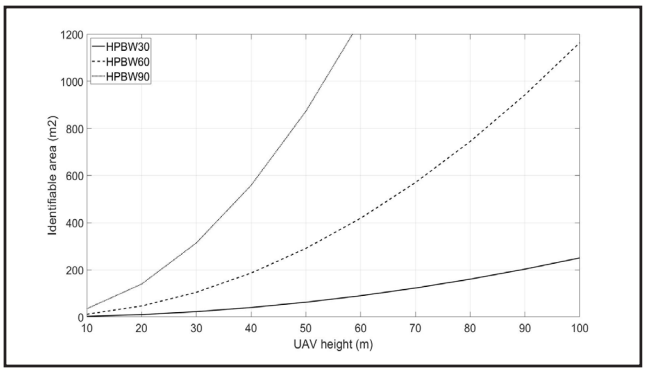

Figure 12. *Fine-grained localization of an unauthorized UAV operator.*

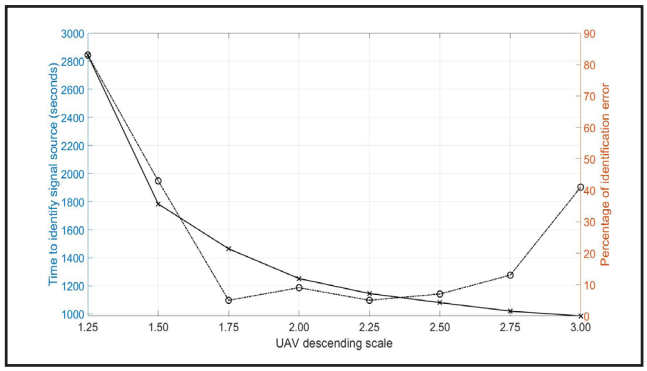

Figure 13. *Effect of UAV descending scale on time to identify an unauthorized UAV operator and its corresponding percentage of identification error.*

4.2 Time to Identify an Unauthorized UAV Operator

Time to identify an unauthorized UAV operator is defined as the time the system takes, from deploying the UAV until the location of an unauthorized UAV operator is determined. It is undeniable that this is the most important key performance metric of the system and it is also preferable to have the lowest value possible. The system that offers low time to identify signal source implies that the location of an unauthorized UAV can be determined promptly and further security measures can be carried out in timely manner. Moreover, since the UAV spends less time in the air, the energy consumption per detection and localization cycle is lower. As a result, the duty cycle of the system is higher and hence improving the system availability. Figure 13 depicts an effect of UAV descending scale on time to identify an unauthorized UAV operator and its corresponding percentage of identification error. As mentioned previously, UAV descending scale has to be carefully chosen as it can drastically affect the system performance. It is obvious that choosing an arbitrary value of UAV descending scale is not a good idea. In this case, the UAV with HPBW of 60 degrees begins the detection of an unauthorized UAV operator at service ceiling of 1,000 meters. The UAV descending scale is varied from 1.25 to 3.00 with 0.25 step size. It is clear the time to identify an unauthorized UAV operator is not linearly dependent with the UAV descending scale, that is, the time to identify an unauthorized UAV operator exponentially increases once the UAV descending scale is less than 2.0 while it exhibits linear increase with decreasing value of UAV descending scale elsewhere.

It is straight forward to choose the largest value of UAV descending scale if the identification error is omitted. However, it is crucial to investigate as many aspects of the system. Here, the percentage of identification error, defined as the percentage that the system fails to determine the location of an unauthorized UAV operator, is examined for different values of UAV descending scale. It is interesting that it does not exhibits either linear or exponential behavior with UAV descending scale. On the contrary, the percentage of identification error decreases with decreasing value of UAV descending scale, remains constant shortly, and then increases with decreasing value of UAV descending scale. In other words, the percentage of identification error yields a local minima. Figure 13 provides an invaluable information about the optimal choice of UAV descending scale, that is, the value of UAV descending scale in which the system yields the optimal performance. It is obvious that the UAV descending scale of 2.35 is the optimal choice since it is where the time to identify signal source and percentage of identification error cross.

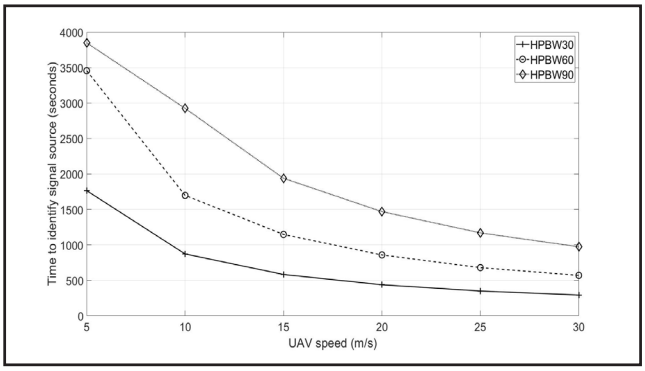

Figure 14. *Effect of UAV speed on time to identify an unauthorized UAV operator.*

The effect of UAV speed on time to identify an unauthorized UAV operator is shown in Figure 14. The UAV speed is varied from 1.25 to 3.00 with 0.25 step size and shown on X-axis while Y-axis shows the time to identify an unauthorized UAV operator. The system is set to terminate detection and localization when UAV service ceiling reaches 40 meters

which corresponds to 200 m2 of an identifiable area for UAV equipped with HPBE of 60 degrees. It is obvious that by increasing the UAV speed, the time to identify an unauthorized UAV operator decreases. Otherwise speaking, the time to identify an unauthorized UAV operator is inversely proportion to the UAV speed. However, the relationship among the two are not linear. The rate of reduction of the time to identify an unauthorized UAV operator is higher during UAV speed of 5 to 15 m/s while it tapers off towards higher UAV speed.

The HPBW of the antenna also has an effect on the time to identify an unauthorized UAV operator. Three values of HPBW, 30, 60, and 90 degrees, are investigated in Figure 14. It is clear that all value of HPBW exhibits a similar pattern and the antenna with smaller value of HPBW yields lower value of time to identify an unauthorized UAV operator. However, it should not be concluded that the antenna with a small value of HPBW is preferable since it also offers less coverage area compared to ones with a higher value of HPBW, and vice versa.

5. Conclusions

UAV has seen an exceptional growth in the recent past and it is highly affordable and accessible than ever before. This poses several critical security issues, ranging from merely loss of privacy to life-threatening incident. It is crucial for the system to not only intercept an unauthorized UAV but also able to locate an unauthorized UAV operator. We propose a system to detect and locate an unauthorized UAV operator by equipping the UAV with a directional antenna. This UAV performs an unauthorized UAV operator detection and localization tasks by traveling along the predefined path and narrows down the potential area as time passes. We demonstrate, through simulation studies, how UAV service ceiling, UAV speed, and antenna directivity have an effect on the key performance metrics of the system, together with, the optimal operating condition.

6. References

[1] Cooperative Surveillance for UAVs: Enabling safe, secured and efficient UAV operations, [Online] https://www.eurocontrol.int/sites/default/files/events/presentation/session5.5-thales-utm-aperspective.pdf

[2] R. Peng and M. L. S ichitiu, "Angle of arrival localization for wireless sensor networks." *In Proceedings of 3rd Annual IEEE Communications Society on Sensor and Adhoc Communications and Networks*, January, 2006.

[3] S. Tomic, M. Beko, and M. Tuba. "A linear estimator for network localization using integrated RSS and AOA measurements." *IEEE Signal Processing Letter*, Vol. 26, No. 3, pp. 405-409, March, 2019.

[4] N. Garcia, H. Wymeersch, and D. T. M. Slock. "Optimal precoders for tracking the AoD and AoA of a mmWave path." *IEEE Transactions on Signal Processing*, Vol. 66, No. 21, pp. 5718-5729, November 2018.

[5] C.-H. Park and J.-H. Chang. "TOA source localization and DOA estimation algorithms using prior distribution for calibrated source." *Digital Signal Processing,* Vol. 71, pp. 61-68, December, 2017.

[6] M. R. Gholami, S. Gezici, and E. G. Ström. "TW-TOA based positioning in the presence of clock imperfections." *Digital Signal Processing*, Vol. 59, pp. 19-30, December, 2016.

[7] Y. Liu, F. Guo, L. Yang, and W. Jiang. "Source localization using a moving receiver and noisy TOA measurements." *Signal Processing*, Vol. 119, pp. 185-189, February, 2016.

[8] E. Kazikli and S. Gezici. "Hybrid TDOA/RSS based localization for visible light systems." *Digital Signal Processing*, Vol. 86, pp. 19-28, March, 2019.

[9] D. Wang, J. Yin, T. Tang, X. Chen, and Z. Wu. "Quadratic constrained weighted least-squares method for TDOA source localization in the presence of clock synchronization bias: Analysis and solution." *Digital Signal Processing*, Vol. 82, pp. 237-257, November, 2018.

[10] Y. Sun, K. C. Ho, and Q. Wan. "Solution and analysis of TDOA localization of a near or distant source in closed form." *IEEE Transactions on Signal Processing*, Vol. 67, No. 2, pp. 320-335, January, 2019.

[11] P. Abouzar, D. G. Michelson, and M. Hamdi. "RSSI-based distributed self-localization for wireless sensor networks used in precision agriculture." *IEEE Transactions on Wireless Communications*, Vol. 15, No. 10, pp. 6638-6650, October, 2016.

[12] A. E. Lagias, T. D. Lagkas, and J. Zhang. "New RSSI-based tracking for following mobile targets using the law of cosines." *IEEE Wireless Communication Letter*, Vol. 7, No. 3, pp. 392-395, Junuary, 2018.

[13] J. Luomala and I. Hakala, "Analysis and evaluation of adaptive RSSI based ranging in outdoor wireless sensor networks." Ad Hoc Networks, Vol. 87, pp. 100-112, May, 2019.

[14] Z. Na, Y. Wang, X. Li, J. Xia, X. Liu, M. Xiong, and W. Lu. "Subcarrier allocation based simultaneous wireless information and power transfer algorithm in 5G cooperative OFDM communication systems." *Physics Communications*, Vol. 29, pp. 164-170, August, 2018.

[15] Z. Na, J. Lv, M. Zhang, B. Peng, M. Xiong, and M. Guan, "GFDM based wireless powered communication for cooperative relay system." *IEEE Access*, Vol. 7, pp. 50971-50979, April, 2019.

[16] T. S. Rappaport. *Wireless communications*, *principles and practice*. Prentice Hall, 1996.

[17] L. Gui, M. Yang, P. Fang, and S. Yang. "RSS-based indoor localization using MDCF." *IET Wireless Sensor Systems*, Vol. 7, No. 4, pp. 98-104, August 2017.